N cycling and microbial dynamics in pasture soils

Md Sainur Samad

University of Otago

June 2017

This dissertation is submitted in publication format

for the degree of Doctor of Philosophy.

Declaration

This dissertation is the result of my own work and contains nothing which is the outcome of work done in collaboration with others, except where clearly stated.

No part of this dissertation has been submitted for any other degree or qualification.

This thesis project was undertaken in the laboratory of Dr Sergio E. Morales in the Department of Microbiology and Immunology, University of Otago in Dunedin, New Zealand between February 2014 and April 2017. A portion of this research was also performed in the laboratory of Prof. Lars R. Bakken at the Department of Environmental Sciences, Norwegian University of Life Sciences in Ås, Norway between May 2014 and July 2014.

Thesis by publication format

This dissertation has been submitted by publication format. The Otago School of Medical Science and the Department of Microbiology and Immunology provided consultation on how to submit this format. This thesis is presented in accordance with their guidelines.

Chapter two and three are primary research papers that have been accepted for publications. Chapter four has been prepared as a manuscript. Chapter five has been prepared and submitted to a journal. The extended introduction and summary sections were written specifically for this thesis. They serve to place the work in a wider context and bring together the findings as a whole. In accordance with requirements, each chapter has been reformatted for consistency.

I took the leading role in the work presented here. For each study, I designed experiments, performed research, analyzed data and interpreted results, except where clearly stated. I contributed significantly to writing and revising each manuscript as first-author. Each publication also contains contributions by co-authors of varying size and importance, and this is clearly stated for each manuscript. Author contributions are detailed using the initials of each author at the start of each chapter.

Abstract

Pasture soils are a significant source of the greenhouse gas, nitrous oxide (N_2O) and as such they contribute to global warming. It has been reported that N_2O is approx. 300 times more potent than carbon dioxide (CO_2) as a greenhouse gas. Thus, understanding the mechanisms for controlling N_2O emissions from soil is key to developing new soil management strategies to counter or prevent climate change throughout the world. Despite this, very little is known about the key regulators of production and consumption of N_2O in pasture soils, especially under urine patch conditions. To address this, we used pasture soils representing both Northern (Ireland) and Southern (New Zealand) Hemispheres in experiments designed to understand both phenotypic and genotypic characteristics associated with N_2O emissions. We used a combination of gas kinetics, soil physicochemical characterization, metagenomics, 16S amplicon sequencing and quantitative PCR (of denitrifier: *nirS, nirK, nosZI* and *nosZII;* and nitrifier: bacterial and archaeal *amoA* genes) to link physical, chemical and biological parameters associated with emissions. This thesis work was able to show how in nitrate-amended pasture soils the rate of carbon mineralization under oxic and anoxic conditions is positively linked to the rate of denitrification. In addition, the emission ratio of N_2O is negatively linked to pH. Both pH and N_2O emission ratio were significantly associated with 16S microbial community composition as well as microbial richness. This result confirms that pH imposes a general selective pressure on the entire community and that this is associated with changes in emission potentials. This supports the general ecological hypothesis that with increased microbial diversity, efficiency of N_2 production increases (i.e. more efficient conversation of N_2O to N_2). Worked performed in a simulated urine patch (oxic conditions) suggested other pathway (e.g., nitrifier-denitrification) as a source of N_2O emissions. No clear trend was observed between emission ratio of N_2O under urine patch condition and emission ratio under true denitrification conditions (i.e. under anoxic environment). The urine patch accelerated the rate of C mineralization about 10 times, concurrent with a decrease in prokaryotic richness and a shift in community composition. Community response identified two major groups of responders: negatively affected prokaryotes we hypothesized utilized energy from N-linked redox reaction for maintenance and positively responding populations that use this energy for growth. Overall, this study

provides new insights into the N_2O emissions and microbial dynamics for reduction of N_2O in pasture soils.

Acknowledgements

First of all, I would like to express my sincere gratitude to my supervisor, Dr Sergio E. Morales for his enormous support, guidance and inspiration throughout my PhD study. I am grateful to Sergio for the funding I have received for this work from the New Zealand Fund for Global Partnerships in Livestock Emissions Research. I would like to thank my co-supervisors Professor Greg Cook and Professor Clive Ronson and all other members in my PhD committee for their valuable suggestions and feedbacks.

I am grateful to the University of Otago for Doctoral Research Scholarship award. I am also grateful to Department of Microbiology & Immunology for the travel award and departmental scholarship support.

Special thanks to my collaborators Professor Lars R. Bakken from Norwegian University of Life Sciences, Professor Tim J. Clough from Lincoln University, Dr Cecile A. M. de Klein from AgResearch, Dr Karl G. Richards & Dr Gary J. Lanigan from Teagasc-Ireland for their valuable suggestions and feedbacks. I thank all members of the nitrogen group at the Norwegian University of Life Sciences for their assistance and technical advice in gas kinetics work when I was in Norway in 2014. My gratitude to Dr Xochitl Morgan for her technical assistance that helped me to learn GraPhlAn analysis. Thanks to Dr Ambarish Biswas for his assistance in metagenomics. I thank all members in the Morales lab, 5th floor colleagues & friends, and other members in the department of Microbiology & Immunology for their support and encouragement.

Lastly, my countless thanks to my beloved parents and my wife for their continuous support and encouragement that helped me to complete my PhD.

Contents

List of Figures

Abbreviations

AFP	Air filled porosity
AMO	Ammonium monooxygenase
ANOVA	Analysis of variance
AOA	Ammonia-oxidizing archaea
AOB	Ammonia-oxidizing bacteria
ATP	Adenosine Triphosphate
BLAST	Basic local alignment search tool
C	Carbon
C:N	Carbon and nitrogen ratio
$CaCl_2$	Calcium chloride
CEC	Cation exchange capacity
CO_2	Carbon dioxide
Cu	Copper
DI	Deionized water
DNA	Deoxyribonucleic acid
DNRA	Dissimilatory nitrate reduction to ammonium
dNTP	Deoxynucleotide triphosphates
e^-	Electron
ECD	Electron capture detector
Fe^{2+}	Ferrous
FID	Flame ionization detector
g	Gram
GC	Gas chromatography
GHG	Greenhouse gas
GWP	Global Warming Potential
h	Hour
H^+	Proton
H_2	Hydrogen
H_2O	Water

ha	Hectare
ha^{-1}	Per hectare
HAO	Hydroxylamine oxidoreductase
He	Helium
HM	High moisture
HURM	Hydroxylamine/hydrazine-ubiquinone-redox-module
/N_2O	N_2O production index
KCl	Potassium chloride
kg	Kilogram
kPa	KiloPascals
LM	Low moisture
M	Molar
Mg m^{-3}	Megagrams per cubic meter
ml	Milliliter
mm	Millimeter
Mn^{2+}	Manganese
Mo-bis-MGD	Molybdenum-bis-molybdopterin guanine dinucleotide
mRNA	Messenger RNA
N_2/N	Dinitrogen/Nitrogen
N_2O	Nitrous oxide
N_2OR	Nitrous oxide reductase
nar	Nitrate reductase
NH_2OH	Hydroxylamine
NH_3	Ammonia
NH_4^+	Ammonium
nir	Nitrite reductase
NMDS	Non-metric multidimensional scaling
NO	Nitric oxide
NO_2^-	Nitrite
NO_3^-	Nitrate
NOB	Nitrite-oxidizing bacteria
nor	Nitric oxide reductase
nos	Nitrous oxide reductase
O_2	Oxygen

^{o}C	Degrees celsius
OTUs	Operational Taxonomic Units
PMF	Proton-motive force
ppb	Parts per billion
Ps az	Pseudoazurin
Q/QH2	Ubiquinone-ubiquinol pool
qPCR	Quantitative PCR
rDNA	Ribosomal DNA
RNA	Ribonucleic acid
rRNA	Ribosomal RNA
rrn	Operon copy number
SD	Standard Deviation
SE	Standard Error
SIMPER	Similarity percentage analysis
SO_4^{2-}	Sulfate
TCD	Thermal conductivity detector
Tg	Teragram
UQH_2	Ubiquinol
WFPS	Water filled porosity
yr^{-1}	Per year
µl	Microliter
µm	Micrometer

CHAPTER 1

General introduction

1.1. N_2O in the atmosphere

Nitrous oxide (N_2O) is an intermediate product in the natural process of nitrogen (N) cycling and is known as a greenhouse gas (GHG). N_2O is about 298 times more effective at trapping heat than carbon dioxide (CO_2) over a 100-year period and has an atmospheric life of approximately 121 years (IPCC, 2007; Myhre *et al.*, 2013). It is the second most important GHG after CO_2, and is known to deplete the stratospheric ozone layer (Ravishankara *et al.*, 2009). The concentration of N_2O in the atmosphere has increased by 20 % from 271 ppb to 324 ppb over the last 260 years (Myhre *et al.*, 2013). Soils, sediments, and water bodies all contribute to the production of N_2O as part of microbial and abiotic processes. The major source of N_2O are agricultural soils (Cole *et al.*, 1997; Paustian *et al.*, 2004; Mosier *et al.*, 1998), especially direct N_2O emissions from fertilized soils, animal production (from urine) as well as indirect N_2O emissions from nitrogen (N) used in agriculture (e.g. leaching and runoff, atmospheric deposition) (Mosier, 1998; Syakila and Kroeze, 2011). Combined, emissions from N fertilizer application and animal production (4.3-5.8 Tg N_2O-N yr^{-1}), and emissions from natural soils (i.e., unmanaged soils; 6-7 Tg N_2O-N yr^{-1}) represent 56-70% of all global N_2O sources (Syakila and Kroeze, 2011; Butterbach-Bahl *et al.*, 2013). More importantly, grazed pasture soils contribute 41% of global N_2O emissions (direct and indirect) through animal excreta (Oenema *et al.*, 2005).

In New Zealand, pastoral farming is the dominant agricultural sector and is characterized by year-round grazing of clover-based pastures. As a result, N-deposition by grazing animals is the single largest source of direct N_2O emissions in New Zealand contributing over 50% of emissions (de Klein *et al.*, 2003). An additional 30% of emissions were from indirect emission (e.g. leached and volatilized excreta-N) (de Klein *et al.*, 2003). More details about urine patch and how it contributes to N_2O emission in section 1.3.

1.2. The nitrogen (N) cycle

The N cycle involves several redox reactions (i.e. oxidation and reduction ranging from +5 to -3 as illustrated in Figure 1.1) catalyzed by different enzymes within bacteria, archaea and some fungi. This cycle can be broken down into modular reactions which include: ammonification, assimilation, nitrification, denitrification, nitrogen fixation, anammox and dissimilatory nitrate reducing to ammonium (DNRA) pathways.

In pasture ecosystems, N is deposited in soil as urea via urine patches. Urea is an organic compound, which under goes several N transformation processes; for examples, ammonification, nitrification, denitrification. Ammonification is a process in which organic nitrogen is converted to ammonia (NH_3). This process can be performed by many microbes, plants and animals. Ammonia can be exited in the form of ammonium (NH_4^+) in acidic or neutral environments. NH_4^+ can be assimilated by many microbes and plants, where they are incorporated into amino acids and other nitrogen-containing biomolecules. In nitrification, NH_3 or NH_4^+ are oxidized to nitrite ions (NO_2^-), which is further oxidized to nitrate ions (NO_3^-) (Figure 1.1). Nitrate ions can be incorporated or assimilated by a wide range of organisms (e.g. bacterial, fungal and algal species) into organic matter via assimilatory NO_3^- reduction. Under anaerobic conditions, nitrate ions can act as terminal electron acceptors. This process is known as nitrate respiration, or dissimilatory nitrate reduction. One of the dissimilatory nitrate reduction pathways is called denitrification. In denitrification, NO_3^- is first converted into NO_2^- then gaseous N (NO, N_2O and N_2). As a result of denitrification, soils lose NO_3^- which is one of the important nutrients for farming. However, denitrification can play an important role for removal of NO_3^- from wastewater treatment to prevent eutrophication (Knowles, 1982). Other pathways in N cycling includes N fixation, DNRA and anammox. In N fixation, soils gain N from the atmosphere as an inorganic source through N fixation (N_2 to NH_4^+) using nitrogenase enzyme. In DNRA, NO_3^- can be transformed into the NH_4^+ which is a reverse process of nitrification. In anammox (anaerobic ammonium oxidation), NH_4^+ and NO_2^- are directly converted into N_2. This process has a great interest in wastewater treatment. A detailed description of denitrification and nitrification is given below as both are involved in urine patch kinetics.

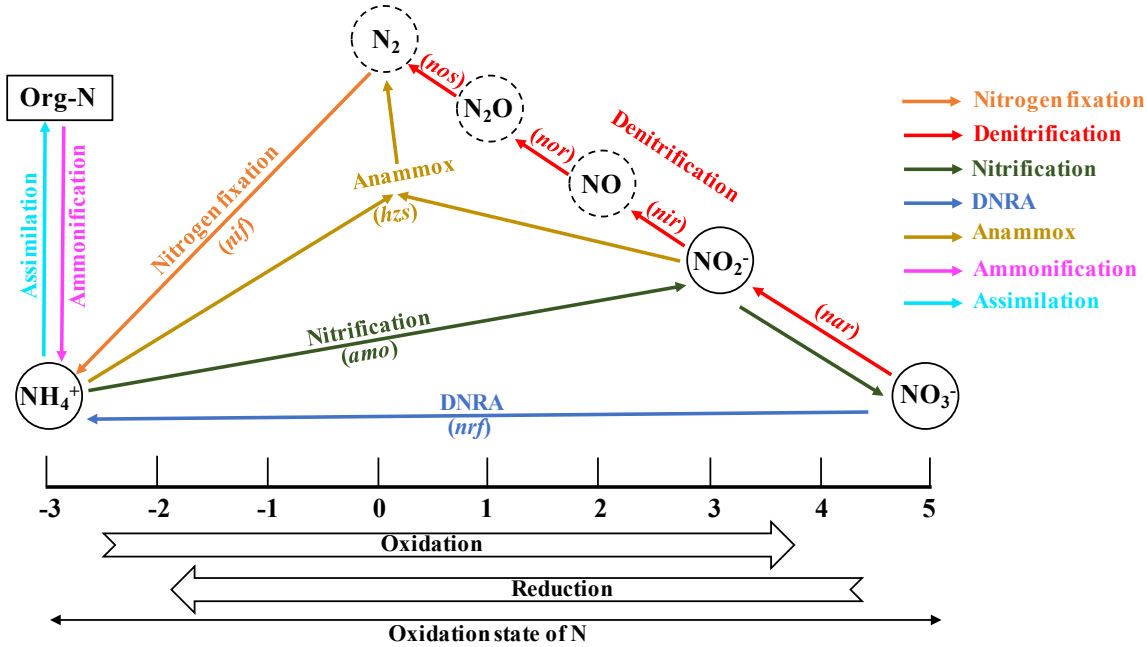

Figure 1.1. Microbial transformations within the N cycle. "Org-N" refers to organic nitrogen (e.g. urine/urea). N-transformation pathways and genes denoted as colored arrows and italic-text.

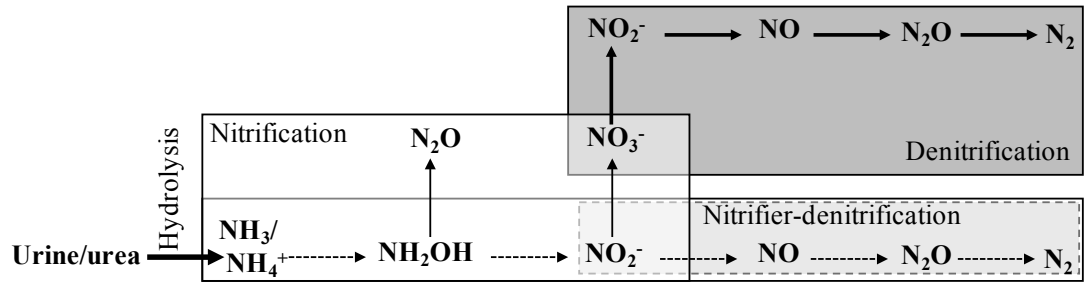

Figure 1.2. Nitrogen transformations within a soil urine patch (modified from Wrage *et al.*, (2001)). For explanation see text.

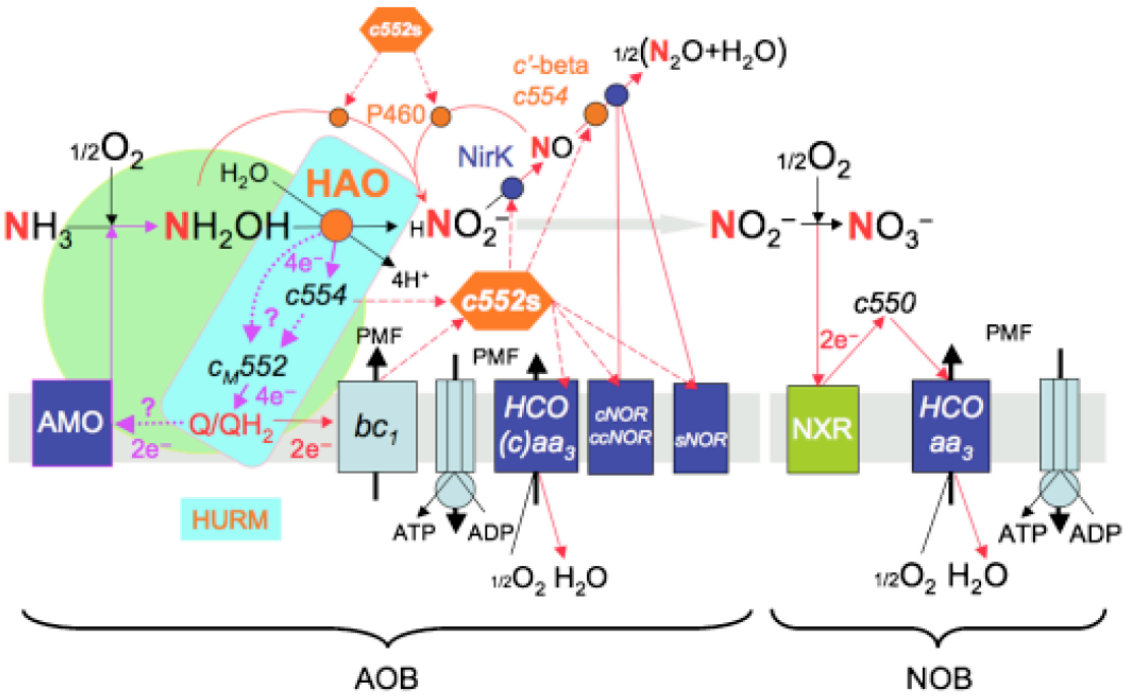

Figure 1.3. Schematic diagram illustrating the nitrification process by ammonia-oxidizing bacteria (AOB) and nitrite-oxidizing bacteria (NOB) at the cellular level. Solid lines represent experimentally verified reactions, dotted lines (with question marks) indicate lack of experimental verification of reactions. Abbreviation: HURM, hydroxylamine/hydrazine-ubiquinone-redox-module; (c)aa3, cytochrome (c)aa3; bc1, cytochrome bc1 (complex II); NirK, Cu-dependent nitrate reductase; c'-β, cytochrome c'- β; c550, cytochrome c552; c_M552, cytochrome c_M552; c554, cytochrome c554; NXR, nitrite oxidoreductase; P460, cytochrome P460; PMF, proton-motive force; Q/QH2, ubiquinone-ubiquinol pool; sNOR, cNOR, ccNOR, nitric oxide reductase with differing electron acceptor mechanasim. See text for more details. Figure taken from Klotz and Stein (2007).

1.2.1. Nitrification

In general, nitrification is a two-step aerobic oxidative process where NH_3/NH_4^+ is first oxidized to NO_2^- and subsequently NO_3^- by two different specialist prokaryotic groups, namely the ammonia oxidizing bacteria and/or archaea (AOA & AOB) and the nitrite-oxidizing bacteria (NOB) (van Kessel *et al.*, 2015) (Figure 1.2). The transformation of NH_4^+ to NO_2^- produces hydroxylamine (NH_2OH) which is one of the first several intermediates during nitrification. This transformation is catalyzed by the enzyme ammonium monooxygenase (AMO). The NH_2OH is then oxidized to NO_2^- by hydroxylamine oxidoreductase (HAO), and finally NO_2^- is oxidized to NO_3^- by nitrite oxydoreductase (NRX). Soil NO_3^- can be lost through leaching and/or can be transformed further to gaseous N (NO, N_2O, N_2) through denitrification. N_2O can be produced during nitrification as a result of decomposition of NH_2OH or reduction of NO_2^- to N_2O and N_2 via nitrifier-denitrification by autotrophic ammonia oxidizers (Wrage *et al.*, 2001; Zhu *et al.*, 2013).

1.2.2. Enzymes involved in nitrification

1.2.2.1. Key enzymes of AOB

NH_3 is utilized by AOB as the sole source of energy and the reductant requires four specialized proteins: AMO, HAO, cytochromes c554 and cM552 (Whittaker *et al.*, 2000; Arp *et al.*, 2007) (Figure 1.3). AMO is a membrane-bound hetero-trimeric copper enzyme encoded by three gene subunits, *amoA* (31.4 kDa), *amoB* (38 kDa) and *amoC* (31.4 kDa) (Ge *et al.*, 2015). HAO is located in the periplasmic space and composed of multi-c-heme and homotrimer (64 kDa) subunits (Arp *et al.*, 2002). This enzyme is encoded by the *hao* gene cluster (1710 bp). The AMO initiates NH_3 catabolism by oxidizing NH_3 to NH_2OH. Subsequently, the oxidation of NH_2OH to NO_2^- is catalyzed by HAO. As a result of the oxidation process catalyzed by HAO, four electrons are released which then follow a redox cascade via the two tetrahem cytochromes c554 and cM552 to the electron transport chain at the level of ubiquinone (Hooper *et al.*, 1997; Arp *et al.*, 2007). Among the four electrons that are released from the oxidation of NH_2OH by HAO, two are moved towards the oxidation of NH_3 in the next cycle and the remaining two are utilized for other reductant-requiring cellular processes, for example biosynthesis and ATP generation (Arp *et al.*, 2007). After generation of NO_2^- from the oxidation of NH_2OH by HAO, the NO_2^-

can be either transformed into NO_3^- through the NXR enzyme or it can be transformed into NO→ N_2O→ N_2 through the process of nitrifier-denitrification.

1.2.2.2. Key enzymes of NOB

NOB gain energy through the one-step oxidation process of NO_2^- to NO_3^- by the key enzyme NXR (Figure 1.3). NXR is a membrane-bound iron-sulfur molybdoprotein, which shuttles two electrons per oxidized NO_2^- into the electron transport chain (Meincke *et al.*, 1992; Lücker *et al.*, 2010). NXR consists of 3 subunits: NxrA (α), NxrB (β) and NxrC (γ) (Lücker *et al.*, 2010). The subunit NxrA is known as the substrate-binding site and is located in the periplasmic space in *Nitrospira* (Lücker *et al.*, 2010; Koch *et al.*, 2015), *Nitrospina* (Lücker *et al.*, 2013), and 'Candidatus Nitromaritima'(Ngugi *et al.*, 2016). However, in some bacteria (e.g. *Nitrobacter*, *Nitrococcus*, and *Nitrolancea*) NxrA is located in the cytoplasm (Spieck *et al.*, 1996; Starkenburg *et al.*, 2006; Sorokin *et al.*, 2012). The periplasmic NXR contributes proton motive force (PMF) (where the proton is derived from water) as part of the cell's energy budget whereas in the cytoplasmic NXR the protons do not contribute to creating a PMF (Lücker *et al.*, 2010; Daims *et al.*, 2016). The periplasmic NXRs are phylogenetically affiliated with the type II enzyme of the DMSO reductase family, whereas cytoplasmic NXRs are phylogenetically linked to nitrate reductase (NARs). It is proposed that two types of NXR evolved independently and likely spread by lateral gene transfer into different organisms, representing the large phylogenetic diversity of NOB (Sorokin *et al.*, 2012; Lücker *et al.*, 2010; 2013).

1.2.3. The role of microbes in nitrification

The nitrifiers are chemolithoautotrophic meaning they use chemical energy from nitrification to fix CO_2 as their source of carbon (C). Both AOB and AOA are involved in the oxidation of NH_3/NH_4^+. AOA are generally found in higher abundance in most soils compared to AOB, but their contribution to nitrification varies (Leininger *et al.*, 2006; Heil *et al.*, 2015). In nitrogen-rich grassland soils, the contribution of AOA is predicted to be small, despite being present in large numbers compared to AOB, suggesting that nitrification is mainly driven by bacteria rather than archaea with the application of ammonia substrate (Di *et al.*, 2009). This means that AOB gain comparative advantage over archaea in fertilized soils due to biochemical adaptation in high nutrient environment. On the other hand, archaea are comparatively better

adapted than bacteria in a low nutrient environment, or in extreme pH, or both (Valentine, 2007; Di *et al.*, 2009).

In addition, a phylogenetically wide range of heterotrophic bacteria and fungi oxidize NH_3 using two proposed pathways (De Boer and Kowalchuk, 2001; Heil *et al.*, 2015). In the first pathway, heterotrophic bacteria (e.g. *Paracoccus denitrificans*) use similar enzymes to their autotrophic counterparts (Moir *et al.*, 1996). Some nitrifying bacteria, for example *Thiosphaera pantotropha,* combine their nitrification activity with aerobic denitrification (Kuenen and Robertson, 1994). The second pathway is restricted to fungi and involves N compounds that react with hydroxyl radicals when hydrogen peroxide and superoxide are both present (De Boer and Kowalchuk, 2001). This process can occur during cell lysis and lignin degradation by fungi when oxidases and peroxidases are released into the environment.

1.2.4. Recent discovery in NOB

Recent studies suggest that some strains of NOB (e.g. *Nitrospira*) are complete ammonia oxidizers in a process termed 'comammox' (Daims *et al.*, 2016). Organisms able to carry out 'comammox' perform complete nitrification (e.g. $NH_4^+ \rightarrow NO_2^- \rightarrow NO_3^-$) as they harbor the full genetic complement for both ammonia and nitrite oxidation.

1.2.5. Factors affecting the nitrification process

Nitrification can be influenced by physical, environmental, chemical, and biological factors. The list of factors is shown in Table 1.

Table 1 List of factors that influence the nitrification process *(Sahrawat, 2008)*

Physical & environmental factors	**Chemical factors**	**Biological factors**
Substrate concentrations (e.g. urea, NH_4^+)	Soil pH	Microbial biomass
Soil matrix	Nutrient availability	Abundance and diversity of nitrifiers
Moisture content	C:N ratio	Soil respiration
Soil temperature		
Clay content		
O_2 availability		
Soil organic matter		
Soil management practices		

1.2.6. Denitrification

Denitrification encompasses a series of transformations performed primarily by a wide range of heterotrophic bacteria. This process is also known as a major microbial respiratory process that reduces the anionic form of N (NO_3^- and NO_2^-) to gaseous products of NO, N_2O and N_2 under anoxic conditions. A wide range of diverse microbial genes (mostly bacteria and fungi) are involved in this process ($NO_3^- \rightarrow NO_2^- \rightarrow NO \rightarrow N_2O \rightarrow N_2$) (Figure 1.1). For example, $NO_3^- \rightarrow NO_2^-$, is the first step of denitrification and is catalyzed by a nitrate reductase encoded by either *narG* or *napA* genes. The second step ($NO_2^- \rightarrow NO$) is catalyzed by a nitrite reductase which is encoded by one of two different genes (*nirS* and *nirK*). The third step ($NO \rightarrow N_2O$) is catalyzed by a nitrite reductase encoded by the *nor* gene (e.g. *cnorB*, *qnorB*). The final step in the denitrification process ($N_2O \rightarrow N_2$) is catalyzed by the nitrous oxide reductase (N_2OR) encoded by the *nosZ* gene. The N_2OR is the only known enzyme capable of reducing N_2O to N_2 (Jones *et al.*, 2013; Sanford *et al.*, 2012; Hu *et al.*, 2015). Recent studies show that *nosZ* is represented by two subtypes (clade I and II) each harbored by taxonomically distinct and non-overlapping groups of prokaryotes (Sanford *et al.*, 2012; Jones *et al.*, 2013). The *nosZ* (clade II) gene is comparatively more diverse compared to *nosZ* (clade I) gene. The major difference between *nosZ*I and *nosZ*II is secretory pathway (Tat vs. Sec) used to transport proteins across the cytoplasmic membrane. All *nosZ* (clade I) process the Tat (Twin-arginine translocation) pathway which catalyze the translocation of secretory proteins in their folded state, whereas *nosZ* (clade II) process the Sec pathway (i.e. general secretory pathway) which catalyze the translocation of secretory proteins in their unfolded state (Sanford *et al.*, 2012; Natale *et al.*, 2008). It should be noted that not all denitrifiers harbor the *nosZ* genes; for example, *Agrobacterium tumefaciens* and *Thauera* (some strains) lack the *nosZ* gene (Philippot *et al.*, 2011; Bakken *et al.*, 2012). This suggests that the process is modular – and that organisms may able to do part of the process i.e. they can lack any part of the chain but not just *nosZ*.

1.2.7. Enzymes involved in denitrification

Four different reductase enzymes are involved in the complete denitrification process (Figure 1.4). To understand this process at the cellular level we use *Paracoccus denitrificans* as a model organism for explanation.

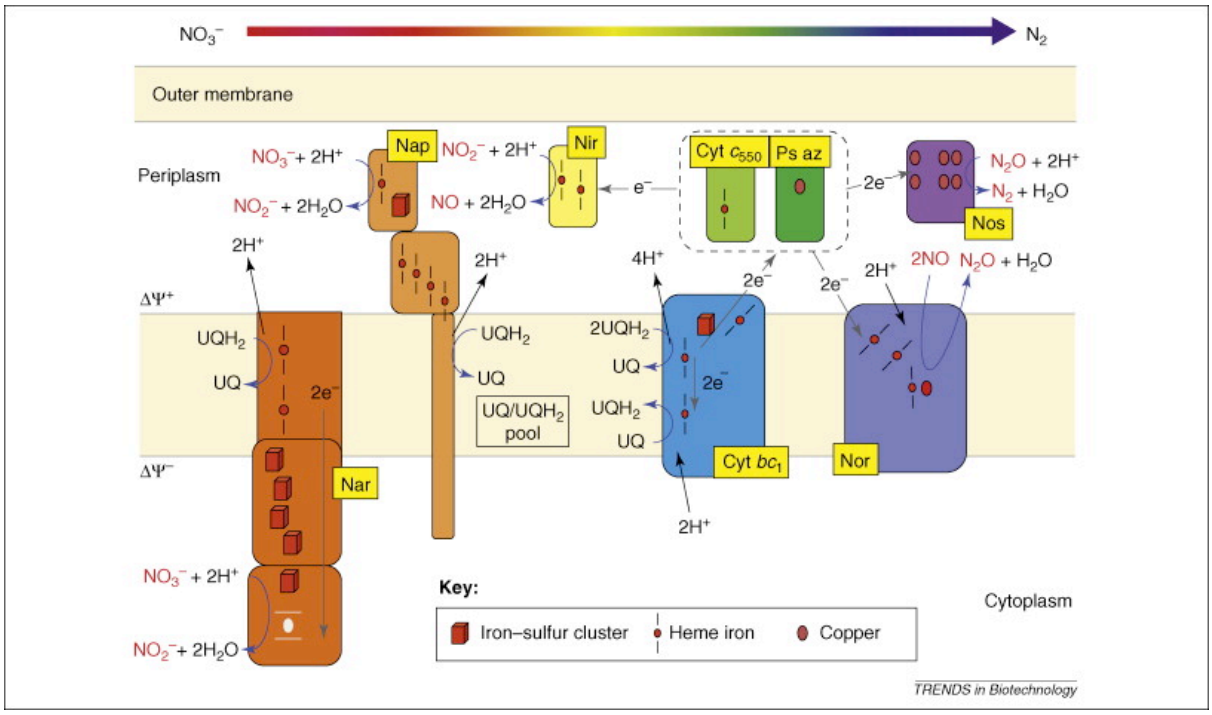

Figure 1.4. The schematic diagram illustrating the denitrification process at cellular level in *Paracoccus denitrificans*. Abbreviation: Nap & Nar, nitrate reductase; Nir, nitrite reductase; Nor, nitric oxide reductase; Nos, nitrous oxide reductase. Cyt c_{500}, Cytocrome c_{500}, Ps az, pseudoazurin. Figure taken from Richardson *et al*. (2009).

1.2.7.1. Nitrate reductase

Nitrate to nitrite is catalyzed by nitrite reductase according to the following reaction:

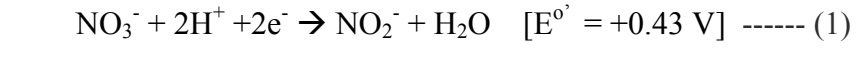

$$NO_3^- + 2H^+ + 2e^- \rightarrow NO_2^- + H_2O \quad [E^{o'} = +0.43\ V] \text{ ------ } (1)$$

There are two types of nitrate reductase: a periplasmic nitrate reductase, which is known as Nap, and a membrane-bound nitrate reductase, which is known as Nar (Figure 1.4). Nar has 3 subunits: *narGHI.* (Moura *et al.,* 2004). The catalytic site is encoded by *narG*. Nar receives electrons from ubiquinol (UQH_2) at the P-side (positive side) of the membrane. Two protons (2H+) discharge to the periplasm and two electrons (2e-) pass to the cytoplasmic membrane via the cofactor known as Mo-bis-MGD (Molybdenum-bis-molybdopterin guanine dinucleotide). The inward movement of e^- is equivalent to the transfer of H^+ from the cytoplasm to the periplasm which generates proton motive force (PMF) by a redox loop mechanism. The periplasmic nitrate reductase (Nap) is a heterodimer of two subunits (NapA (93 kDa) and NapB (16 kDa)), encoded by the *napEDABC* gene cluster (Berks *et al*., 1995). NapA also contains a Mo-bis-MGD cofactor which is similar to the co-factor of the membrane-bound nitrate reductase. The tetra-haem c-type cytochrome (NirC) is an electron-transfer component. The e- is transfered from the UQH_2 to NapA via NapC (Nicholls and Ferguson, 2013).

1.2.7.2. Nitrite reductase

Nitrite to nitric oxide is catalyzed by NO_2^- reductase which is located in the periplasm. The reaction is given below:

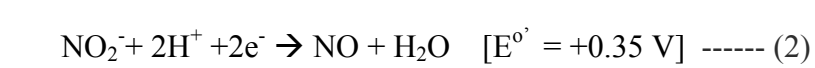

$$NO_2^- + 2H^+ + 2e^- \rightarrow NO + H_2O \quad [E^{o'} = +0.35\ V] \text{ ------ } (2)$$

There are two types of NO_2^- reductase: cytochrome cd_1 (both c- and d_1-type haem centers, cd_1Nir) and a copper containing NO_2^- reductase (CuNir). The cd_1Nir and CuNir are respectively encoded by the *nirS* and *nirK* genes (Zumft, 1997). Each of the nitrite reducers contains either *nirS* or *nirK* genes. (Coyne *et al*., 1989).

P. denitrificans harbors periplasmic NO_2^- reductase (cd_1Nir), which is a homodimer (approx. 65 kDa) and contains both c- and d_1-type haem centers. (Ohshima *et al*., 1993; Zumft, 1997). The c-type acts as an electron transfer center and the d_1-type acts as a catalytic center. The NO_2^- reductase can get electrons from cyt bc_1 via either a haem containing cytochrome C500 (Cyt c_{500}) or a copper containing pseudoazurin (Ps az) (Figure 3) (Moir *et al*., 1993).

Cu-containing CuNir is a homotrimer with two distinct Cu centers (type 1 Cu-center, T1Cu and type 2 Cu-center, T2Cu) in each monomeric unit (Godden *et al*., 1991; Howes *et al*., 1994). In general, T1Cu mediate electron transfer, and T2Cu act as active sites where substrate-binding and reduction take place (Howes *et al*., 1994)

1.2.7.3. Nitric oxide reductase (NOR)

NOR is a membrane bound enzyme that catalyzes the conversation of NO to N_2O. The reaction is given below:

$$2NO + 2H^+ + 2e^- \rightarrow N_2O + H_2O \quad [E^{o'} = +1.18\ V] \text{ ------ (3)}$$

There are 3 types of respiratory NORs (cNOR, qNOR, qCu_ANOR) reported from bacteria, but the best characterized NOR (cytochrome-c-dependent, cNOR) is the NorBC enzyme from *P. denitrificans,* which is a two-subunit complex (Field *et al*., 2008; Richardson *et al*., 2009). The NorC subunit (17 kDa) contains an N-terminal transmembrane helix that anchors to the periplasmic face of the cytoplasmic membrane. The NorC accepts electrons from two periplasmic electron donors: cytochrome C_{550} and pseudoazurin. The NorB (56 kDa) is a catalytic subunit which consists of 12 transmembrane helices (van der Oost *et al.*, 1994; Field *et al.*, 2008; Richardson *et al.*, 2009).

1.2.7.4. Nitrous oxide reductase (N_2OR)

The reduction of N_2O is only possible by the enzyme N_2OR which represents the last step of denitrification ($N_2O \rightarrow N_2$). This is the only known biotic sink for N_2O. The reaction requires two protons (H^+) and two electrons (e^-). See equation (4) (Zumft *et al*., 2006):

$$N_2O + 2H^+ + 2e^- \rightarrow N_2 + H_2O \quad [E^{o'}\text{ (pH 7.0)} = +1.35\text{ V}; \Delta G^o = -339.5\text{ KJ/mol}] \text{ ------ (4)}$$

This reaction shows high positive redox potential at pH 7, $E^{o'}$ = +1.35 V. N_2OR is a soluble enzyme which is usually located in the bacterial periplasm. The crystal structure of N_2OR is known from several denitrifier species: *Paracoccus denitrificans*, *Pseudomonas nautica*, and *Achromobacter cycloclastes*. All structures of N_2OR look virtually identical (Richardson *et al*., 2009); and they are homodimers and carry multi-copper ions in each monomer. Each monomer consists of two domains: a C-terminal cupredoxin domain (Cu_A) and an N-terminal seven-bladed beta-propeller domain (Cu_z) (Haltia *et al*., 2003). The Cu_z is known as an active site or a catalytic center, and electrons pass from Cu_A to Cu_z. The N_2O binds to the active site of Cu_z (between Cu1 and Cu4) which is suggested by a docking experiment and hence the reduction of N_2O occur by N_2OR (Haltia *et al*., 2003). The N_2OR can be inactivated when it is exposed to O_2. This is apparently due to the trap of cofactor Cu_z in a redox-inactive form of the state $[Cu_4S]^{3+}$(Rasmussen *et al*., 2002). The activity of N_2OR is also sensitive to the acidic environment (e.g. pH). This was tested in vitro analysis using methylviologen as an electron donor and showed more N_2OR activity at pH>7. A transcriptome study suggests that reduction of N_2O to N_2 is hampered due to posttranscriptional interference with the expression of *nosZ* (Liu *et al*., 2014). Therefore, the activation and deactivation of N_2OR in bacterial cells play an important role for the production and consumption of N_2O in soils or any other environments.

1.2.8. Factors affecting denitrification and N_2O emissions

Denitrification can be affected by physiochemical properties (e.g. pH, organic C, mineral N, aeration, and water content), field management practices (e.g. fertilization, liming, irrigation, and tillage) and even genetic potential (e.g. available of genes for denitrification) in soil. These factors can be classified into two groups: proximal and distal controls (Wallenstein *et al*., 2006). The "proximal controls" on denitrification are defined as environmental conditions and resources that affect immediate changes of denitrification rate and has less direct effects on denitrifier communities in long term. The proximal controls are pH, O_2, C availability, and temperature. Whereas the "distal controls" on denitrification are defined as those factors that control the diversity and composition of denitrifier communities over the long term (Figure 1.5). The distal controls include both environmental factors and biotic factors.

The availability of N as NO_3^- in soil can be one of the most important factors that regulate denitrification. The concentration of NO_3^- varies and depends on nitrification, N-mineralization, plant N uptake, microbial immobilization and NO_3^- leaching or diffusions (Tiedje *et al.*, 1980; Saggar *et al.*, 2013; Zaman *et al.*, 2007). The ratio of denitrification (N_2O:N_2) is also influenced by the availability of nitrate, where the higher concentration of NO_3^- influences the higher N_2O:N_2 ratio (Senbayram *et al.*, 2012; Firestone *et al.*, 1980).

The rate of denitrification can be influenced by available organic C. Denitrifiers are heterotrophs and they use organic C as an electron donor. With greater availability of organic C, there is an enhancement of denitrification rate under anoxic conditions (Reddy *et al.*, 1982; Burford and Bremner, 1975; McCarty and Bremner, 1992; Senbayram *et al.*, 2012)

Soil pH is considered an important factor that regulates the denitrification process; more importantly it regulates the emission ratio of N_2O. Denitrification can occur in wide range of pH. Soils with acidic pH have a significant negative relationship with the N_2O:N_2 ratio; hence, decreasing the pH leads to enhanced emission ratio of N_2O (Bakken *et al.*, 2012; Senbayram *et al.*, 2012; Liu *et al.*, 2014; Šimek and Cooper, 2002; Qu *et al.*, 2014). In contrast, the alkaline soils show more N_2 as the end product of denitrification which represents a low product ratio of N_2O

(Richardson *et al*., 2009). The probable reason is that under low pH conditions the activity of nitrous oxide reductase (N_2OR) enzyme is inhibited due to lack of enzyme assembly in the periplasm (Liu *et al.*, 2014).

Denitrification is an anaerobic process, hence, the availability of oxygen inhibits or represses the process (Knowles, 1982). Oxygen diffusion between soil and atmosphere depends on soil moisture which affects denitrification. In contrast, available oxygen can enhance the production of N_2O through nitrification, especially nitrifier-denitrification. It was demonstrated that AOB strain (in batch culture) contributed 11-26% and 43-87% of N_2O under 20% and 0.5% O_2 respectively as a result of nitrifier-denitrification (Frame and Casciotti, 2010).

There are other factors such as moisture content, temperature, soil type, soil management practices and genetic potentials (e.g. availability of functional genes for denitrification) that can affect the denitrification and N_2O emissions. Moisture content regulates the diffusion of oxygen in the soil which affects denitrification. In general, microbial growth is driven by temperature which controls denitrification. Different soil types (e.g. clay, loam and so on) have different components and can play an important role in denitrification.

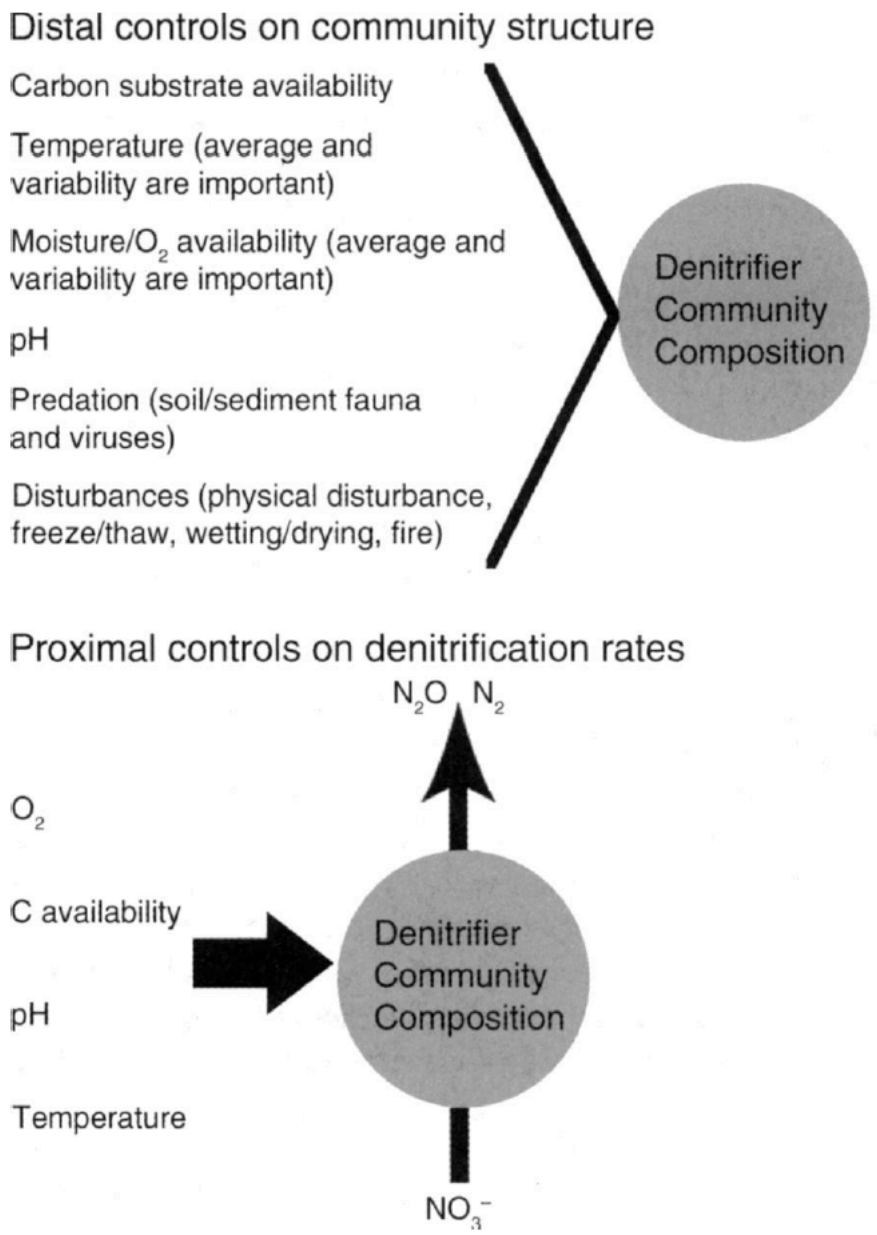

Figure 1.5. A conceptual schematic diagram of proximal and distal controls on denitrifiers and denitrification. Figure taken from Wallenstein *et al*. (2006).

1.3. How the urine patch is linked to N_2O emissions?

Pastoral agriculture is an important livestock production system where animals graze outdoor pastures. This is a traditional practice for livestock production in many parts for the world including New Zealand. In such a system, the dominant source of N_2O is animal excreta, particularly urine, that deposits to the soil during grazing. The rate of N deposition to the pasture soil from a single urination of a dairy cattle can be as high as 700-1000 kg N ha^{-1} (Di and Cameron, 2016). This N deposition from urine is mostly in the form of urea. Urea is hydrolyzed by urease enzyme and produced NH_3 (gas) and NH_4^+ ions. Most of the NH_4^+ (cation) can be retained or absorbed by negatively charged soil cation exchange complex, particularly soil clays and organic matter, despite some NH_3 loss through volatilization (Di and Cameron, 2016). The NH_4^+ leaching is negligible due to its high cation exchange capacity (CEC). However, NH_4^+ can be rapidly oxidized and produce NO_3^- as an end product through nitrification, followed by denitrification where consecutive reductions of NO_3^- to NO_2^- and gaseous products (NO, N_2O and N_2) is occurring. This process is also called coupled nitrification-denitrification, as the end product of NO_3^- or NO_2^- can be utilized for denitrification (Wrage *et al*., 2001). The details about nitrification and denitrification processes have been discussed in the earlier sections. The coupled nitrification-denitrification process should not be confused with the term of nitrifier-denitrification. Nitrifier-denitrification is a pathway of nitrification, where oxidation of NH_4^+/NH_3 to NO_2^- is followed by the reaction of NO_2^-, N_2O and N_2 (Wrage *et al*., 2001) (Figure 1.2). A recent study suggests that N_2O can be produced from NH_2OH by AOB (e.g. *Nitrosomonas europaea*) without following the nitrifier-denitrification pathway (Caranto *et al*., 2016).

1.4. Importance of microbial diversity for N_2O emissions

Denitrifiers are highly diverse and phylogenetically heterogeneous groups of microorganisms, mostly bacterial species from the phyla Bacteroides, Firmicutes, Actinobacteria, Chloroflexi, Verrucomicrobia, Aquificae and Proteobacteria (Philippot, 2002; Jones *et al*., 2013). They are also physiologically heterogeneous microorganisms including aerobic & anaerobic taxa, heterotrophs & autotrophs, nitrifiers, N_2-fixers, methylotrophs, thiosulfate oxidizers and even extremophiles (Butterbach-Bahl *et al*., 2013). Denitrifying bacterial communities can be tracked, for

instance, by *nirS* and *nirK* encoding NO-reductase that are highly diverse in soil and their abundance can be affected by soil types and soil management practices (Szukics *et al*., 2010). Another study demonstrated the abundance of *nirK* gene rapidly increased under wet conditions until the substrate (NO_3^-) was limited (Azziz *et al*., 2017). Changes in the community structure were observed in *nirK* and AOA, indicating dynamic populations, whereas distinct adaptation (i.e. changes in community structure appear after a certain period of time) of the AOB communities, indicating higher stability (Szukics *et al*., 2010).

Our knowledge about denitrification is mostly related to bacterial denitrification. However, some fungi can produce N_2O from NO_3^- and NO_2^- under anaerobic conditions. All strain of *Fusarium oxysporum* (except strain IFO 9967) produce N_2O from NO_2^- (Shoun *et al*., 1992). Some other fungi also exhibited denitrifying activities, for example, *Gibberella fujikuroi*, *Trichoderma hamatum*, *Cylindrocarpon tonkinense*, *Fusarium decemcellulare*, *Fusarium lini, Fusarium solani*, *Chaetomium* sp. and *Talaromyces flacus*. (Shoun *et al*., 1992). Still, our knowledge is limited about the overall contribution to N_2O emissions from fungi and their ecological role in pasture soils.

NO-reductase, encoding the *nirK* gene, has also been identified among extreme halophiles representing an archaeon (e.g. *Haloferax denitrificans*) (Inatomi and Hochstein, 1996). Archaea are widely distributed and highly abundant in soils (Leininger *et al*., 2006), although, little is known about archaeal denitrification in soils as they are difficult to culture. Ammonia oxidizing archaea (AOA) have a great importance in the nitrification process. Based on enrichment culture, it was reported that AOA may be a major source of the oceanic N_2O, (Santoro *et al*., 2011). Another isotopic study reported that N_2O can be produced by AOA (strains from soil) and followed two different pathways (i.e. ammonia oxidation and nitrifier-denitrification) (Jung *et al*., 2014).

The relationship between the functional genes of denitrification and N_2O emissions and microbial community composition is not well understood. The integration of knowledge about physicochemical, gas kinetics, functional genes, as well as microbial community composition, will help us to understand the role of denitrifier communities and their process for the production and reduction of N_2O in pasture soils.

1.5. Thesis outline

The overall aim of this study is to determine the N cycling process (i.e. denitrification and nitrification) in pasture soils to understand the emission potential of N_2O through the analysis of the edaphic factors, gas kinetics, the microbial community structure, and functional gene analysis. To date, significant progress has been made yet the following questions are still poorly addressed:

Denitrification profile of pasture soils:

- Which are the most important drivers of denitrification (and particularly potential N_2O emission) in pasture soils?
- Can we predict the denitrification rate based on the rate of C mineralization?

Microbial community profile and its link to pH and N_2O emissions:

- What is the role of microbial diversity and richness in terms of soil N_2O emissions?
- Are there any potential links between the abundance of denitrification genes with pH as well as N_2O emissions?

Urine patch kinetics profile of pasture soils:

- How do urine patches contribute to N_2O emissions in pasture soils?
- What is the potential relationship between oxic urine patch kinetics and anoxic nitrate-amended denitrification kinetics?

Microbial community dynamics under urine patches:

- How and which microbes respond to urine addition?
- What are the impacts of N deposition on microbial community dynamics at genome and transcription levels?
- What are the relative contributions of AOA and AOB under urine patches?
- What is the relative contribution of microbes at different taxonomic levels (Phylum to Species)?
- What are the microbial life strategies (growth vs. maintenance)?

This thesis has addressed the above questions completely or partially in the following chapters (Chapter 2 to 5). Each chapter is presented here as a manuscript format.

CHAPTER 2 | HIGH-RESOLUTION DENITRIFICATION KINETICS IN PASTURE SOILS LINK N_2O EMISSIONS TO PH, AND DENITRIFICATION TO C MINERALIZATION

Denitrification is a microbial mediated process where soils loose nitrogen as N_2O and/or N_2. The objective of this chapter is to determine the denitrification kinetics profile of 13 pasture soils (New Zealand and Ireland) and how the rate of denitrification is linked to C mineralization. The other objectives were to compare the effect of different soil pH and its relationship to the emission ratio of N_2O and N_2O index.

CHAPTER 3 | PHYLOGENETIC AND FUNCTIONAL POTENTIAL LINKS pH AND N_2O EMISSIONS IN PASTURE SOILS

Soil pH regulates the reduction of N_2O to N_2, however, it can affect microbial community composition and the N_2O emission ratio of pasture soils. This chapter is aimed to link phenotypes (Chapter 2) to genotypes (functional potential and community composition) in order to understand the relationship between pH, microbial diversity and N_2O emissions.

CHAPTER 4 | RUMINANT URINE PATCH REVEALS SIGNIFICANT SOURCES OF N_2O

This chapter focuses on the simulated urine patch kinetics under oxic conditions. Artificial urine was applied in 13 different pasture soils (same soils that were used in Chapter 2 & 3) under microcosm study. The objective of this chapter is to determine the N transformation process under oxic urine patch conditions and to compare its relationship with denitrification kinetics (Chapter 2 & 3).

CHAPTER 5 | RESPONSE TO URINE PATCH REVEALS METABOLIC AND ECOLOGICAL STRATEGIES OF SOIL BACTERIA

The nitrogen cycle represents one of the most well-studied processes in soil, yet taxonomic diversity is mostly unknown or linked to poorly characterized microbial populations. In this study, urea was applied to soil to mimic the ruminant urine

deposition event and its impact on microbial community composition in temporal scale. The hypothesis was that the changes in transcription, or population size, could serve to determine life strategies of microbes utilizing each intermediate (i.e. whether they are used for growth vs. maintenance).

CHAPTER 2

High-resolution denitrification kinetics in pasture soils link N_2O emissions to pH, and denitrification to C mineralization

Md Sainur Samad, Lars R. Bakken, Shahid Nadeem, Timothy Clough,

Cecile de Klein, Karl G. Richards, Gary J. Lanigan, Sergio E. Morales*

Article Published: PLoS ONE

Author Contributions: Authors are listed in order of magnitude of their contribution in each role. Corresponding author is indicated by an asterisk (*). Conceived and designed the experiments: SEM, LRB, MSS, CAMdK, TJC, KGR and GJL. Performed the experiments: MSS and SN. Analyzed the data: MSS and LRB. Contributed reagents/materials/analysis tools: SEM, LRB, CAMdK, TJC, KGR, GJL. Supervisory roles: SEM and LRB. MSS wrote the manuscript. MSS produced all figures and tables. All authors revised the paper.

Abstract

Denitrification in pasture soils is mediated by microbial and physicochemical processes leading to nitrogen loss through the emission of N_2O and N_2. It is known that N_2O reduction to N_2 is impaired by low soil pH yet controversy remains as inconsistent use of soil pH measurement methods by researchers, and differences in analytical methods between studies, undermine direct comparison of results. In addition, the link between denitrification and N_2O emissions in response to carbon (C) mineralization and pH in different pasture soils is still not well described. We hypothesized that potential denitrification rate and aerobic respiration rate would be positively correlated in soils. This relationship was predicted to be more robust when a high resolution analysis is performed as opposed to a single time point comparison. We tested this by characterizing 13 different temperate pasture soils from Northern and Southern hemispheres sites (Ireland and New Zealand) using a fully automated-high-resolution GC detection system that allowed us to detect a wide range of gas emissions simultaneously. We also compared the impact of using different extractants for determining pH on our conclusions. In all pH measurements, soil pH was strongly and negatively associated with both N_2O production index (IN_2O) and $N_2O/(N_2O+N_2)$ product ratio. Furthermore, emission kinetics across all soils revealed that the denitrification rates under anoxic conditions ($NO+N_2O+N_2$ µmol N/h/vial) were significantly correlated with C mineralization (CO_2 µmol/h/vial) measured both under oxic (r^2 = 0.62, p=0.0015) and anoxic (r^2 = 0.89, p<0.0001) conditions.

2.1. Introduction

Nitrous oxide (N_2O) is a potent greenhouse gas contributing 8% of anthropogenic global warming (Lesschen *et al.*, 2011; IPCC, 2007; Myhre *et al.*, 2013) and responsible for depleting stratospheric ozone (Ravishankara *et al.*, 2009). The N_2O molecule has a Global Warming Potential (GWP) 298 times higher than carbon dioxide (CO_2) over a 100-year period and an atmospheric life of approximately 121 years (Myhre *et al.*, 2013). In the atmosphere, N_2O has increased by 20% over the last 260 years (1750 to 2011) from 271 ppb to 324 ppb (Myhre *et al.*, 2013). Currently, the major anthropogenic source of N_2O is agricultural soils (Cole *et al.*, 1997; Paustian *et al.*, 2004). In these N_2O emitting soils denitrification is thought to be the most important pathway leading to N_2O loss (Mosier, 1998; Ostrom *et al.*, 2010), although a recent study showed that ammonia oxidation pathways and nitrifier denitrification are significant sources of N_2O and NO under low oxygen availability (Zhu *et al.*, 2013).

Denitrification is the stepwise process of reducing nitrate (NO_3^-) to N_2O or N_2, via nitrite (NO_2^-) and nitric oxide (NO). Four reductase enzymes catalyze the steps: nitrate reductase (NAR), nitrite reductase (NIR), nitric oxide reductase (NOR) and nitrous oxide reductase (N_2OR) (Regaert *et al.*, 2015; Bakken *et al.*, 2012). The key requirements for biological denitrification, and complete reduction of nitrate to N_2, can be summarized into two components: 1) the presence of microbes harboring the genetic ability to perform all the steps in denitrification, and 2) suitable environmental conditions for expression of the genetic potential. Changes in these two components can modify N_2O emissions from soils (Saggar *et al.*, 2013; Morales *et al.*, 2015). For example, some organisms (complete denitrifiers) contain all the genetic information needed to produce the four enzymes, while others (incomplete denitrification) lack a subset of the enzymes and can only catalyze portions of the denitrification process (Regaert *et al.*, 2015; Bakken *et al.*, 2012). Alternatively, changes in the concentration and ratio of electron donors (i.e. available organic carbon compounds), available terminal electron acceptors (e.g. NO_3^-, NO_2^-, NO or N_2O), and soil redox potential can modulate environmental conditions and thus the efficiency of denitrification in soils (Saggar *et al.*, 2013; Jahangir *et al.*, 2012). The addition of nitrogen fertilizers or manures increases denitrification rates especially when there is an adequate supply of carbon (Lampe *et al.*, 2006; Senbayram *et al.*, 2012). This is due to the fact that, denitrifiers require C to be readily available for reduction of NO_3^-

to occur (Senbayram *et al.*, 2012). The rate of C mineralization in soils is influenced by many factors (e.g. temperature, drying-wetting, tillage, liming, crop residues, fertilizer application, root exudates) and which ultimately have a major impact on the denitrification rate (Saggar *et al.*, 2013).

Known regulators can be difficult to assess in agricultural settings, and even more complicated to manipulate. An important factor that is more amenable for manipulation, and is a strong regulator of soil denitrification at both proximal and distal scales, is pH (Čuhel *et al.*, 2010). Soil pH is a key driver of the microbiological processes affecting N_2O and N_2 production (Regaert *et al.*, 2015; Saggar *et al.*, 2013), and influences the $N_2O/(N_2O+N_2)$ product ratio and N_2O production index of soils. Proximal control by pH implicates direct changes in N_2O-reductase activity, while distal control by pH implicates changes in the denitrifier community, which is an important component affecting N_2O emission rates (Čuhel *et al.*, 2010). The mechanisms producing such effects are not well understood however, recent findings based on gene transcription, protein expression and the kinetics of electron flow at the cellular level have provided promising clues. In the model organism *Paracoccus denitrificans,* environmental pH hinders the posttranslational assembly of a functional N_2O-reductase enzyme (Bakken *et al.*, 2012; ISO, 2005; Gawlik *et al.*, 2003). The inactivity of this enzyme results in the accumulation of N_2O, which in results in soils becoming net N_2O sources. Since soil pH can be controlled at field scales it represents a potential tool for mitigating N_2O emissions from soils, but integrating knowledge across studies is made complicated due to variations in methodologies, most commonly the type of extractant used for pH measurements. Several different extractants (e.g. water, $CaCl_2$ and KCl) are widely used for measuring soil pH (Bergaust *et al.*, 2011; Liu *et al.*, 2014). However, the KCl based pH measurement is less commonly used for agricultural soils because it's strong nature can alter the original properties of the sample being studied (Liu *et al.*, 2014) . This variability limits our capacity to integrate results over studies since the effects these changes can have on measurements are not fully understood.

Here we used a fully automated high-resolution GC detection system for measuring gas emissions under standardized oxic and anoxic conditions in order to assess factors linked to pasture soil N_2O emission and denitrification potential across soils representing both Northern and Southern hemispheres. Our objectives were: (1) to determine the denitrification kinetics of pasture soils, (2) to determine the effect changing methods (extractant type) for determining soil pH has on observed

relationship with N_2O flux, (3) to compare two methods of quantifying N_2O emissions from soils (an emission index and ratio), and (4) to investigate the relationship between denitrification and C mineralization in soils.

2.2. Materials and methods

Soil samples were collected (May 2014) from 13 different sites (Figure 2.1) in the Northern and Southern hemispheres: (Ireland- Moorepark, Johnstown, Solohead and New Zealand- Warepa, Otokia, Wingatui, Tokomairiro, Mayfield, Lismore, Templeton, Manawatu, Horotiu, Te Kowhai). Soil properties are presented in Table S2.1. Permission for sampling was not required or in the case of sites located on private land, owner permission was secured for sampling.

At each site multiple (>3) soil cores (25 mm diameter by 100 mm long, and excluding the grass layer) were collected and sieved to 2-4 mm, composited and immediately couriered to the Norwegian University of Life Sciences, Norway for analysis. Soil samples were stored at 4°C in the lab until analyzed (within one week).

2.2.1. Soil pH measurements

Soil pH was measured using three different extraction methods: i) deionized (DI) water, ii) 0.01 M $CaCl_2$ and iii) 2M KCl. All pH measurements were carrying out using a 10 ml soil sample (field moist) measured using a volumetric spoon and transferred to a plastic vial. The respective pH treatment solutions (DI water, 0.01 M $CaCl_2$ or 2M KCl) were added (25 ml) and the vials were sealed and then, mixed thoroughly by hand shaking for 1 minute and left to settle overnight. Immediately prior to measuring the pH, samples were shaken well and allowed to settle for 10 minutes. All pH measurements were done using an Orion 2-star pH Benchtop pH meter (Thermo Scientific) equipped with an Orion 8175BNWP electrode (Thermo Scientific).

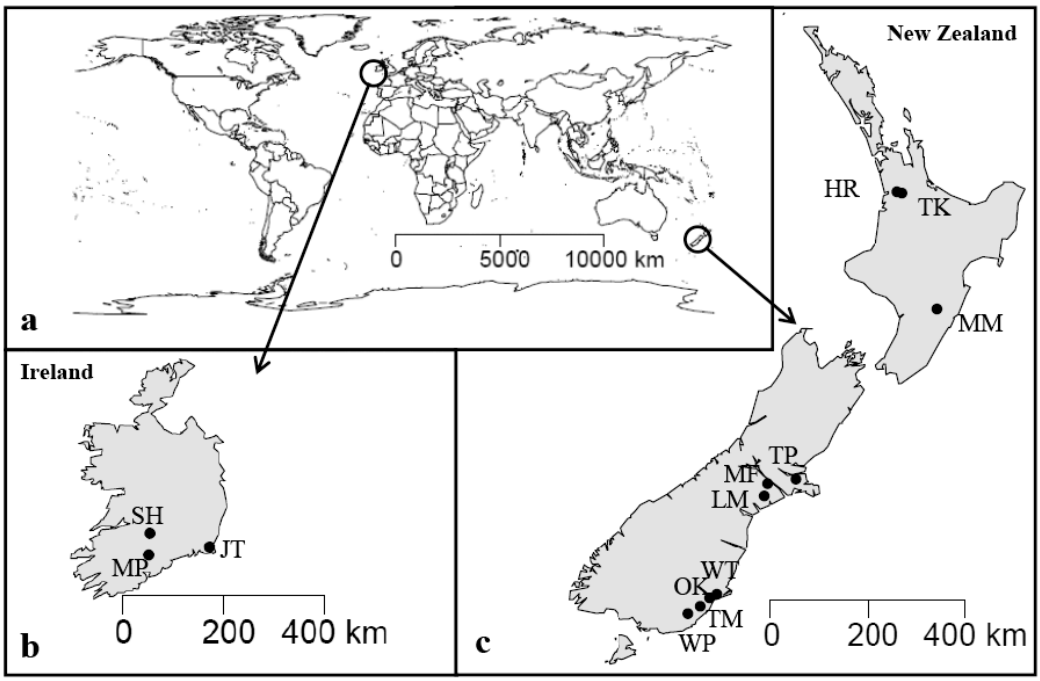

Figure 2.1. Geographical location of soil samples. Map showing origin of soil samples used in the study (a) world map, (b) Ireland [Moorepark (MP), Johnstown (JT), Solohead (SH)] and (c) New Zealand [Warepa (WP), Otokia (OT), Wingatui (WT), Tokomairiro (TM), Mayfield (MF), Lismore (LM), Templeton (TP), Manawatu (MM), Horotiu (HR), Te Kowhai (TK)]. The map was generated using open source "R-program (packages 'maps' and 'mapdata').

2.2.2. Nitrate adjustment

Individual soil samples (100 g dry weight) were placed in 500 ml filter funnels (Millipore) with 4.5 cm diameter (0.2 µm) Millipore membrane filters and subsequently flooded with a 2 mM NH_4NO_3 solution for 10 minutes. Samples were then drained using a vacuum in order to obtain a homogeneous distribution of NO_3^- in the soils. The moisture content of the soil samples was determined (dried overnight at 105°C) after draining and dry weight equivalents were used for subsequent gas kinetic experiments (Table S2.2). The cation exchange capacity (ECE) is different in all soils and its effect is not tested after addition of NH_4NO_3.

2.2.3. Gas kinetics under oxic and anoxic conditions

All incubations were performed using slightly modified methods described previously (Raut *et al.*, 2012; Qu *et al.*, 2014; Molstad *et al.*, 2007). In brief, following NO_3^- adjustment, 20 g (dry weight equivalent) of soil was transferred to a 120 ml serum vial and sealed with an airtight butyl-rubber septa and an aluminum crimp cap. Triplicate vials were prepared from each soil sample and incubated at 20 ^{o}C using an automated GC system (Molstad *et al.*, 2007). The GC (Agilent GC -7890A) system was equipped with three detectors (an electron capture detector (ECD), a thermal conductivity detector (TCD), a flame ionization detector (FID)) and one Chemiluminescence NOx analyzer (NOx analyzer Model 200A, Advanced Pollution Instrumentation, San Diego, USA). The GC system was integrated with an automated sampling robot (CTC GC PAL). All data presented were from experiments performed over two runs, which included independent standards for each run. Duplicates of four different gas standards were used in this experiment. All standards were prepared using evacuated vials (120 ml with septum) filled with commercially produced standard gases (supplied by AGA). Headspace samples (approx. 1 ml) were taken via needle and measured sequentially every 5 hours. The samples were incubated under oxic conditions for approx. 40 hours and subsequently incubated under anaerobic conditions for the remainder of the incubation (approx. 200 hours total). In order to create anoxic conditions, sampling vials were flushed and evacuated three times with high purity helium (He) gas, and over pressure was released from the vials before GC analysis.

2.2.4. Calculation of C mineralization and denitrification rates

Oxic respiration (i.e. oxic C mineralization) was calculated using the mean production rates of CO_2 (µmol/h per vial) within the first 40 hours when oxygen was present. Denitrification rates and anoxic C mineralization rates were calculated using the mean production rates of $NO+N_2O+N_2$ (µmol N/h per vial) and CO_2 (µmol/h per vial) respectively, within the first 40 hours following removal of O_2 by replacement of the headspace with helium.

2.2.5. Calculation of N_2O production index and (N_2O/N_2O+N_2) ratio

Characterization of N_2O emissions from each soil were done using two methods: 1) the N_2O production index (IN_2O) as described by Liu *et al*. (2010) and Qu *et al*. (2014) and 2) the N_2O product ratio (N_2O/N_2O+N_2) as described by Raut *et al*. (2012). Calculation of IN_2O was done using a 5 hours interval (i.e. 0 h – 5 h, 5 h – 10 h, 10 h – 15 h, and so on), while the $N_2O/(N_2O+N_2)$ ratio only took into account a single time point (i.e. 0 h, 5 h, 15 h, and so on). All soils were compared based on a 50 h anoxic incubation period for IN_2O. The $N_2O/(N_2O+N_2)$ ratio was calculated using the maximum value during the same 50 h period. Calculation of the N_2O production index (IN_2O) was done using the formula:

$$IN_2O = \int_0^T N_2O\,(t)\,dt / [\int_0^T N_2O\,(t) + \int_0^T N_2\,(t)]\,dt$$

where N_2O (t) is the accumulated flux of N_2O at any time t, N_2 (t) is the accumulated flux of N_2 at any time, and T is the time when a certain amount of NO_3^-- N g^{-1} soil is recovered as (NO_2^-, NO, N_2O and N_2)-N. Here we considered 50 h as T.

Linear regressions performed on JMP 10 (SAS Institute) were used to identify relationships between variables.

2.4. Results

2.4.1. Gas kinetics

Soil samples incubated under oxic conditions did not produce quantifiable amounts of NO, N_2O or N_2 after 40 h of incubation despite active respiration as determined by consumption of O_2 and production of CO_2 (Figure 2.2). Upon removal of O_2, immediate production of NO, N_2O and N_2 were detected. For all soils, NO and N_2O were converted to N_2, but the kinetics of the conversion varied. Accumulation of NO (mean ± SD) ranged between 100 ± 2.9 and 8390 ± 802 nmol N/vial, corresponding to Templeton and Lismore soils, respectively. While N_2O

accumulation ranged between 2.6 ± 0.5 to 56.5 ± 2.3 µmol N/vial, corresponding to Templeton and Horotiu, respectively.

2.4.2. IN_2O and $N_2O/(N_2O+N_2)$

The N_2O production index (IN_2O) and the $N_2O/(N_2O+N_2)$ product ratio were calculated based on the kinetics observed during anoxic incubation (Figure 2.3). Except for Solohead and Otokia, soil samples displayed higher IN_2O (approx. 10%) than $N_2O/(N_2O+N_2)$ with a mean value of 0.77 ± 0.27 and 0.67 ± 0.20 respectively (Fig S2.2). The Solohead soil had both the lowest N_2O production index (IN_2O = 0.02) and $N_2O/(N_2O+N_2)$ product ratio (0.23), while the Lismore soil had the highest (IN_2O = 1 and $N_2O/(N_2O+N_2)$ = 0.89). Values for IN_2O and $N_2O/(N_2O+N_2)$ were from all soils positively correlated (r^2 = 0.84 p<0.001).

2.4.3. Soil pH and N_2O emissions

Soil pH values were moderately acidic to neutral across all soils (Table S2.1). The pH measurements in the water-based method resulted in a wider range of values (5.57-7.03), while values for the KCl based method resulted in pH values clustered within the acidic range (4.40-6.39). The influence of soil pH on N_2O emissions was examined by comparing pH values obtained, with each of the different pH extraction methods, with the $N_2O/(N_2O+N_2)$ ratio and the IN_2O for all soils (Figure 2.4). Soil pH explained a significant proportion of the variation in relationship to IN_2O regardless of method used to determine pH (r^2 = 0.85 in DI H_2O; r^2 = 0.75 in $CaCl_2$; r^2 = 0.71 in KCl; p<0.05 all cases). Strong relationships (p<0.05) were also observed between pH and the $N_2O/(N_2O+N_2)$ product ratios regardless of soil pH extraction method (r^2 = 0.82 in DI H_2O; r^2 = 0.68 in $CaCl_2$; r^2 = 0.54 in KCl). Among the soil samples, one (Solohead) displayed very low N_2O emissions resulting in an outlier (Figure 2.4). To assess its impact, it was removed, and the IN_2O and $N_2O/(N_2O+N_2)$ ratio were recalculated and correlated to pH. Only the DI water-based pH measurement was significantly correlated, but the resulting r^2 was lower (In case of IN_2O and pH: r^2 = 0.62 p=0.0025 in DI H_2O; r^2 = 0.29 p=0.07 in $CaCl_2$; r^2 = 0.13 p=0.24 in KCl, and in case of $N_2O/(N_2O+N_2)$ product ratios and pH: r^2 = 0.69 p=0.0009 in DI H_2O; r^2 = 0.43 p=0.019 in $CaCl_2$; r^2 = 0.17 p=0.178 in KCl).

2.4.4. Links between denitrification and C mineralization

The rate of soil denitrification under anoxic condition ($NO+N_2O+N_2$ µmol N/h/vial) was significantly linked to the rate of C-mineralization (CO_2 µmol/h/vial) under both oxic (r^2 = 0.62, p=0.0015 and anoxic (r^2 = 0.89, p<0.0001) conditions (Figure 2.5).

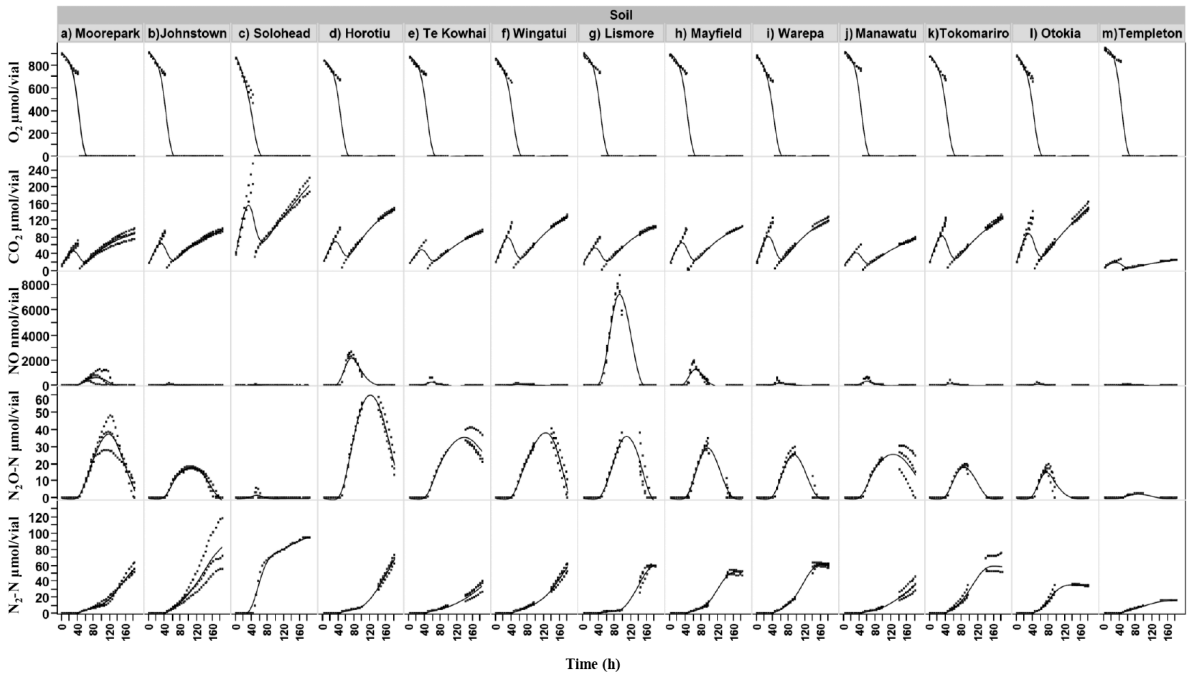

Figure 2.2. Gas kinetics profile of IR and NZ soils under oxic and anoxic conditions. O_2, CO_2, NO, N_2O and N_2 emission kinetics during incubation of 13 different temperate soils (3 Ireland (a,b,c) and 10 New Zealand (d to m)) amended with 2 mM nitrate (flooding and draining immediately before incubation). Soil samples (20 g dry weight) were incubated under oxic (first 40 hours) and subsequently anoxic conditions. Dots represent three replicate vials and smooth line is the fitted line for all data.

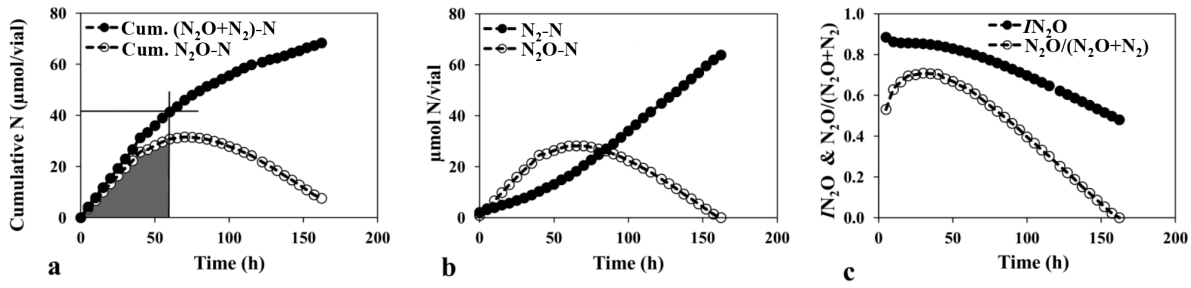

Figure 2.3. Demonstration of calculation of IN_2O and $N_2O/(N_2O+N_2)$. Representative curves for a) cumulative N accumulation, b) measured N, and c) N_2O production index (IN_2O) and $N_2O/(N_2O+N_2)$ product ratio over time for one soil (Moorepark). N_2O production indices were calculated as [$IN_2O = \int_0^T N_2O\ (t)\ dt / [\int_0^T N_2O\ (t) + \int_0^T N_2\ (t)]\ dt$]. Curves represent a single flask result. Each vial contained 20 g (dry weight) soil incubated in a 120 ml serum vial under anoxic conditions. Results for all other soils can be found in appendix section Fig S2.1.

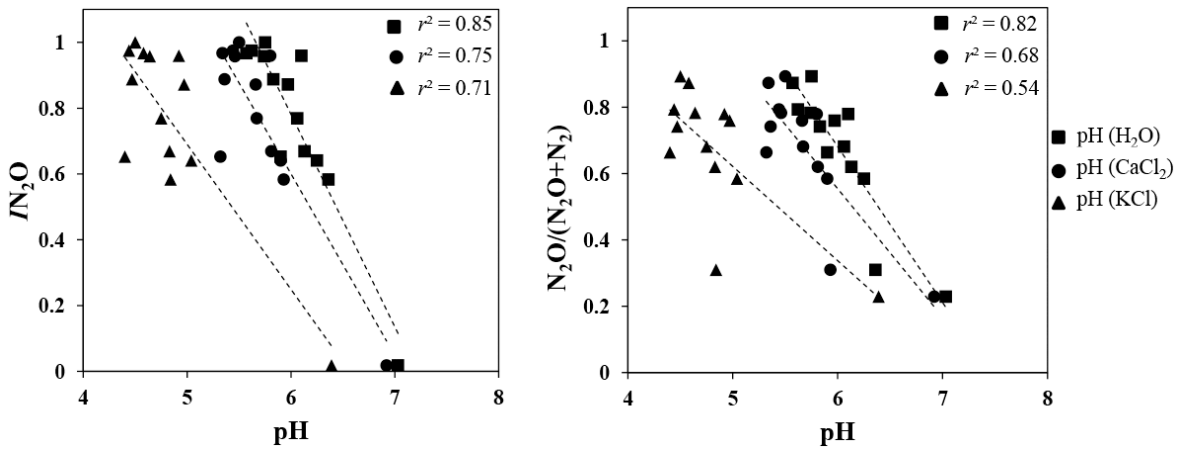

Figure 2.4. Relationship between pH and N_2O emissions. Effect of method (extractant type) for determining soil pH on correlation with (a) N_2O production index (IN_2O) and (b) $N_2O/(N_2O+N_2)$ ratio. Calculation of both index and ratio was based on N_2O emission within the curve (see Fig S1 for each sample) at 50 h under anoxic incubation. Soil pH was measured using three different extractants: i) DI water (■), ii) 0.01 M $CaCl_2$ (●), and iii) 2M KCl (▲). Dotted lines represent regression lines. Points represent the mean triplicate vials results.

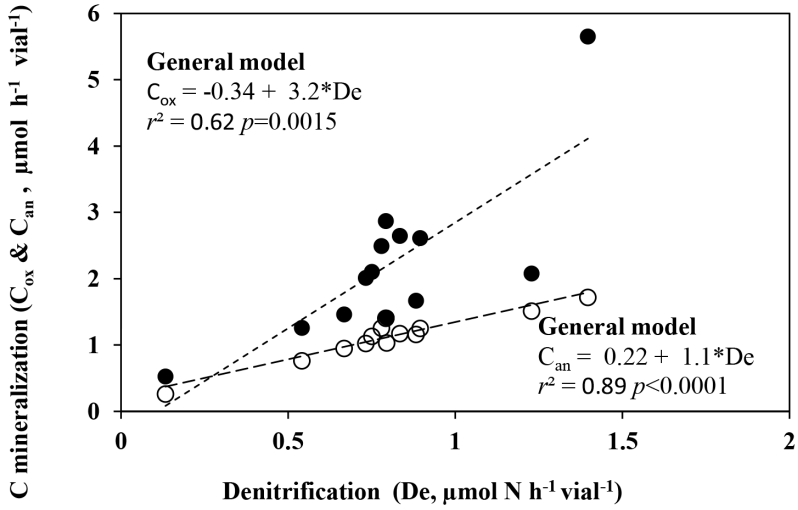

Figure 2.5. Links between denitrification and C mineralization. Relationship between C mineralization rate during both oxic [closed circles] and anoxic phase [open circles] and denitrification (De; i.e. production rates of $NO+N_2O+N_2$). Each point represents mean of triplicates. Linear regression function is shown for both oxic (C_{ox}) and anoxic (C_{an}) C mineralization.

2.5. Discussion

It is known that soil pH plays a strong role in regulating the loss of N gases (Mørkved *et al.*, 2007). One problem with understanding the pH effect on N_2O emissions is consolidating the many studies done to date, and their sometimes-conflicting observations (Šimek and Cooper, 2002). Here we tested soil pH using the three most commonly used extractants and found that soil pH measurements vary across all three extractants (approx. 1-2 units within pH range) (Figure 2.4 and Table S2.3). This is likely due to the differences in protons (H^+) and hydronium ions (OH^-) attracted to exchange sites for each buffer, which causes an electrical potential to develop. Although the different pH extractants yield different soil pH values, the relative ranking of the soils from highest to lowest pH was entirely conserved across all extractants. Thus absolute values of soil pH across studies will be hard to compare but their relative placement within a gradient (higher vs. lower pH) can be used to compare results across independent studies. Evidence in the literature supports the claim for reduced N_2O reduction and denitrification in low pH systems (Raut *et al.*, 2012; Firestone *et al.*, 1980), leading to the N_2O production index being strongly correlated with pH (Qu *et al.*, 2014; Liu *et al.*, 2010). The underlying mechanisms involved in the pH control over N_2O emission have begun to be unraveled in part by the use of model organisms, including *Paracoccus denitrificans.* Recent work demonstrated that the relative activity of the N_2O reductase enzyme decreased with lowering of the pH. This decrease in activity was associated with a post-transcriptional effect wherein the assembly of the N_2OR enzyme was inhibited by low pH (ISO, 2005). However, further work showed that when N_2OR was expressed at pH 7.0, it remained functional over the entire pH range tested (5.7 to 7.6), suggesting that the role of pH is specific to the folding of the protein upon expression (Gawlik *et al.*, 2003). It is important to understand that although pH in this scenario plays a role as a proximal regulator, it can also play a role as a distal regulator as well by controlling community composition (Rousk *et al.*, 2010) making interpretation complicated.

Independent of the methods used to measure soil pH or the mechanism controlling the pattern, we observed that the IN_2O was higher than the $N_2O/(N_2O+N_2)$ ratio in each soil sample (except for Solohead and Otokia soils). This is likely due to the fact that the IN_2O takes into account a time period (the emission occurring between two given time points), as opposed to single time points as used in the

$N_2O/(N_2O+N_2)$ ratio calculations. As seen in the kinetic profiles (Figure 2.3), the shape of the curve is not always similar and although heights (i.e. maximum values) might be similar, a gentler slope (i.e. slower but more prolonged rates) can lead to an extended period of emissions not accounted for by height alone. The fact that $I N_2O$ and $N_2O/(N_2O+N_2)$ were strongly correlated (r^2= 0.84) suggests that both parameters can be used as a measure of the soils' contrasting propensities to emit N_2O. As the N_2O production index ($I N_2O$) is calculated using at least two time points and the area under the curve, it is possibly the best predictor of the propensity of the soils to emit N_2O, as dependent on the ability of the denitrifying community to express N_2O reductase. It cannot be taken as a direct predictor of N_2O emission to the atmosphere under field conditions, primarily because the fraction of denitrification products lost to the atmosphere as N_2O depends on soil moisture content; high soil moisture content retards N_2O diffusion and hence increases the fraction of N_2O reduced to N_2.

Aside from pH, O_2 is also a known 'master' regulator of denitrification. Soil samples in this study were incubated in two phases (oxic and anoxic). During the oxic phase, microbial respiration was active as determined by monitoring of the CO_2 produced but there were no emissions of NO, N_2O or N_2. However, upon removal of O_2, emissions of NO, N_2O and N_2 were observed in all soil samples independent of pH. This confirms prior work (Raut *et al.*, 2012; Qu *et al.*, 2014; Liu *et al.*, 2010) indicating that in the hierarchy of regulators of denitrification, O_2 serves as a primary control with pH serving a secondary role, not in controlling the rate of denitrification but the kinetics of the product ratio. Both measurements of emission potential ($I N_2O$ and $N_2O/(N_2O+N_2)$) are strongly related to soil pH (r^2 = 0.53 to 0.85) transient accumulation of N_2O.

In both oxic and anoxic conditions, the C mineralization rates (CO_2 production) for all soils provide an indirect indication of denitrification rates, and serve as a good proxy for predicting N cycling activity (Figure 2.5). Oxic respiration rates (or C mineralization) were 3.2 times higher than the rates of denitrification, likely due to the larger pool of organisms capable of carrying out this general process. When the anoxic C mineralization rate was compared to the rate of denitrification, a strong relationship (r^2 = 0.89) was observed, suggesting that denitrification was the dominant pathway for energy generation and responsible for respiration from the selected soils under the experimental conditions. This is expected given the conditions used in this study favor denitrification, and its

intermediates represent the most energetically advantageous alternative electron acceptor. However, we observed that C mineralization rates under anoxic conditions were 10% higher than denitrification rates, which may be due to fermentation process and/or the presence of other alternative electron acceptors in soils (e.g. Fe^{2+}, Mn^{2+}, SO_4^{2-}, etc.). Apart from microbial respiration and fermentation, another probable source of CO_2 is from inorganic carbonate (e.g. lime). As denitrification rate is strongly associated with the production rate of CO_2 under anoxic conditions, therefore, this may indicate that the sources of CO_2 is mainly from C mineralization.

Although measures like C mineralization and denitrification rates, $/N_2O$ and $N_2O/(N_2O+N_2)$ allow us to assess the impact of potential regulators, as well as providing easy comparison to prior work, they do not convey all the differences observed. By using a continuous monitoring system, we observed that the gas emission profile (kinetics) (i.e. the production and consumption of the gas intermediates in denitrification) of pasture soils varied greatly across all soils. Some soils (e.g. Lismore, Horotiu, Mayfield and Moorepark) were more prone to producing NO compared to others, but the profiles generated could not be summed based on a single gas. The data generated from these 13 soils suggests that our inability to accurately predict emissions is in part due to the uniqueness of each soil, which is reflected here in their unique gas profiles. Soils such as the Solohead soil would likely generate results that are difficult to interpret based on single time point measurements due to its kinetic profile (extremely fast rates of almost all measured variables). Despite these difficulties, certain conclusions can be made. Soil pH is one of the most important soil factors affecting the denitrification products (i.e. N_2O or N_2). Here we showed that differences in extractants for measuring pH could account for discrepancies in observations across prior studies. However, a consistent trend of increased N_2O emissions with lowering pH was observed independent of pH extractants. Further, two approaches for representing emissions ($/N_2O$ than $N_2O/(N_2O+N_2)$) were examined and shown to be positively correlated, providing alternatives for reporting emissions. Finally, as denitrification rate is closely related to soil C mineralization, therefore C mineralization could be used as an indirect tool for predicting the denitrification rate of NO_3^- amended pasture soils.

CHAPTER 3

Phylogenetic and functional potential links pH and N_2O emissions in pasture soils

Md Sainur Samad, Ambarish Biswas, Lars R. Bakken, Timothy J. Clough, Cecile A. M. de Klein, Karl G. Richards, Gary J. Lanigan, Sergio E. Morales*

Article Published: Scientific Reports

Author Contributions: Authors are listed in order of magnitude of their contribution in each role. Corresponding author is indicated by an asterisk (*). SEM, MSS, LRB, CAMdK, TJC, KGR and GJL designed the experiments. MSS, CAMdK, TJC, KGR and GJL collected samples and processed. MSS, AB, SEM and LRB analyzed the data. SEM and LRB had supervisory roles. MSS produced all figures and tables. MSS and SEM wrote the manuscript. All authors revised the paper.

Abstract

Denitrification is mediated by microbial, and physicochemical, processes leading to nitrogen loss via N_2O and N_2 emissions. Soil pH regulates the reduction of N_2O to N_2, however, it can also affect microbial community composition and functional potential. Here we simultaneously test the link between pH, community composition, and the N_2O emission ratio ($N_2O/(NO+N_2O+N_2)$) in 13 temperate pasture soils. Physicochemical analysis, gas kinetics, 16S rRNA amplicon sequencing, metagenomic and quantitative PCR (of denitrifier genes: *nirS, nirK, nosZI and nosZII*) analysis were carried out to characterize each soil. We found strong evidence linking pH to both N_2O emission ratio and community changes. Soil pH was negatively associated with N_2O emission ratio, while being positively associated with both community diversity and total denitrification gene (*nir* & *nos*) abundance. Abundance of *nosZII* was positively linked to pH, and negatively linked to N_2O emissions. Our results confirm that pH imposes a general selective pressure on the entire community and that this results in changes in emission potential. Our data also support the general model that with increased microbial diversity efficiency increases, demonstrated in this study with lowered N_2O emission ratio through more efficient conversion of N_2O to N_2.

3.1. Introduction

The Anthropocene has resulted in a loss of global biodiversity and enhanced greenhouse gas emissions (Vitousek *et al.*, 1997). A major driver of change has been the transformation of land for agriculture purposes, needed to sustain the expanding global populations (Tilman *et al.*, 2002). These changes are expected to drive further reductions in biodiversity and the loss of associated ecosystem services (Tilman *et al.*, 2001). Of the greenhouse gases associated with agriculture, nitrous oxide (N_2O) is of particular concern due to its global warming potential (> 300 times more powerful as CO_2) and ozone-depleting capabilities (Robertson, 2000; Ravishankara *et al.*, 2009; Pachauri *et al.*, 2014; Tian *et al.*, 2016).

The mechanisms that control N_2O production and loss from soils are still being debated, with identified regulators comprising physical, chemical and biological factors (Saggar *et al.*, 2013). Soil pH has been identified as a master regulator of gaseous N emissions, with the propensity of soils to release N_2O over N_2 tightly linked to this (Samad *et al.*, 2016a). Two mechanisms have been proposed for explaining the role of pH: i) a distal impact on the genetic potential in soils through re-arrangements of the microbial community and ii) a proximal impact driven by modulation of the direct reactions catalyzing the conversion of N_2O to N_2 by microbial enzymes (Wallenstein *et al.*, 2006). However, emissions of N_2O are controlled at multiple levels: i) the available genetic potential within the soil microbial community (genotype) (Braker and Conrad, 2011), ii) the activation or de-activation of the potential in response to an environmental signal (transcriptional regulation controlling expression of genotype) (Kern and Simon, 2015; Qu *et al.*, 2016), iii) the translation of transcripts leading to an immature or apoprotein (translational regulation) (Dreusch *et al.*, 1997), iv) maturation of a protein resulting in an active enzyme (post-translational regulation) (Dreusch *et al.*, 1997), v) export of enzymes when activity is not cytoplasmic (e.g. sec / tat dependent secretion as is the case for *NosZ*) (Bernhard *et al.*, 2000; Heikkilä *et al.*, 2001; Simon *et al.*, 2004), and vi) degradation or turnover rate of enzymes once active (Vogel and Marcotte, 2012). These controls cover both the production of N_2O and the consumption, or turnover, into N_2 by a different process. As a result emissions are limited by what may be summarized as: i) genetic potential, ii) transcriptional regulation, and iii) enzymatic activity. The outcome is a complex array of regulators and processes that are likely to change across time and space.

Despite the complexity, observations support the role of both distal and proximal regulators (Philippot *et al.*, 2011; Bakken *et al.*, 2012). Distal impacts by pH are proposed to be driven by selecting for community shifts at both functional and phylogenetic levels (Morales *et al.*, 2015) with shifts in available potential (functional gene abundances) resulting in shifts in phenotypes (observed emissions) (Nishizawa *et al.*, 2014; Shiina *et al.*, 2014). Proximal impacts by pH provide a clearer mechanism. Low pH causes a shift in active organisms (Brenzinger *et al.*, 2015), but more importantly pH disrupts the activity of the N_2O reductase by interfering with assembly (Bergaust *et al.*, 2010; Liu *et al.*, 2010; 2014). Although evidence supports the role of pH in regulating emissions and community structure (Nicol *et al.*, 2008; Lauber *et al.*, 2009; Čuhel *et al.*, 2010; Rousk *et al.*, 2010) studies linking all three remain sparse.

An additional consideration is the role of biodiversity in supporting ecosystem processes like N (nitrogen) cycling. It has been proposed that biodiversity is a universal regulator of ecosystem processes (Tilman, 1999). Although microbial studies that support the role of microbial diversity in controlling productivity (Ptacnik *et al.*, 2008; Schnitzer *et al.*, 2011), N cycling (Griffiths *et al.*, 2000; Wertz *et al.*, 2006; Wittebolle *et al.*, 2009) and even N_2O emissions (Wagg *et al.*, 2014) exist, these rely on single manipulated soils or small sample sizes. However, such studies serve to establish a hypothesis that aligns with ecological theory. That is, with increasing diversity there is increased redundancy and efficiency of ecosystem processes (Loreau *et al.*, 2001; Tilman *et al.*, 2014). This has been observed in some microbial studies (Griffiths *et al.*, 2000; Levine *et al.*, 2011), including those associated with N_2O emissions (Domeignoz-Horta *et al.*, 2015), while others showed no direct effects (Griffiths *et al.*, 2001; Wertz *et al.*, 2006). However, a detailed study linking gaseous emissions (NO, N_2O and N_2), pH and microbial diversity, over soils with varying parent materials and climates, is lacking.

In this study we aimed to link phenotypes (emission potential) to genotypes (functional potential and community composition) across 13 soils with varying pH (5.57 - 7.03) representing both Northern and Southern Hemisphere soils. These soils were selected as they represent the normally observed pH range in agronomic grasslands (recommended pH optima = 6.2-6.5). Using this dataset our goal was to simultaneously explore the relationship between pH, diversity and emissions. We hypothesized that the effect of pH on emissions would be linked to changes in whole communities, and not solely to denitrification functional potential. To test this, we

quantified the abundance of genes involved in denitrification using quantitative PCR and metagenomic analysis, and examined their relationship with the emissions potential (N_2O ratio = $N_2O/(NO+N_2O+N_2)$). We also determined the microbial community composition and diversity of each soil and identified patterns linked to both changes in pH and emissions.

3.2. Materials and Methods

3.2.1. Sample collection and processing

Soil samples used in this study and their physio-chemical properties have been described previously (Samad *et al.*, 2016a). Soils were selected to represent intensive agricultural grasslands with a representative pH range close to the agronomic optimum of 6.5. Briefly, soil samples were collected from 13 permanent grasslands (managed agricultural) sites in Ireland (Johnstown, Moorepark, Solohead) and New Zealand (Horotiu, Lismore, Manawatu, Mayfield, Otokia, Te Kowhai, Templeton, Tokomairiro, Warepa, Wingatui), representing Northern and Southern hemisphere sites. Soil cores (n>3) were collected randomly from each site using a corer (25 mm diameter by 100 mm long), and excluded the grass layer. For each site, replicate cores were sieved to <4 mm, composited and immediately shipped to the Norwegian University of Life Sciences, Norway for analysis. Soil samples for kinetics were stored at 4°C in the lab until analyzed (within one week). Soils for DNA extraction were immediately frozen and stored at -20°C until extracted. Three separate DNA extractions were performed from 0.25 g of soil material from each site (total 39) with the PowerLyzer® PowerSoil® DNA Isolation Kit (MoBio, Carlsbad, CA) as per manufacturer's instructions. DNA concentration, purity and contamination with humics were assessed with a Nanodrop Spectrophotometer, ND-1000 (Thermo Scientific). DNA yields ranged between 8-21 ng/µl (median = 13; standard error = 0.6) with no detection of humic acids (median absorbance at 320nm = 0.008; standard error = 0.0010) indicating high quality extractions.

3.2.2. Gas kinetics

Gas kinetics methods were described in detail in Samad *et al.*, 2016 (Samad *et al.*, 2016a). Briefly, soils (100 g dry weight) were provided with nitrate (2 mM NH_4NO_3) by flooding in 500 ml filter funnels (Millipore) with 4.5 cm diameter (0.2 µm)

Millipore filters at least three times for 10 minutes. To obtain a homogeneous distribution of NO_3^- and to remove excess liquid from soils a vacuum was applied. After NO_3^- adjustment, 20 g (dry weight equivalent) of each soil was transferred to a 120 ml serum vial and sealed with an air-tight butyl-rubber septa and an aluminum crimp cap. For each site triplicate vials were prepared and incubated at 20°C using an automated GC system (Molstad *et al.*, 2007). The soils were first incubated for 40 h under oxic conditions and then incubated under anoxic conditions for over 200 h. The emission of NO, N_2O and N_2 were measured at 5 h intervals under anoxic conditions. The product ratio of N_2O (i.e. $N_2O/(NO+N_2O+N_2)$) was calculated and the maximum value observed during incubation for each soil was used. The maximum value represents the highest potential of each soil to emit N_2O. While NO_3^- concentrations are likely to see a small increase due to nitrification of the added NH_4^+ (NH_4NO_3) during oxic incubation, resulting in soil-to-soil differences in available NO_3^- at the beginning of the anoxic incubations, these differences are unlikely to affect the kinetics of denitrification (and the product ratios) since the NO_3^- concentration applied (2 mM) was 2-3 orders of magnitude higher than *Ks* for NO_3^- reductases (Hassan *et al.*, 2016). Further, wetting of soils did not result in emissions with kinetics only measurable in the presence of exogenously added N.

3.2.3. Quantification of bacterial community and functional gene abundance

Quantitative PCR (qPCR) was performed on all 39 extractions to determine total bacterial abundance and the abundance of four denitrification functional marker genes (*nirS, nirK, nosZ* (Clade I) & *nosZ* (Clade II)) in each soil. Reactions were performed in 96-well plates using the ViiA7 real-time PCR system (Applied Biosystems, Carlsbad, CA). Standards for qPCR were generated using a 10-fold serial dilution (10^8 to 10^1) of known copy numbers of pGEM-T easy (Promega, Madison, Wisconsin, USA) cloned template (i.e. specific genes [*nirS*, *nirK, nosZ*I, & *nosZII*] were inserted in the cloning vector). All quantifications were performed using 4 technical replicates for each DNA sample loaded into the same plate, with each plate containing replicated standards and no template controls (PCR efficiencies shown in Supplementary Table S3.1. Amplification of *nosZ* Clade II and *nirK* targets was not possible with multiple tested polymerase brands even after optimization. As a result, two different master mixes (ABI and Thermo Scientific) were used as specific below. All reactions were performed in 20 µl volumes containing: 1× Master

Mix (ABI for *nirS* & *nosZ*I or Thermo Scientific for *nirK* & *nosZII*), 0.5-1 µM of each primer (0.5 µM for *nirS* & *nosZ*I and 1µM for *nirK* & *nosZII*), 5 ng of template DNA and autoclaved Milli-Q H_2O to a final volume of 20 µl. Primers and qPCR conditions are summarized in Supplementary Table S3.1. A melt curve analysis (95°C for 15 s, 60°C for 1 min then increasing 0.05^{o}C/s (data acquisition) until 95°C) was performed at the end of reactions to test for specificity and to confirm no amplification in the negative control. No inhibition was observed and all samples tested amplified.

3.2.4. Analysis of 16S rRNA gene by amplicon sequencing

16S rRNA gene libraries were created for each DNA extraction using bacterial/archaeal primers 515F/806R targeting the V4 region of the 16S rRNA gene. Library preparation and sequencing were conducted according to the standard protocol (Version 4_13) of the Earth Microbiome Project (Caporaso *et al.*, 2012) and libraries were paired-end sequenced using the Illumina MiSeq platform. Preliminary processing was carried out in Qiime (version 1.9.0) using default parameters (Caporaso *et al.*, 2010). Sequences were clustered into Operational Taxonomic Units (OTUs) at 97% sequence similarity using the SILVA version 119 reference library (Quast *et al.*, 2012) and UCLUST (Edgar, 2010). Taxonomic classification was assigned using BLAST analysis against the SILVA database (Altschul *et al.*, 1990). Samples were then rarified and randomly subsampled 10 times (using the Qiime command 'multiple_rarefactions_even_depth.py') to equal depths (16,000). Samples below that threshold (1) were removed for a total of 38 samples retained. All 10 OTU tables per sample were subsequently merged and exported for processing in R. All downstream analysis were performed in R (R Development Core Team, 2008) and described in detail in supplemental information. The 16S rRNA amplicon sequences were summited to NCBI, SRA database (SRA accession: SRP080971).

3.2.5. Metagenomic sequence analysis

Six sites (Ireland: Johnstown, Moorepark, Solohead and New Zealand: Horotiu, Lismore, Templeton) representing a range of emission profiles from each country were selected for metagenomic analysis. Libraries for each metagenome were generated using the Illumina Nextera XT library preparation kit. Duplicate

MiSeq 2 X 250 base paired end runs were carried out for each of the 6 samples. Sequences were submitted to and annotated using the MG-RAST server (Meyer *et al.*, 2008). Metagenomic data is available through the MG-RAST server (ID numbers 4644147.3 to 4644142.3). Sequence counts ranged from 2,634,050- 4,851,047 before quality control. Sequences were classified taxonomically using the SILVA SSU ribosomal databases and functionally using KEGG with default settings.

3.2.6. Metagenome quantification of nosZI and nosZII

To differentiate between Clade I and II variants of the *nosZ* gene, a total of 1463 sequences annotated as being *nosZ* using the KO (KEGG Orthology) database were retrieved from the metagenomic libraries in our study. In order to classify them based on clade and to provide a taxonomic placement a reference database was generated. NosZ amino acid sequences were downloaded from the FunGene database (Fish *et al.*, 2013) and classified as Clade I (*nosZI* [PRK02888;Tat dependent]) or Clade II (*nosZI* [nitrous_nosZ_Gp; Sec dependent]) based on conserved protein domains using CD-Search (Marchler-Bauer and Bryant, 2004). Classification was confirmed by detection of signal peptides using the PRED-TAT algorithm (Bagos *et al.*, 2010). Taxonomy for each reference sequence was retrieved from NCBI using accession numbers associated to reference sequences. Metagenome extracted *nosZ* sequences were annotated by identifying their closest match to the reference database using BLASTX (word_size: 3, E-value:10). Matches with 60% identity and 40 amino acids coverage (cutoff) were retained and classified based on the best match. A total of 974 sequences of the original 1463 were annotated.

3.2.7. Statistical analyses

All statistical analyses were performed in R (R Development Core Team, 2008) using the phyloseq (McMurdie and Holmes, 2013), pvclust (Suzuki and Shimodaira, 2006) and vegan (Oksanen *et al.*, 2013) packages. Detailed descriptions can be found in supplemental methods.

3.3. Results

3.3.1. pH dependent changes in emissions linked to denitrifier community size as well as to total community diversity and composition

The preferential loss of N from soils as N_2O, or alternatively the efficiency of conversion of N_2O to N_2, as determined using the N_2O ratio ($N_2O/(NO+N_2O+N_2)$) was negatively associated with soil pH (R^2 = 0.83, p<0.001) (Figure 3.1A). However, when individual gases produced during denitrification were considered, pH was only strongly and inversely associated with emissions of N_2O (R^2 = 0.62, p<0.01), with other gases showing no clear pattern (NO [R^2 = 0.12, p=0.25], N_2 [R^2 = 0.21, p=0.11]) (Supplementary Fig. S3.1). The N_2O ratio was negatively, and pH was positively, associated with microbial diversity (R^2 = 0.57, p<0.01; R^2 = 0.49, p<0.01), as well as to total denitrification gene (*nir* & *nos*) abundance (R^2 = 0.57, p<0.01) (Figure 3.1B-1C and Supplementary Fig. S3.2). Across all soils the Proteobacteria, Actinobacteria and Firmicutes phyla were the dominant phyla, and represented >75% of total microbial populations in pasture soils (Figure 3.1D). Comparison of samples based on 16S rRNA community composition visualised with a non-metric multidimensional scaling (NMDS) plot, using a Bray-Curtis dissimilarity matrix, also displayed a significant link to the N_2O emission ratio and pH (Figure 3.1E and Supplementary Fig. S3.3-S3.4). A Mantel test, however, supported the correlation between microbial community structure and both the N_2O ratio (r = 0.57, p<0.001) and pH (r = 0.61, p<0.001). A pvclust analysis (hierarchical clustering with p-values calculated via multiscale bootstrap resampling, Supplementary Fig. S3.5) demonstrated that while at a 95% confidence level the clusters formed represented replicates for the same site, at lower confidence levels (<95%) soils could be clustered geographically (4 clusters: 1 Ireland; 3 New Zealand: Otago, Canterbury and North Island).

3.3.2. pH and the N_2O ratio correlate to distinct microbial populations

Operational taxonomic units (OTUs at 97% sequence similarity) significantly associated to changes in emissions, or pH, were identified using Spearman's rank correlation (Figure 3.2). A total of 590 OTUs displaying both a statistically significant result (p<0.05) and a strong effect (r ≥0.5 or r≤-0.5), based separately on either variable, were analyzed. The number of detected OTUs was 2.5-fold larger for pH (554 OTUs) than for N_2O ratio (224 OTUs) (Figure 3.2). Surprisingly, the number of

OTUs either positively or negatively correlated, to either variable, was relatively conserved indicating an almost 1:1 replacement of OTUs along the gradient. For pH, 49.2% of detected OTUs were positively and 50.7% were negatively correlated, whereas for the N_2O ratio 47.8% were positively and 52.2% were negatively correlated. As a general trend, taxa showed a strongly conserved antiparalelism in relationship to pH and N_2O ratio consistent with prior trends (Figure 3.1). While certain phyla displayed conserved patterns (e.g. Chloroflexi and Bacteroidetes), all phyla had examples of contrasting responses suggesting diverse life strategies. However, certain lineages at lower taxonomic levels did present consistent patterns (e.g. class Ktedonobacteria within the Chloroflexi, Subgroup 1 & 2 of the Acidobacteria, and Frankiales within the Actinobacteria). Lineages with known functional roles associated to N cycling like the Nitrospirae (positive correlation to pH and a negative correlation to N_2O ratio) and the Thaumarchaeota (mostly negative correlation to pH and a positive correlation to N_2O ratio) showed clear responses. It is also worth noting that candidate phyla (WD272, WS3) as well as other poorly studied phyla (e.g. Armatimonadetes) showed strong correlations with the N_2O ratio. For full taxonomic lineages and corresponding response to pH and emissions see Supplementary Table (Samad *et al.*, 2016b).

3.3.3. Linking denitrifying genes with pH and N_2O emissions

To determine the effect of varying pH on the genetic potential for denitrification, qPCR analysis was performed for key denitrification genes. Results confirmed a link between pH and the denitrification potential of soils (total [sum] abundance of all measured denitrification genes [*nirS*, *nirK*, *nosZI*, *nosZII*]). A positive association with pH (R^2 = 0.41, $p<0.05$) was observed, with an inverse response observed based on emissions (negative association with N_2O ratio [R^2 = 0.57, $p<0.01$]) (Figure 3.3). To confirm observations, and to account for potential biases associated with primers and PCR, we determined the total abundance (per 2.63 million reads per sample) of denitrification genes in metagenomes created from 6 soils (Figure 3.3 and Supplementary Fig. S3.6). Trends based on total denitrification gene abundance were conserved between approaches (R^2 = 0.66, $p<0.05$), however, discrepancies were observed when clade specific *nosZ* gene correlations were performed. For Clade I trends were similar based on either qPCR or metagenome, although these were not statistically significant (R^2 = 0.44).

However, results for Clade II based on metagenomic data showed a strong and statistically significant link to both pH (R^2 = 0.69, $p<0.05$) and N_2O ratio (R^2 = 0.63, p=0.059) that was not consistent with qPCR results. Despite low PCR efficiencies (average 66%), the abundance of *nosZ* genes belonging to Clade II were consistently higher than Clade I for both methods (~5-fold based on metagenome and 1.02-fold based on qPCR) (Figure 3.3-3.4). Irish soils had significantly higher numbers (1.9-fold, $p<0.05$, Welch's *t*-test on metagenome data) of *nosZ* genes compared to New Zealand. It was also observed that taxonomic richness and diversity for Clade II was approximately 3-fold higher than for Clade I. A total of 11 different phyla (Bacteroidetes, Firmicutes Verrucomicrobia, Gemmatimonadetes, Thermomicrobia, Proteobacteria [Alpha, Beta, Delta and Gamma], Spirochaetes, Aquificae, Euryarchaeota, Crenarchaeota, and Chloroflexi) were identified based on *nosZ* sequences. The Bacteroidetes dominated those belonging to Clade II (*nosZ*) while the Alphaproteobacteria dominated within Clade I (Figure 3.4 and Supplementary Fig. S3.7). We also examined the *nirS and nirK* genes individually, and found a positive association with pH (R^2 = 0.53, $p<0.05$) and negative association with N_2O ratio (R^2 = 0.38, $p<0.05$) for *nirS* (Supplementary Fig. S3.8). However, no significant associations were observed for the *nirK* gene.

3.3.4. Linking functional richness with pH and N_2O emissions

To account for changes in community metabolic potential outside of those previously explored, trait (function) specific patterns, associated to pH and emissions, were explored by determining the functional richness at two different levels: general N metabolism (all N cycling related genes detected) and total functional potential (total number of different genes detected). No pattern was observed between functional richness (total functional richness as well as functional richness of N-metabolism) and pH or N_2O emission ratio in the soil (Supplementary Fig. S3.9).

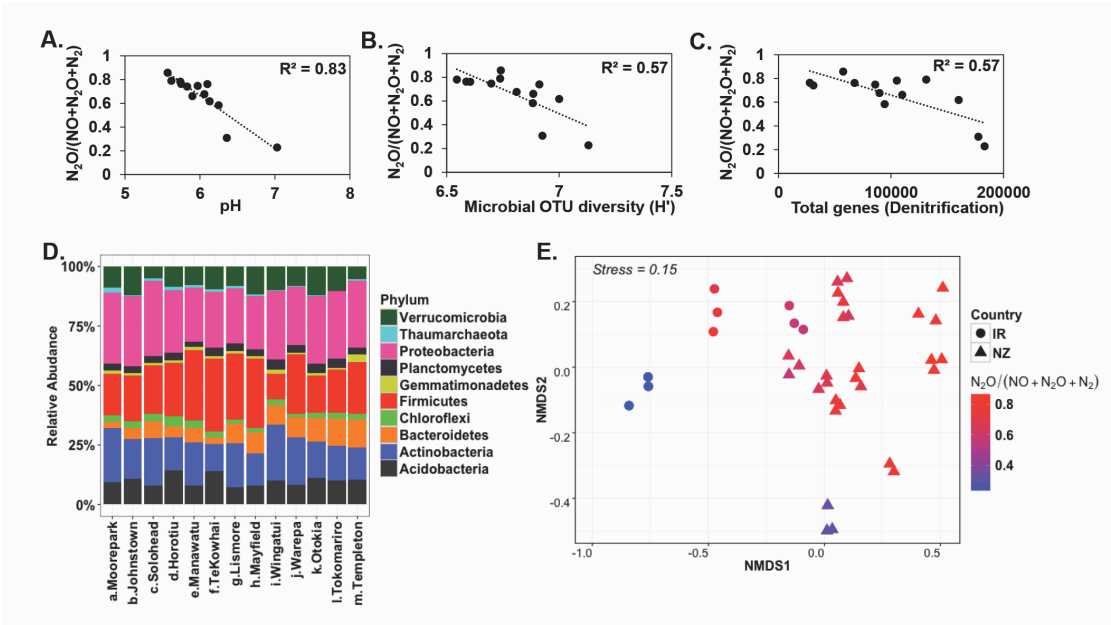

Figure 3.1. Relationship between soil pH, N_2O emission ratio, community phylogenetic and functional potential. Relationships of $N_2O/(NO+N_2O+N_2)$ with pH (A), Shannon diversity based on 16S OTUs clustered at 97% sequence similarity (B), and total gene abundance (gene abundance per 5 ng soil DNA) for denitrification genes (*nirS*, *nirK*, *nosZI* and *nosZII*) based on qPCR (C). Changes in community composition at phylum level for Irish (IR) and New Zealand (NZ) soils ranked by country (a-c: IR: Ireland soils, d-m: NZ: New Zealand soils) and decreasing N_2O emission ratio (D). Microbial community dissimilarities of soils with different emission profiles as determined using NMDS (Bray-Curtis) ordination (E).

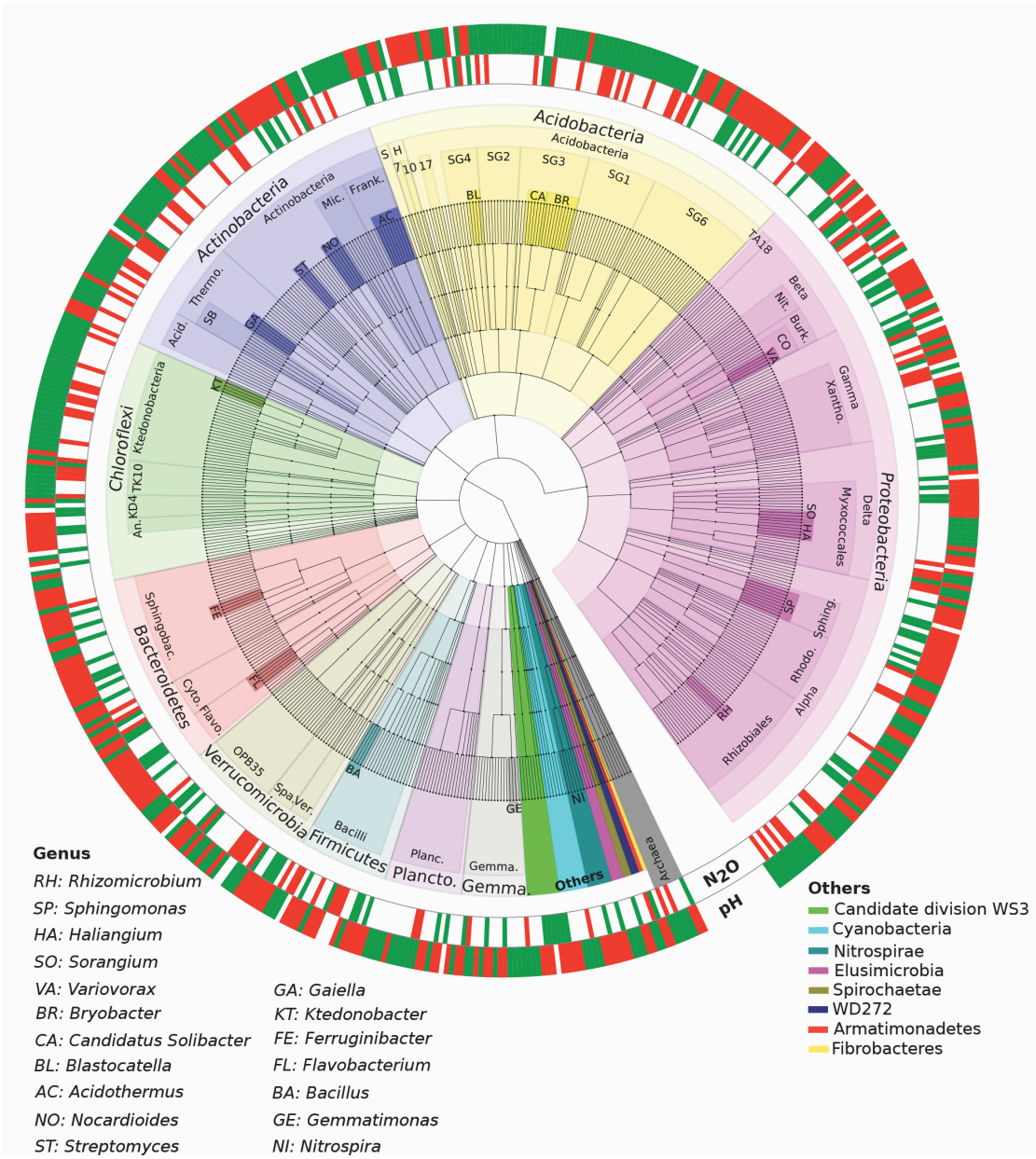

Figure 3.2. Taxonomic summary of OTUs significantly associated ($p<0.05$ after BH correction; $r \geq 0.5$ [Red] or ≤ -0.5 [Green]) to either pH or N_2O emissions ratio. The graph represents a cladogram of 590 OTUs. Nodes on the tree (moving outwards from center) correspond to taxonomic level [Domain, Phylum, Class, Order, Family, Genus and OTUs]. Shaded areas of branches delineate defined taxonomic groups. Abbreviations: S, Subgroup-22; H, Holophagae; SG, 7, 10 and 17 denotes Acidobacterial orders (subgroups); Rhodo., Rhodospirillales; Sphing., Sphingomonadales; Xantho., Xanthomonadales; Burk., Burkholderiales; Nit., Nitrosomonadales; Frank., Frankiales; Mic., Micrococcales; Thermo., Thermoleophilia; Acid., Acidimicrobiia; KD4, KD4-96; An., Anaerolineae; Sphingobac., Sphingobacteriia; Cyto., Cytophagia; Flavo., Flavobacteriia; Spa., Spartobacteria; Ver., Verrucomicrobiae; Plancto., Planctomycetes; Planc., Planctomycetacia; Gemma., Gemmatimonadetes; SB, Solirubrobacterales; CO, Comamonadaceae.

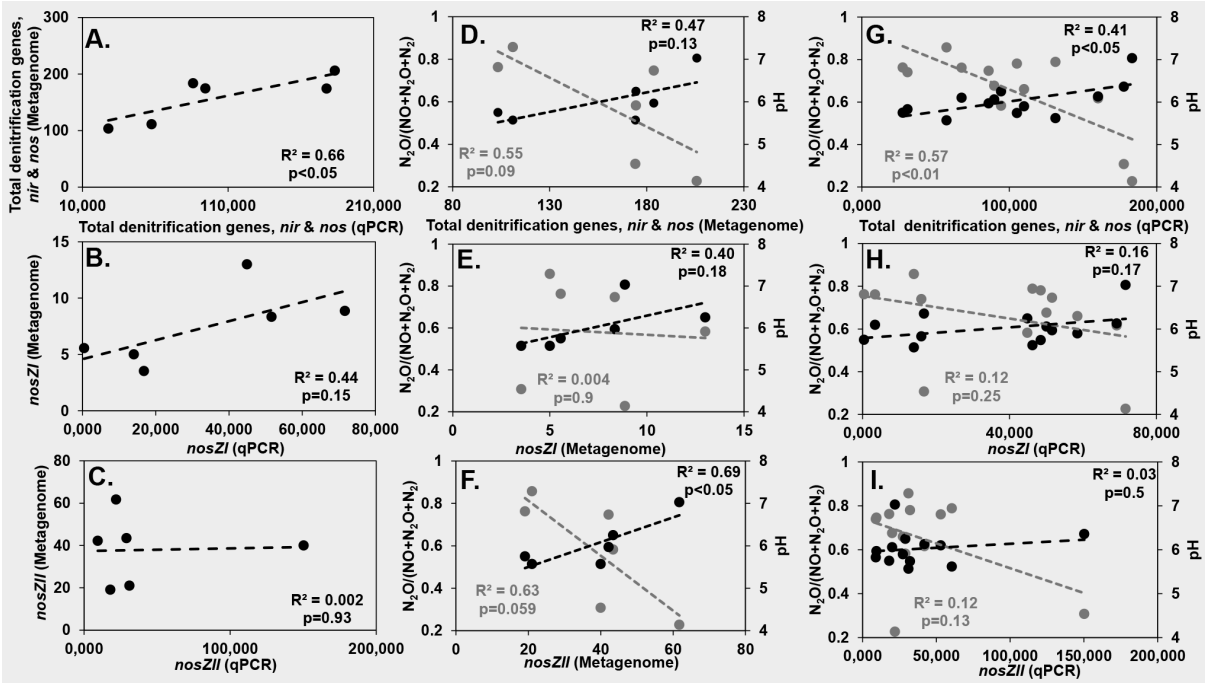

Figure 3.3. Relationship between abundance of denitrification genes (based on absolute quantification of metagenome & qPCR abundance of *nirS*, *nirK*, *nosZI*, *nosZII*), $N_2O/(NO+N_2O+N_2)$ and pH. (A-C) Comparison of gene abundances based on either metagenomic (i.e. gene abundance per 2.63 million reads) or qPCR analysis (gene abundance per 5 ng soil DNA) for 6 soils. (D-F) Response of total denitrification genes, nosZ Clade I and II abundances based on metagenomic analysis for 6 soils against $N_2O/(NO+N_2O+N_2)$ (gray) and pH (black). (G-I) Response of total denitrification genes, nosZ Clade I and II abundances based on qPCR analysis for all 13 soils against $N_2O/(NO+N_2O+N_2)$ (gray) and pH (black).

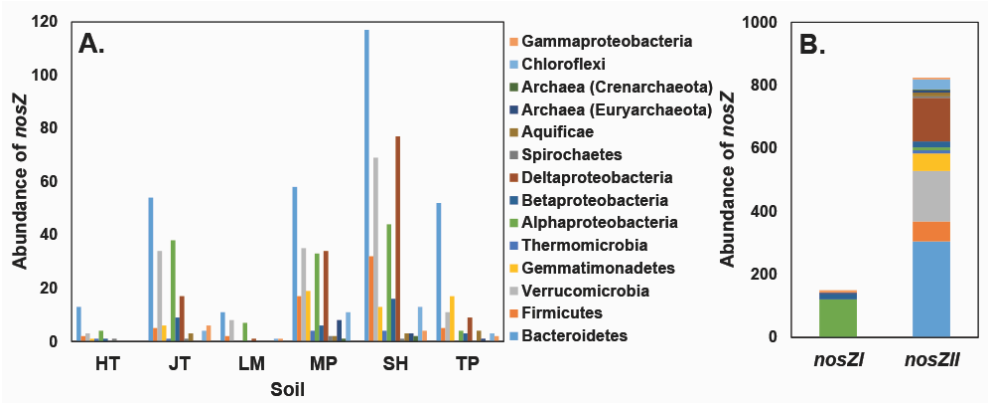

Figure 3.4. Abundance (genes per 2.63 million reads) and predicted taxonomy of nitrous oxide reductase (*nosZ*) genes by soil (3 New Zealand [HT, Horotiu; LM, Lismore; TP, Templeton] and 3 Ireland soils [JT, Johnstown; SH, Solohead; MP, Moorepark]). (A), and summarized by Clade (B), based on metagenomics analysis. Clade I: Total abundance (150), Richness (4), Shannon Diversity (0.68), Evenness (0.49). Clade II: Total abundance (824), Richness (14), Shannon Diversity (1.87), Evenness (0.46).

3.4. Discussion

Results support the role of native soil pH in shaping community composition and diversity. Microbial community changes were associated to both geographic changes (country and region) as well as to N_2O emissions potential, as has been described previously (Morales *et al.*, 2010; 2015). It is important to note that N_2O emissions potential, or ratio, as defined in this study ($N_2O/(NO+N_2O+N_2)$) refers to the propensity of soils to emit N_2O over other denitrification gas intermediates. Here this is accomplished using a controlled environment where all other factors were held constant. While this does not reflect the absolute (total amount) of N lost through the process, it is possibly the best predictor of the propensity of the soils to emit N_2O (Saggar *et al.*, 2013; Samad *et al.*, 2016a). However, this potential, and the observed phenotype, can be modulated by fluctuating factors and require observations at the denitrification level through expression profiling (transcriptional/translational level) to identify real time drivers of N_2O emissions (Liu *et al.*, 2010; 2014; Brenzinger *et al.*, 2015). Despite these limitations our observations highlight a conserved response to pH in both Northern and Southern Hemisphere soils. This suggests pH is part of a universally conserved mechanism selecting for both emissions and microbial communities. The range of pH observed in our soils (5.57 - 7.03) was sufficient to capture the range at which the N_2O reductase and N_2O emissions fluctuate in response to pH (Liu *et al.*, 2010; Obia *et al.*, 2015; McMillan *et al.*, 2016; Russenes *et al.*, 2016). Soil pH controls not only the assembly of the N_2O reductase (Liu *et al.*, 2010; 2014), but also alters general expression patterns (Brenzinger *et al.*, 2015) and selects for shifts in microbial community composition (Rousk *et al.*, 2010) indirectly influencing the abundance and type of functional genes in soils. Thus pH can have confounding effects due to its role in shaping the genotype, expression and eventual phenotype associated with denitrification.

While our findings support prior work, we show that of all the three measured gases only N_2O had a significant association with pH when compared to maximum emission levels, with maximum observed N_2O emissions decreasing with higher pH (Fig S3.1). This was consistent with a lack of correlation between pH and individual denitrification genes. This is potentially due to the modular nature of denitrification (Zumft, 1997; Philippot, 2002; Philippot *et al.*, 2011) where different steps within the pathway are encoded in distinct operons which do not necessarily depend on nor are associated with each other. Despite no strong correlations between emissions and

denitrification specific genes, we found that of the two clades of *nosZ* gene one was dominant. Both qPCR and metagenome results show that Clade II are highly abundant, despite amplification efficiencies being poor (66%) for Clade II primers. Further, trends between metagenomic and qPCR data did not match and suggested that Clade II primers do not provide an accurate view of the abundance within our soils. Despite an apparent under representation (based on qPCR) for *nosZII*, the average Clade II/Clade I abundance ratio was >1 both for PCR-based and metagenomics analysis and is in line with prior observations of their dominance in certain soils (Orellana *et al.*, 2014). It also aligns with reports linking the abundance of Clade II with the emissions potential of soils (Jones *et al.*, 2014). Our results also support the predicted diversity based on clade, with Clade II being represented in almost 3-times more phyla (Fig. 4) (Jones *et al.*, 2013). Despite evidence supporting the taxonomic conservation for the two clades (different *nosZ* types are found restricted to certain microbial groups) (Sanford *et al.*, 2012; Jones *et al.*, 2013; 2014) our data shows that these organisms can be associated with soils displaying contrasting pH and emissions ratios.

Despite the lack of correlation between specific denitrification genes and pH, we did observe a trend of decreasing abundance of denitrification genes and overall diversity (based on 16S analysis) with decreasing pH. The role of diversity in regulating ecosystem processes has been long debated (Loreau *et al.*, 2001; Tilman *et al.*, 2014). The significance of microorganisms in this debate has only vaguely been addressed, relative to their predicted diversity (Locey and Lennon, 2016), despite their expected importance (Van Der Heijden *et al.*, 2008; Graham *et al.*, 2014). Available studies suggest that when specific microbial functional groups (i.e. methanotrophy vs. respiration) are used to test diversity/ecosystem process relationships, significant trends can be uncovered (Griffiths *et al.*, 2000; Wertz *et al.*, 2006; Wittebolle *et al.*, 2009; Levine *et al.*, 2011). For N_2O, studies suggest that diversity plays a role, with decreases in diversity leading to increases in emissions (Philippot *et al.*, 2013; Wagg *et al.*, 2014). Our results support and expand on those observations indicating a role for diversity-mediated responses at multiple levels (from whole community, to specific populations linked to denitrification). Though our data do not allow a mechanism to be determined, we hypothesize that an increase in diversity ensures a steady population of microbes that are capable of sustaining a process (e.g. N_2O reduction) over a range of conditions. This diversity is still under

the proximal control of regulators thus it can be modulated based on spatially and temporally controlled factors.

Identification of specific organisms responding to either pH or emissions highlighted co-varying trends. For example, while many organisms associated to changes in pH were identified as being associated to changes in emissions, not all organisms were. This implies that while certain organisms are selected by pH, they may not play a role in controlling emissions. Alternatively, some organisms that do play a role, might not be selected for by pH alone. While such correlations allow for development of new hypotheses they serve only as a first step in identifying the mechanisms controlling emissions and the role individual organisms may play. Our study also does not address the role or contributions other pathways (like nitrification) might play in regulating N_2O emissions.

CHAPTER 4

Ruminant urine patch reveals significant sources of N_2O

Md Sainur Samad, Lars R. Bakken, Shahid Nadeem, Timothy Clough,

Cecile de Klein, Karl G. Richards, Gary J. Lanigan, Sergio E. Morales*

Article in Preparation: Soil Biology and Biochemistry

Author Contributions: Authors are listed in order of magnitude of their contribution in each role. Corresponding author is indicated by an asterisk (*). SEM, LRB, and MSS designed the experiments. MSS, SN, CAMdK, TJC, KGR and GJL collected samples and processed. MSS and LRB analyzed the data. SEM and LRB had supervisory roles. MSS wrote the manuscript. MSS produced all figures and tables.

Abstract

Nitrous oxide (N_2O) emissions in soils predominantly arise from denitrification under anoxic conditions. However, the emission of N_2O under oxic conditions is poorly understood or sometimes underestimated. Here we used high-resolution automated gas-chromatography to track the urine patch kinetics profile (NO, N_2O and N_2) of 13 different pasture soils from Northern (New Zealand) and Southern hemispheres (Ireland) under oxic conditions. We observed significant production of NO and N_2O compared to controls (no urine) which may indicate other process apart from denitrification. Urine addition elevated the C-mineralization (i.e. production of CO_2) by approx. 10-fold. The production rate of N (i.e. $NO+N_2O+N_2$ μmol/h) from the urine patch was significantly associated (R^2= 0.9, $p<0.001$) with the maximum emission of N_2O ratio (i.e. $N_2O/(NO+N_2O+N_2)$). This means higher denitrification rates enhance the emission ratio of N_2O. No significant relationship was observed between pH and the emission ratio of N_2O under this simulated urine patch, although such relation was obvious under true denitrification process (i.e. anoxic conditions). Multiple correlation analysis is showed that NO_2^- concentration has significantly correlated to both pH and the emission ratio of N_2O. In addition, oxic respiration (O_2 rate) was negatively correlated with gaseous N rate but positively correlated with ammonia oxidizing bacteria (AOB).

4.1. Introduction

Nitrous oxide (N_2O) is a potent greenhouse gas about 298 times more effective in trapping heat than carbon dioxide (CO_2) (IPCC, 2007; Myhre *et al*., 2013), while also contributing to the depletion of the stratospheric ozone layer (Ravishankara *et al*., 2009). The concentration of N_2O in the atmosphere has increased by 20 % from 271 ppb to 324 ppb over the last 260 years (Myhre *et al*., 2013). The major source of this N_2O is agricultural soils (Cole *et al.*, 1997; Paustian *et al.*, 2004; Mosier *et al.*, 1998), with ruminant urine representing a significant source of nitrogen (N) linked to global N_2O emissions (Oenema *et al*., 2005; van Groenigen *et al*., 2008).

Grazed pasture soils receive N as organic urea in the form of ruminant excreta, with urine being the dominant source. A single ruminant urination event contributes a fertilization equivalent of approx. 1000 kg N (per ha) to the soil (Di and Cameron, 2002). The transformation of urine to N_2O or dinitrogen (N_2) is regulated through both biotic (e.g. nitrification, nitrifier-denitrification and denitrification) and abiotic processes (e.g. chemodinitrification) (Van Cleemput and Samater, 1996; Saggar *et al.*, 2013). Urine is first hydrolyzed into ammonia (NH_3) or ammonium ions (NH_4^+), and depending on site conditions (i.e. pH, oxic status) can proceed down different pathways, with coupled nitrification-denitrification expected to be the dominant pathway (Wrage *et al*., 2001). Nitrification is a stepwise aerobic process where biological NH_3 or NH_4^+ is first converted into nitrite (NO_2^-) by nitrifying or ammonia-oxidizing bacteria, and then into nitrate (NO_3^-) by nitrite-oxidizing bacteria. Further conversions are carried out via a denitrification cascade. Denitrification is an anaerobic stepwise process catalyzed by predominantly heterotrophic bacteria where NO_3^- is converted first into nitric oxide (NO), then into N_2O, and finally into N_2. While this process is divided amongst the different group of prokaryotes, the alternative process of nitrifier-denitrification combines both stages within the same organism (Wrage *et al*., 2001). In this combined pathway, AOB emit N_2O along with other gases under oxic conditions without following the anoxic denitrification pathway (Zhu *et al.*, 2013; Stein and Yung, 2003). In this pathway (by AOB), the oxidation of NH_3 to NO_2^- occurs first, followed by the reduction of NO_2^- to NO, N_2O, and N_2. In addition, NO_3^- is not produced under nitrifier-denitrification process, which is a linking compound between two pathways (nitrification-denitrification). However, recent findings suggest that N_2O production could completely bypass denitrification with

N_2O production under anaerobic conditions occurring immediately through hydroxylamine oxidoreductase (Caranto *et al*., 2016).

The complex array of potential transformations leading to N_2O suggests that soil conditions can alter the contributions of each pathway (Zhu *et al*., 2013), but it also implies that chemical transformations within each pathway can transiently alter the conditions overriding intrinsic regulators. This is especially true for pH, considered a master regulator of N cycling and N_2O emissions (Čuhel *et al.*, 2010). Under true (anaerobic) denitrification in soils, the emission ratio of N_2O and pH are negatively associated with each other (Šimek and Cooper, 2002; Bakken *et al.*, 2012; Raut *et al.*, 2012; Qu *et al.*, 2014; Samad *et al.*, 2016a). The current hypothesis is that low pH hinders the posttranslational assembly of a functional N_2O-reductase enzyme (Bakken *et al.*, 2012; Bergaust *et al.*, 2010; Liu *et al.*, 2014). However, most studies have utilized nitrate or nitrite as an N source. Within urine patches the dominant N source is urea, and its hydrolysis and sequential transformation can result in large pH fluctuations (Sherlock and Goh, 1985; Clough *et al.*, 2017; Samad *et al.*, 2017). An initial 'liming' effect is consistently recorded and suggests that regulation by intrinsic soil pH can be decoupled allowing other regulators to become more important within urine patches.

Here, we used a fully automated high-resolution gas chromatography (GC) system for measuring gas kinetics immediately after applying artificial urine in 13 different soils representing Northern (Ireland) and Southern Hemispheres (New Zealand) soils. Our objectives were: (1) to determine the urine patch kinetics of soils, (2) to investigate the relationship between pH and the emission ratio of N_2O (i.e. $N_2O/(NO+N_2O+N_2)$) under a urine patch, (3) to determine if regulators identified under denitrification conditions still exert a role within urine patches, and finally (4) to determine which variables are linked to production of gaseous N rate (i.e. $NO+N_2O+N_2$ µmol/h) as well as emission ratio of N_2O.

4.2. Materials and methods

4.2.1. Study sites, and sample collection

Soil samples were collected from 13 different sites in both Northern (Ireland [Moorepark, Johnstown, Solohead]) and Southern (New Zealand [Warepa, Otokia,

Wingatui, Tokomairiro, Mayfield, Lismore, Templeton, Manawatu, Horotiu, Te Kowhai]) hemispheres as described previously (Samad *et al*., 2016a).

4.2.2. pH measurements

Soil pH was measured using deionised (DI) water as in (Samad *et al*., 2016a). All pH measurements were done using an Orion 2-star pH Benchtop pH meter (Thermo Scientific) equipped with an Orion 8175BNWP electrode (Thermo Scientific).

4.2.3. Nitrate adjustment

Nitrate levels in soils (150 g dry weight) were adjusted by placing samples in 500 ml filter funnels with 4.5 cm diameter (0.2 µm) Millipore membrane filters and subsequently flooding them with a 2 mM NH_4NO_3 solution for 10 minutes. Samples were immediately drained by applying a vacuum. The moisture content of drained samples was determined and dry weight equivalents were used for gas kinetic experiments.

4.2.4. Artificial urine preparation

Artificial urine was prepared by following the protocol of Kool *et al*., (2006) and pH adjusted if needed (pH = 7). There are some reasons why artificial urine was used instead of ruminant urine. N concentration is fixed in the artificial urine and easy to reproduce for multiple experiments at any time. Nitrogen concentration and volume was adjusted to simulate a urine patch in the field (final dose was equivalent to 1000 kg N/ha, or 13.3mg N/vial delivered in a 1.29 ml dose for a final concentration of 0.66 mg N/g of soil (dry weight)).

4.2.5. Gas kinetics of urine cascade

All samples were processed using a slightly modified version of the method described previously (Samad *et al*., 2016a). For each sample, 20 g (dry weight equivalent) of nitrate adjusted soil was placed inside a 120 ml serum vial and compressed to obtain 70% water filled porosity (WFPS) and 30% air filled porosity (AFP) which mimicked natural soil conditions. Vials were sealed with an air-tight butyl-rubber septa and an aluminium crimp cap, followed by three rounds of flushing and evacuating using 20% pure O_2 (80:20 He:O_2 mix). Urine treated vials received 1.29 ml (13.3mg N/vial) of artificial urine delivered via a syringe needle one minute

before the first GC reading of all samples. For each soil and treatment (urine and without urine), triplicate vials were prepared and incubated at 20°C using an automated GC system (Molstad *et al.*, 2007). All data presented were from experiments performed in two runs, with each run containing independent standards (duplicates of four different gas standards). All standards were prepared using evacuated vials (120 ml with septum) filled with commercially produced standard gases (supplied by AGA). Headspace samples (approx. 1 ml) were measured every 5 hours (O_2, CO_2, NO, N_2O, N_2) using an autosampler. To prevent anaerobiosis additional pure O_2 (final conc. ~20%) was injected (1-4 times depending on O_2 consumption rate) to the vials throughout the incubations. Incubations lasted approx. 180 hours. The emission ratio of N_2O (i.e. $N_2O/(NO+N_2O+N_2)$ was determined at every time points and the maximum observed value was used for downstream analysis.

4.2.6. Nitrite (NO_2^-) measurements

To allow destructive sampling and monitoring of NO_2^- levels, 7 additional vials per soil (12 ml serum vials, each containing 2 g of soils (dry weight) under the same treatment) were used and kept offline (not processed for gas kinetics). These vials were only incubated for 25 hours, with sampling occurring at different time intervals. NO_2^- concentrations were determined by distilled water extractions (4 ml per vial and shaking for 1 minute). A 1ml aliquot of extract was transferred to a microcentrifuge tube and centrifuged at 10,000 rpm for 5 minutes. The supernatant was removed and NO_2^- concentration was measured immediately using a Sievers Nitric Oxide Analyzer (NOA 280i; GE Instruments, USA).

4.2.7. Calculation of gaseous N ($NO+N_2O+N_2$) emissions and C mineralization rates

Gaseous N emissions and C mineralization rates were calculated using the mean production rate of $NO+N_2O+N_2$ (µmol/h per vial) and CO_2 (µmol/h per vial) respectively, within the first 40 h.

4.2.8. Quantification of ammonia oxidizers

The ammonia oxidizers (archaeal [AOA] & bacterial [AOB] ammonia monooxygenase gene; *amoA*), and total prokaryotes (16S rRNA genes) were

quantified by quantitative (qPCR). All reactions were performed in 384-well plates using the QuantStudio 6 real-time PCR (Applied Biosystem, CA, USA). Absolute quantification was preformed using a 10-fold dilution series (10^8 to 10^1) of known copy numbers of plasmid templates, generated from pGEM-T easy (Promega, Madison, Wisconsin, USA). Each target was run in separate plates (384-well) and included cloned standards and no template controls. All targets (AOA, AOB and 16S rRNA gene) were run in quadruplicates to determine abundance. The relative abundance of each target was then calculated as a percent ratio (e.g. gene abundance of each target/total prokaryotes (16S rRNA)).

All reactions were performed in 10 µl volumes containing: 1x Master Mix (Fast SYBR Green Master Mix, ABI), 0.2-0.6 µM of each primer [0.2 µM for AOA (Tourna *et al.*, 2008), 0.6 µM for AOB (Avrahami *et al.*, 2003), 0.5 µM for 16S rRNA (Hartman *et al.*, 2009)], 2 µl of target DNA (5 ng total) and autoclaved Mili-Q H_2O to a final volume of 10 µl. qPCR details are summarized in Table S4.1.

4.2.9 Statistical analyses

Analyses were performed in JMP (SAS Institute, Cary, NC, USA) and R (R Development Core Team, 2008). Statistical significance was determined by means of independent t-test for comparison of treatments. Linear regressions were used to identify the relationship between two variables. Multiple correlation tests (Spearman correlation) were performed across variables.

4.3. Results

4.3.1. N kinetics under urine patch

Soil samples were incubated under oxic conditions for 180 hours (Figure 4.1 and Supplementary Figure S4.1). A significant ($p<0.001$) increase in all measured gases was observed in response to urine addition (Supplementary Figure S4.2). Kinetic profiles demonstrate active respiration, with the extent of activity varying across soils as reflected in both oxygen consumption and mineralization rates (Figure 4.1). The rate of CO_2 production as a result of C-mineralization was increased by 10-fold under urine patch conditions compared to control (without urine treatment). The maximum concentrations of NO and N_2O were 24.2 nmol N/vial (mean 16.8±6.9 nmol N/vial) and 19 µmol N/vial (mean 6.7±4.7 µmol N/vial) respectively after urine addition. NO_2^- was produced in all soils upon urine addition. The maximum concentration of NO_2^- was 20.6 nmol/vial (mean 3.5±2.6 nmol/vial [20 g soil]) (Figure 4.2).

4.3.2. Regulators of N_2O emissions under true denitrification (nitrate + anoxic) vs. urine patch (nitrate + urea + oxic) conditions

It was observed that maximum observed N_2O ratios under denitrifying vs. urine patch conditions did not correlate ($R^2=0.1$, Figure 4.3). Further, while pH was a strong driver of N_2O ratio under denitrifying conditions ($R^2=0.83$, $p<0.001$), no relationship was found under urine patches even when soil properties that could affect conditions at the aggregate level (i.e. drainage class) were accounted for. Instead, we found that the N_2O ratio within urine patches increased in a linear manner as the rate of gaseous N ($NO+N_2O+N_2$) increased (Figure 4.4).

4.3.4. Multiple correlation analysis across variables from urine patch, soil properties and ammonium oxidizers (AOA and AOB)

A Spearman correlation test was performed to investigate the relationship across variables including urine patch kinetics, soil chemistry and relative abundance of ammonia oxidizers (AOA & AOB) (Figure 4.5). It was observed that NO_2^- conc. (max.) under urine patch conditions positively correlated with soil pH ($r = 0.61$,

$p<0.05$), the gaseous N rate ($r = 0.66$, $p<0.05$) as well as the emission ratio of N_2O ($r = 0.74$, $p<0.01$). C mineralization rate was positively correlated with moisture content ($r = 0.58$, $p<0.05$), but negatively correlated with pH ($r = -0.77$, $p<0.01$). Oxic respiration rate was positively correlated with AOB (%) ($r = 0.63$, $p<0.05$), but negatively correlated with gaseous N rate. Positive correlation was observed between AOB (%) and AOA (%) ($r = 0.56$, $p<0.05$).

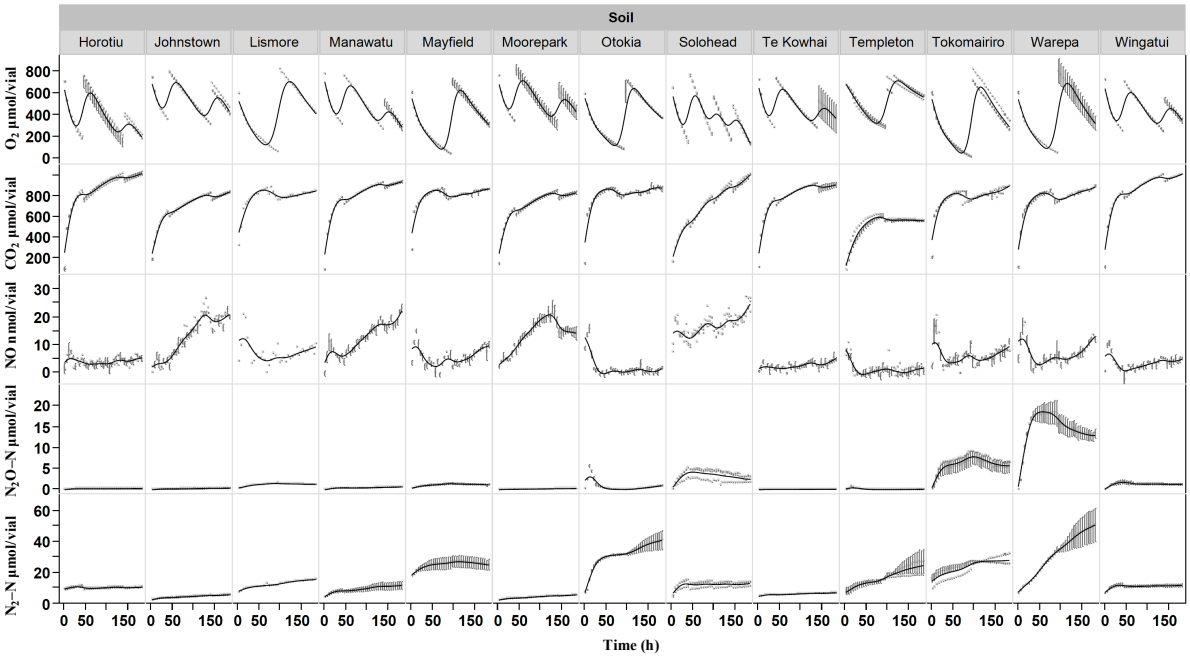

Figure 4.1. Gas kinetics (O_2, CO_2, NO, N_2O, N_2) of urine cascade events in 13 different soil samples (10 New Zealand and 3 Ireland soils) under oxic incubation. Artificial urine (dose was 1000kgN/ha or 13.3 mgN/vial (= 1.29 ml per vial)) simulating the urination event of a cow was injected into each vial just before the first GC measurement. The GC measurements were performed continuously at 5-hour intervals for 180 hours. The top row of the figure represents O_2 conc. of each soil (per vial). To keep the vial under aerobic conditions additional O_2 was added to each vial (2-4 times). Figure represents mean (dot points), SE, and a smooth line which is a fit line of replicates (n = 3).

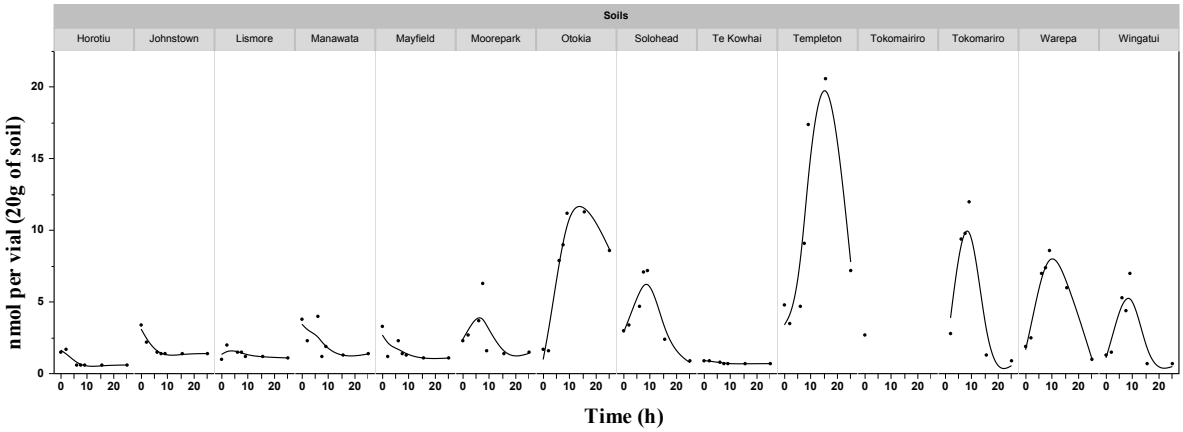

Figure 4.2. Nitrite (NO_2^-) concentration was measured at different time intervals for 25 hours after treatment with urine.

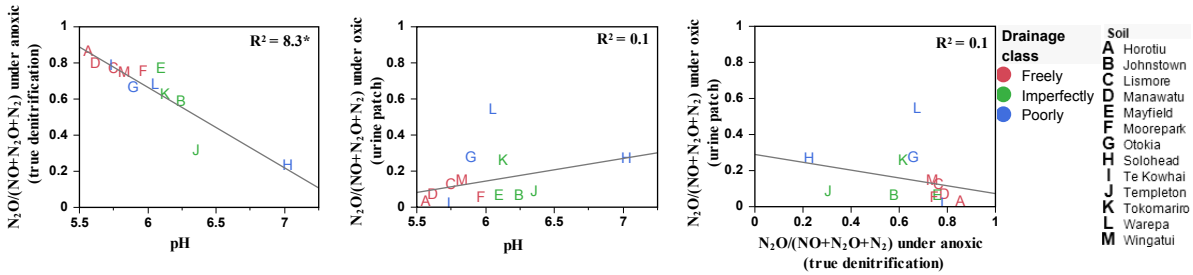

Figure 4.3. Relationship between pH and N_2O emission under both oxic (urine patch) and anoxic (true denitrification) conditions. (A) Relationship between pH and N_2O emission ratio under anoxic condition. (B) Relationship between pH and N_2O emission ratio under oxic condition (with urine treatment). (C) Relationship between N_2O emission ratio under oxic conditions (urine patch) and N_2O emission ratio under anoxic conditions (without urine patch).

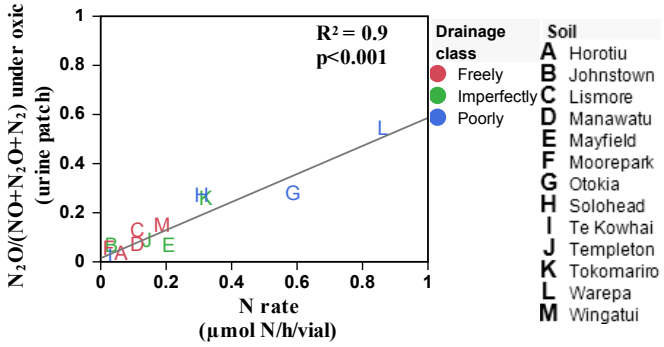

Figure 4.4. Relationship between N rate (i.e. production rate of $NO+N_2O+N_2$) under urine patch conditions and emission ratio of N_2O (i.e. $N_2O/(NO+N_2O+N_2)$ under true denitrification conditions.

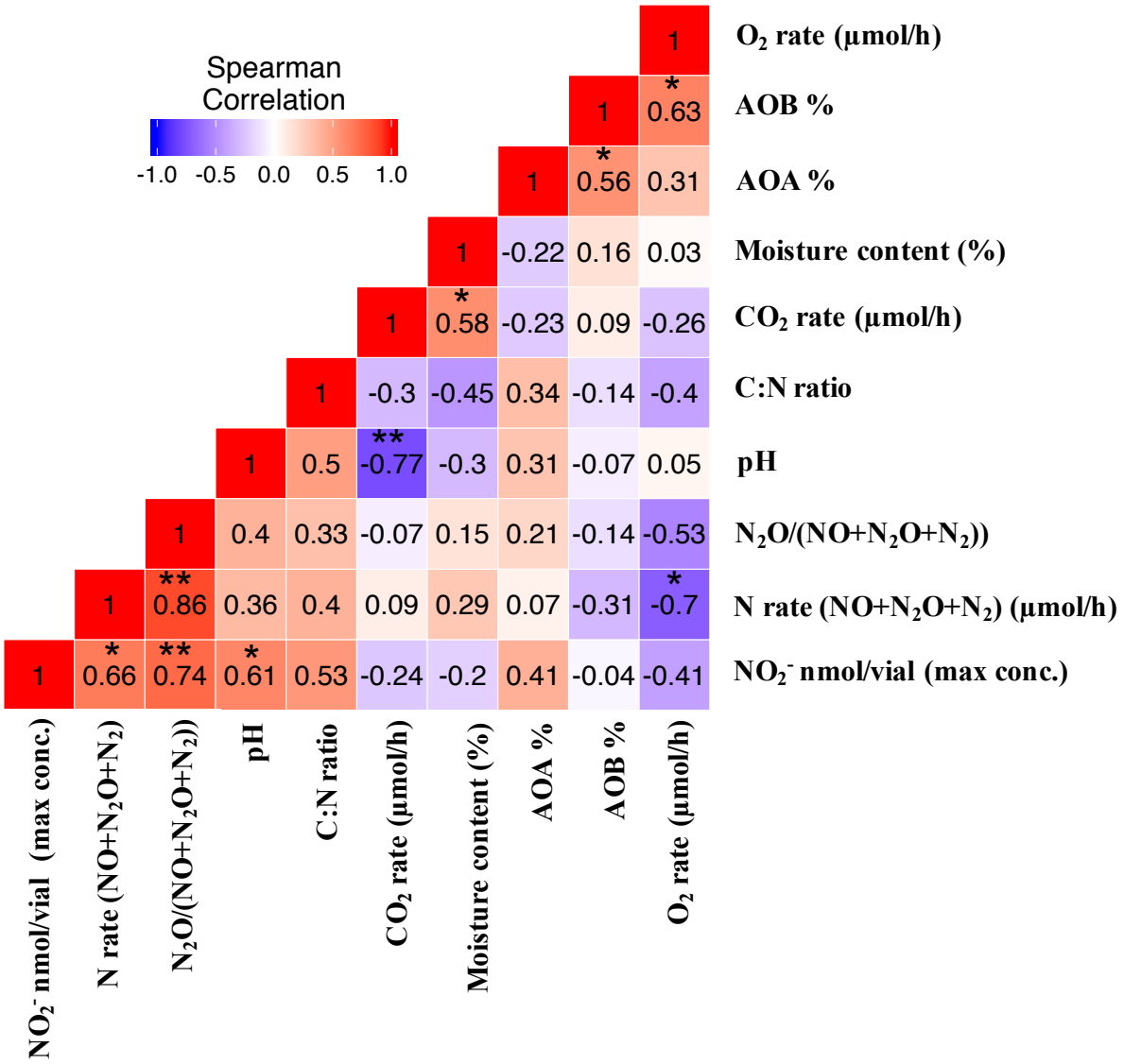

Figure 4.5. Heatmap shows spearman correlations across variables⁻ under urine patch kinetics, soil chemistry and relative abundance of ammonium oxidizing bacteria and archaea (AOB, AOA). Significant values are shown (after BH-corrected) as asterisk (*p<0.05; **p<0.001).

4.4. Discussion

Very little is known about gas kinetics profile of pasture soils, especially N_2O emissions under ruminant urine patches. Here we showed the significant ($p<0.001$) production of NO and N_2O under oxic urine patch conditions in 13 different pasture soils, representing from Northern and Southern Hemispheres. We also observed the production of NO_2^- in almost all soils. Our results probably indicate that apart from denitrification other pathway is dominant under urine patch conditions. This is a rapid and alternative pathway for N_2O emissions under oxic or low oxygen conditions in soils. No isotopic measurements were done in our experiment and that is why we cannot able to specify the pathway. The process has been shown in previous ^{15}N study where significant production of NO and N_2O from urea and ammonium-sulfate amended soils were driven by nitrifier-denitrification under low oxygen availability (Zhu *et al*., 2013).

Soil pH is known to be an important edaphic factor in the regulation of the emission ratio of N_2O (i.e. $N_2O/(NO+N_2O+N_2)$) under true denitrification conditions (Qu *et al*., 2014; Raut *et al*., 2012). The pH interferes with the function of the nitrous oxide reductase enzyme resulting in more N_2O emissions compared to slightly alkaline or neutral pH (Liu *et al.*, 2010; 2014). In our previous studies, we showed that there was a significant linear relationship between pH and emission ratio of N_2O (Samad *et al.*, 2016a; 2016b) where 13 different pasture soils were used. By using the same types of pasture soils in this study, we wanted to investigate further whether the same trend could be observed or not, under urine patch conditions. We observed that emission ratio of N_2O is not significantly associated with pH. The reason could be that the urine addition in soils disrupts or elevates the soil pH due to urea hydrolysis (Sherlock and Goh, 1985; Cabrera *et al.*, 1991). Furthermore, it is completely a different processes (anoxic vs. oxic) and different microorganisms are involved. In general, this process is regulated by ammonia oxidizers; whereas, in denitrification, heterotrophic bacteria are predominantly responsible. These could possibly explain why the emission ratio of N_2O from this process is differed from denitrification and is not linked to pH.

We have observed that the rate of C-mineralization was higher compared to control (without urine treatment) under urine patch conditions. This suggests that

oxic C-mineralization process may support the transformation of NO and N_2O. This trend was observed previously in denitrification under anoxic conditions, where C-mineralization enhanced the denitrification (Reddy *et al.*, 1982; Zimmerman and Benner, 1994; Samad *et al.*, 2016a).

There was a positive linear relationship between the gaseous N rate (i.e. $NO+N_2O+N_2$ µmol/h) and emission ratio of N_2O (i.e. $N_2O/(NO+N_2O+N_2)$). This means, higher N rate can contribute the higher emission ratio of N_2O. Furthermore, the gaseous N rate can be used as an alternative predictor for modeling the emission ratio of N_2O.

Furthermore, we did not observe any strong correlation between ammonia oxidizers (AOA and AOB) with gaseous N rate and emission ratio of N_2O. The AOA and AOB abundance analysis were done based on field soils, and compared here with urine patch kinetics. As a result, this could affect our ability to see the genotypic relation with urine patch kinetics. However, we could generate a hypothesis, for example, the relative abundance of AOB in soil is linked to the oxic respiration (O_2 µmol/h) under urine patch conditions. This gives us an indication where the abundance of AOB can be regulated by the availability of oxygen. Importantly, the higher the rate of oxic respiration could support the growth of AOB.

We observed that NO_2^- concentrations, which play an important role in urine patch to understand the emission ratio of N_2O and gaseous N rate as observed positive correlation. This was also demonstrated in the previous study where NO_2^- intensity was strongly correlated with N_2O emissions (Maharjan and Venterea, 2013).

In summary, we observed the gas kinetics of NO, N_2O and N_2 in urine treated soils in oxic conditions suggest other process apart from denitrification (i.e. nitrifier-denitrification, co-denitrification). As this process was different from denitrification (anoxic), therefore no relationship was observed between soil pH and emission ratio of N_2O under urine patches.

CHAPTER 5

Response to nitrogen addition reveals metabolic and ecological strategies of soil bacteria

Md Sainur Samad, Charlotte Johns, Karl G. Richards, Gary J. Lanigan,

Cecile A. M. de Klein, Timothy J. Clough*, Sergio E. Morales*

Article Accepted: Molecular Ecology

Author Contributions: Authors are listed in order of magnitude of their contribution in each role. Corresponding author is indicated by an asterisk (*). TJC, KGR, GJL, MSS and SEM designed the experiments. MSS, CAMdK, TJC, CJ, KGR and GJL collected samples and processed. MSS, CJ, TJC, KGR and GJL analyzed the data. SEM and TJC had supervisory role. MSS and SEM wrote the manuscript. MSS produced all figures and tables. All authors revised the paper.

Abstract

The nitrogen (N) cycle represents one of the most well studied systems yet the taxonomic diversity of the organisms that contribute to it is mostly unknown, or linked to poorly characterized microbial groups. While progress has allowed functional groups to be refined, they still rely on *a priori* knowledge of enzymes involved, and the assumption of functional conservation, with little connection to the role the transformation plays for specific organisms. Here, we use soil microcosms to test the impact of N deposition on prokaryotic communities. By combining chemical, genomic and transcriptomic analysis we are able to identify and link changes in community structure to specific organisms catalyzing given chemical reactions. Urea deposition led to a decrease in prokaryotic richness, and a shift in community composition. This was driven by replacement of stable native populations, which utilize energy from N-linked redox reactions for physiological maintenance, with fast responding populations that use this energy for growth. This model can be used to predict response to N disturbances and allows us to identify putative life strategies of different functional, and taxonomic, groups thus providing insights into how they persist in ecosystems by niche differentiation.

5.1. Introduction

Modern microbiology techniques have given us unprecedented access to the microbial world (Spiro, 2012; Rinke *et al.*, 2013), yet soil microbial communities remain poorly understood (Delmont *et al.*, 2015). While many studies have focused on the diversity or abundance of key populations (Taylor *et al.*, 2012; Gubry-Rangin *et al.*, 2015; Wei *et al.*, 2015a), fewer have looked at the transcriptional profiles over time (Nicol *et al.*, 2008; Morales and Holben, 2013), and even less have done so for multiple groups at the same time (Liu *et al.*, 2010; Brenzinger *et al.*, 2015). This is particularly true of organisms involved in nitrogen (N) cycling in soils. The complexity of the underlying processes combined with the diversity of microbes contributing to each process provides a large challenge to identifying mechanisms active at any given time (Butterbach-Bahl *et al.*, 2013). Currently we lack enough information to understand basic ecological concepts linked to N cycling *in situ* such as: i) substrate competition at both inter and intra species level, ii) full diversity of both present and active N cycling populations, iii) and the life strategies of these populations which in turn control their responses (both as observed growth or transcriptional changes).

The initial discovery of ammonia oxidizing archaea (AOA) and recognition as important players in the N cycle (Leininger *et al.*, 2006; Hatzenpichler, 2012; Stahl and la Torre, 2012) highlighted the unexpected gaps in knowledge. Later studies have suggested different life strategies for AOA when compared to ammonia oxidizing bacteria (AOB) (Sterngren *et al.*, 2015), but this may be complicated by variance across strains (Bayer *et al.*, 2015). One major unknown is whether observations made in studies, or organisms, from one ecosystem translate to others.

It is well established that individual intermediates in the N cycle can be used for specific reasons (i.e. ammonia oxidation provides electrons, while denitrification intermediates accept reducing equivalents), but the purpose of the reactions for any organism is another major unknown. That is, while some organisms carry out these processes for electrogenic purposes that can result in growth, others do it in order to maintain redox homeostasis (e.g. to dissipate excess reductants) (Green and Paget, 2004). Unfortunately examples where an organism harbors multiple versions of the same enzyme for completely different purposes (respiration vs. redox balance) exist (Hartsock and Shapleigh, 2011), and are likely to limit generalizations.

Despite this, studies focusing on population changes in response to manipulations have consistently recorded conserved patterns (e.g. growth of AOB

but not AOA (Jia and Conrad, 2009; Di *et al.*, 2009; Pratscher *et al.*, 2011)) suggesting that responses by specific populations in a given location or ecosystem are predictable. However, the debate continues on whether niche specialization and differentiation can be determined based solely on correlations, without analyzing the wider array of processes that contribute or influence any given N transformation (Prosser and Nicol, 2012). This is relevant in ecosystems such as agricultural grassland where an understanding of N cycling is crucial for management of both productivity and greenhouse gases (Herrero *et al.*, 2016), of which nitrous oxide (N_2O) is a key player (Reay *et al.*, 2012).

In grazed pastures (i.e. agricultural grasslands) N deposition through ruminant urine drives the emissions of N_2O (Saggar *et al.*, 2013). In this system a full cascade of transformations begins with urea and can result in accumulation of any intermediate depending on conditions, but with a final end product of N_2 or N_2O. While the chemical transformations have been explored (Hamonts *et al.*, 2013; Baral *et al.*, 2014; de Klein *et al.*, 2014a; 2014b), mechanistic understanding of the populations catalyzing the reactions, and the purpose they serve for the organisms is less clear. In this study, we aimed to identify active N-transformation pathways as well as changes in microbial populations/taxa abundance and transcriptional activity for organisms involved in N loss (through gases) in response to urea (simulated ruminant urine deposition event) and varying moisture content. Observed chemical transformations were linked to changes in genotype (functional potential through DNA; a proxy for population changes), expression of genotype (RNA profiles), and total community composition (specific taxonomically defined populations based on the 16S ribosomal rRNA gene). We hypothesized that sequential transformation of nitrogenous intermediates would be coupled to changes in expression of functional genes catalyzing production and consumption of intermediates. Alternatively, transformations not linked to population, or expression changes, would be driven by other (abiotic) pathways. We also hypothesized that changes in transcription, or population size, could serve to determine life strategies of microbes utilizing each intermediate (whether they are used for growth vs. physiological maintenance). To test this we mimicked a ruminant urine-N deposition event using repacked soil cores (soil bulk density= 1.1 Mg m^{-3}) on tension tables monitored for 63 days. Soils were treated with urea under two different moisture contents: high (near saturation; -1.0 kPa) and low (field capacity; -10 kPa) moisture. Simultaneous measurements of soil chemistry, gas kinetics, microbial community composition (by 16S rRNA gene

amplicon sequencing) and functional gene abundance (for nitrification and denitrification) at DNA (gene) and RNA (transcript) levels were performed to determine the active populations and pathways.

5.2. Materials and methods

5.2.1. Sample collection and experimental design

A detailed methodology can be found in (Clough *et al.*, 2017). In brief, soil was collected from a permanently grazed agricultural grassland (dairy pasture) in March (early spring) at the Teagasc Moorepark Research Center, County Cork, Ireland (8°15'W, 52°9'N). The soil is classified as a Typical Brown earth from the Clashmore Series (Gardiner and Radford, 1980). Soil was sampled after the turf was removed and a spade was used to randomly sample the A-horizon (5-20 cm depth, excluding grass layer). To avoid fresh N loading, fields had not been grazed for over a month. Field moist samples were immediately shipped to Lincoln University, New Zealand and kept at 4°C until processed. Prior to use, soil was sieved (≤ 2 mm) to remove any stones, plant roots or earthworms and packed into stainless steel rings (7.3 cm internal diameter, 7.4 cm deep) to a depth of 4.1 cm at *in situ* soil bulk density (1.1 Mg m^{-3} with a gravimetric water content (θg) of 0.24 g water g^{-1} soil). The resulting cores had a total porosity of 0.58 cm^3 pores cm^{-3} soil and were arranged in a factorial experiment replicated four times. Soil cores were maintained at two moisture contents: high (near saturated; -1.0 kPa) and low (field capacity; -10 kPa) moisture using tension tables (Romano *et al.*, 2002). These moisture contents, -1 and -10 kPa respectively, corresponded to 53% and 30% volumetric water content, or 91% and 52% water-filled pore space (WFPS). Nitrogen was applied as a urea solution at 2141 kg urea/ha dry soil (equivalent to a single urination event at the higher rate expected under bovine urine deposition of 1000 kg N ha^{-1}). Four treatments in total were carried out (replicated four times each for a total of 112 cores analyzed) representing two levels of urea and two levels of moisture: urea + high moisture (HM +N; Urea _-1.0kPa), urea + low moisture (LM +N; Urea _-10kPa), no urea + high moisture (HM –N; No Urea _-1.0kPa) and no urea + low moisture (LM –N; No Urea_-10kPa). All cores where held at 20°C for a period of 63 days.

5.2.2. Soil pH, and inorganic-N measurements

Soil pH was monitored throughout the experiment using a flat surface pH electrode (Broadley James Corp., Irvine, California). Inorganic N concentrations (NH_4^+, NO_2^-, NO_3^-) were determined by destructively sampling batches of soil cores (16 soil cores, 4 treatments x 4 replicates) on days 0, 3, 7, 14, 21, 35 and 63. Each core was homogenized and a subsample was extracted (10 g dry soil: 100 ml 2M KCl shaken for 1 hour), filtered (Whatman 42) and analyzed using flow injection analysis (Blakemore *et al*., 1987). N_2O flux was determined by placing a soil core into a 1-L stainless steel tin fitted with a gas-tight lid and rubber septa. The headspace was sampled after 15 and 30 minutes and analyzed using an automated gas chromatograph (8610; SRI Instruments, Torrance, CA), linked to an autosampler (Gilson 222XL; Gilson, Middleton, WI) as previously described (Clough *et al*., 2006).

5.2.3. Nucleic acids extraction

Samples for RNA and DNA extraction were collected simultaneously with samples for inorganic N analysis, but only samples at 0, 7, 14, 21, 35, 63 days were processed for nucleic acids. Each biological replicate was extracted and analyzed separately. For each extraction 2 g (wet weight) of soil were processed using the PowerSoil Total RNA Isolation and DNA Elution Accessory Kits (MoBio, Carlsbad, CA) as per manufacturer's instructions, with slight modifications. Bead beating was done in a Geno/Grinder 2010 (SPEX SamplePrep, LLC, Metuchen, NJ) using two rounds of beating (1750 strokes/min) for 15 s with a 1 min pause in between. The total elution volume for RNA and DNA was 60 µl and 100 µl respectively. RNA was treated with DNase I (RNase-Free) (New England Biolabs, USA) as per the manufacturer's protocol. RNA quality was assessed by denaturing gel electrophoresis. RNA and DNA concentration, purity and humic acid contamination were determined using a Nanodrop Spectrophotometer, ND-1000 (Thermo Scientific). All extractions were stored at -80 ^{o}C until downstream analyses.

5.2.4. Reverse transcription (RT)

Triplicate cDNA conversions (technical replicates) were performed for each RNA extraction using the Maxima H Minus First Strand cDNA Synthesis Kit (Thermo Scientific) according to manufacturer's protocol. Each 20 µl reaction contained: 13 µl of RNA (208 ng Total RNA), 1 µl of random hexamers (100 pmol), 1µl of dNTP mix (0.5 mM final conc.) and 5 µl of master mix (4 µl of 5X RT buffer and 1 µl Maxima H

Minus reverse transcriptase). All technical replicates for a sample were combined and stored at -80°C until further analysis. All further analyses were performed on the same cDNA pool for each sample.

5.2.5. 16S rRNA gene amplicon sequencing

16S rRNA gene amplicon sequencing was performed using primers 515F/806R (V4 region of the 16S gene) and the Earth Microbiome Project conditions (Version 4_13) (Caporaso *et al.*, 2012). All samples were run simultaneously on a single Illumina MiSeq run. Sequences were first processed in Qiime (version 1.9.1) using default parameters (Caporaso *et al.*, 2010). Sequences were clustered into Operational Taxonomic Units (OTUs) at 97% sequence similarity using the SILVA (version 119) reference library (Quast *et al.*, 2012) and UCLUST (Edgar, 2010) following the open-reference Operational Taxonomic Unit (OTU) picking protocol. Taxonomic identification was done using BLAST against the SILVA database (max-e value = 0.001) (Altschul *et al.*, 1990). Subsampling and rarefactions (10 times) were performed to equal read depths of 7,400 per sample, and samples below that threshold were removed. After rarefaction, all 10 OTU tables were merged and exported for further processing in R (R Development Core Team, 2008).

5.2.6. Quantification of gene and transcript abundance

Quantitative PCR (qPCR) was performed in 384-well plates using the ViiA7 real-time PCR system (Applied Biosystems, Carlsbad, CA). Absolute quantification was done using a 10-fold serial dilution (10^8 to 10^1) of known copy numbers of pGEM-T easy (Promega, Madison, Wisconsin, USA) cloned templates as standards. For all targets qPCR runs included cloned standards, no template control and no reverse transcription controls (RNA) run in triplicate. No inhibition or positive amplification on negative controls was observed for any target. All DNA and cDNA samples were run in quadruplicates to determine abundance of: prokaryotes (16S rRNA gene), ammonia oxidizers (archaeal [AOA] & bacterial [AOB] ammonia monooxygenase gene; *amoA*), denitrifiers (cytochrome cd1-type nitrite reductase gene; *nirS,* and Clade I nitrous oxide reductase gene; *nosZI*) and nitrogen fixers (nitrogenase gene; *nifH*).

All reactions were performed in 10 µl volumes containing: 1× Master Mix (Fast SYBR Green Master Mix, ABI), 0.2-0.6 µM of each primer [0.2 µM for AOA (Tourna *et al.*, 2008), 0.6 µM for AOB (Rotthauwe *et al.*, 1997; Avrahami *et al.*, 2003) 0.5 µM for 16S rRNA (Hartman *et al.*, 2009); *nirS* (Throbäck *et al.*, 2004; Yergeau *et al.*, 2007)*, nosZI* (Henry *et al.*, 2006) & *nifH* (Rösch and Bothe, 2005)], 2 µl of template [DNA (1 ng total) or cDNA (80× diluted RT reaction, i.e. total 0.13 ng RNA)] and autoclaved Milli-Q H_2O to a final volume of 10 µl. Primers and qPCR conditions are summarized in Table S5.1. A melt curve analysis (95°C for 15 s, 60°C for 1 min then increasing 0.05^{o}C/s (data acquisition) until 95°C) was performed to test for specificity and to confirm no amplification in the negative controls.

5.2.7. Statistical analyses

All statistical analyses were performed in R (R Development Core Team, 2008) using the phyloseq (McMurdie and Holmes, 2013), pvclust (Suzuki and Shimodaira, 2006), vegan (Oksanen *et al.*, 2013) and mpmcorrelogram packages. Detailed descriptions can be found in supplemental methods.

5.2.8. Growth rate estimation and prediction of rRNA operon (rrn) copy numbers

rrn copy numbers for identified OTUs were predicted using the ribosomal RNA operon copy number database (*rrn*DB) (Stoddard *et al.*, 2015). For each OTU, information from the closest strain available was selected. In instances where a closely related organism was not available, the mean copy number for the closest taxonomic group (i.e. genus, class, etc.) was used. Copy numbers where then compared to the maximum observed abundance and the maximum observed fold change (calculated based on lowest observed abundance for the same organism in a preceding time point for OTUs showing growth or succeeding time points for those decreasing in abundance). An estimated growth rate was calculated for OTUs showing increases in population size in response to N using the following formula:

$$N_t = N_0 * e^{rt}$$

where: N_t: The amount at time t; N_0: The amount at time 0; r: exponential growth rate; t: Time passed

5.2.9. Fit model for *rrn* copy numbers

Both non-linear (Michaelis-Menten) and linear regressions were used to fit *rrn* copy numbers and population changes (i.e. maximum abundance and fold-change), and growth rate (per day). The fit model was performed in R using "drc" and "ggplot2" packages.

5.3. Results

5.3.1. Soil pH and N transformation dynamics in response to urea

Soil pH increased from acidic (pH = 5.5 ± 0.1, i.e. mean ± SD) to alkaline reaching a maximum (pH = 8.7 ± 0.2) at day 3 in urea treated soils. Return to baseline pH was modulated by soil moisture with high moisture (HM; -1.0kPa) soil reaching baseline at day 35 and low moisture soils (LM; -10kPa) doing so at day 53 (Figure 5.1). This shift in pH was linked to a successive N transformation process initiated with urea hydrolysis and leading to nitrification and denitrification: urea → NH_4^+ → NO_2^- → NO_3^- → N_2O →N_2 (Figure 5.1). Sequential peak activity was observed for each transformation with the response modified by moisture. Maximum production (mean µg N g^{-1} soil) for each transformation was observed at day 3, 21 and 35 respectively for NH_4^+ (HM+N = 1758; LM+N= 1730), NO_2^- (HM+N = 79.2; LM+N= 39.7) and NO_3^- (HM+N = 429.2; LM+N= 335). Two distinct production peaks were observed for N_2O, with a short pulse (0 to 5 days) reaching a maximum at day 2 for HM soils (11602.8 µg m^{-2} h^{-1}) and day 3 for LM soils (46.8 µg m^{-2} h^{-1}) (Figure 5.1 and Supplementary Fig. S5.1). A second, longer duration (10 to ~50 days), N_2O pulse reached a maximum at day 28 for HM soils (6405.1 µg m^{-2} h^{-1}) and day 30 for LM soils (448.9 µg m^{-2} h^{-1}). The large N_2O spike (first peak) between days 0 to 5 in the HM+N treatment was about 11.6% of the total N_2O cumulative flux over 63 days, whereas in the LM+N treatment the 0 to 5 day periods accounted for 22.3% of the total N_2O cumulative flux over 63 days.

5.3.2. Population and transcription dynamics for nitrogen related functional groups

Significant changes (ANOVA, $p<0.05$) in relative activity (mRNA abundance/16S rRNA gene abundance) were observed promptly between day 0 & 3 for all functional groups (except AOA and N-fixers in HM soil) in response to urea (Figure 5.1). However, maximum relative transcription did not match maximum

production peaks for corresponding substrates, or products, for each functional group. Nitrifiers (ammonia oxidizers) displayed niche differentiation, with time, length and strength of response differing between bacterial (AOB) and archaeal ammonia oxidizers (AOA). Relative activity of AOA increased (4.6-fold for LM and 1.6-fold for HM) under urea treatments at day 3 only, with a subsequent decrease (-19.3-fold for LM and -7-fold for HM) resulting in lower expression than in untreated soils (Figure 5.1). AOB relative activity also increased but was sustained for a much longer period (3-63 days), with maximum activity (>11-fold change) seen at 21 and 35 days for HM+N and LM+N respectively (Figure 5.1). Denitrifiers (both nitrite and nitrous oxide reducers) showed similar responses as AOA, with peak activity at day 3 and a rapid return to baseline, in the case of nitrite reducers decreasing to levels below those observed in non-urea treated soils (Figure 5.1). To account for endogenous sources of N, N_2 fixers were monitored through the activity of the nitrogenase gene (*nifH*). No significant changes were observed except for day 3 (LM +N only), with a subsequent decrease in activity below background. This decrease below background was observed for all N treated samples.

Changes in the relative contribution to total community composition were calculated by normalizing functional gene abundance to total 16S rRNA gene abundance per sample for each functional group (Figure 5.1). The maximum observed relative abundance of each functional group differed for each group (HM|LM, respectively): AOB, 19|12%; AOA, 8|13%; *nirS*, 6.3|2.9%; *nosZI*, 3.3|3.4%; *nifH*, 4.7|4.32%. Further, large population changes over time were mostly limited to AOB. Generally, AOB comprised <1% of the total community, but in response to urea increased up to 29-fold to make up 19% (day 21 for HM) and 20-fold to make up 12% (day 35 for LM) of the community in urea treated soils. In contrast, AOA were found at consistently high levels (median=4.2%) in untreated soils, but numbers decreased >7-fold in response to urea (~1.3% at least 63 day). Similarly, other functional groups (*nosZI*, *nifH*) decreased or remained stable (*nirS*) in response to urea. Similar patterns for both activity and population changes were observed when absolute values were analyzed (Supplementary Fig. S5.2).

5.3.3. N deposition induces both a genotypic and a transcriptional response at the community level that is modified by soil moisture content

Urea deposition imposed a general negative selective pressure leading to decreases in OTU level prokaryotic diversity (Shannon, -1.2-fold change), richness (-1.5-fold change) and evenness (-1.1-fold change) at DNA level (Figure 5.2a, Supplementary Fig. S5.3). The same pattern was observed when active microbes (based on RNA) were analyzed with decreases in OTU level prokaryotic diversity (Shannon, -1.3-fold change), richness (-1.9-fold change) and evenness (-1.2-fold change). Moisture was found to have a smaller, but significant, effect compared to urea, with LM samples consistently resulting in lower diversity and richness when compared to their HM pairs. Richness and diversity losses were not recovered even after 63 days. In contrast, samples where no urea was applied remained stable (i.e. constant diversity and richness).

Urea deposition significantly altered community structure (Adonis test: $F= 18.04$, $p< 0.001$ for 16S rDNA and $F= 26.27$, $p< 0.001$ for 16S rRNA) as shown in a non-metric multidimensional scaling (NMDS) plot using a Bray-Curtis dissimilarity matrix (Figure 5.2b and Supplementary Fig. S5.4). At both DNA and RNA level community changes along the first axis corresponded with changes in response to urea treatment, with the second axis accounting for changes in moisture. A pvclust analysis (hierarchical clustering with p-values calculated via multiscale bootstrap resampling, Supplementary Fig. S5.5) confirmed two major clusters [100% AU (Approximately Unbiased) and 100% BP (Bootstrap Probability)] formed by urea treated (HM+N and LM+N samples, excluding day 0), vs. untreated soils (HM-N, LM-N, field samples, and HM+N & LM+N at Day 0). Temporal variance within each cluster was confirmed using a Mantel correlogram analysis (Figure 5.2c). Urea treated samples had significant changes in community composition immediately upon treatment (Day 0 to 7), with no return to baseline conditions by the end of the experiment. In contrast, untreated samples did not change significantly over time (Supplemental Fig. S5.6)

Changes in community structure were associated with shifts in major taxonomic lineages (Figure 5.3). In general, phylum level changes in abundance and transcription where correlated to each other (Supplementary Table S5.2 and Fig. S5.7, S5.8). Urea deposition induced temporal changes in phylum level abundance with observed maximum fold changes per group (HM & LM at DNA level) being: Acidobacteria, -4.6 & -3.7; Actinobacteria, 2.4 & 5.3; Bacteroidetes, 4.6 & 2.2; Candidate Division WS3, -10.5 & -7; Chloroflexi, -2.9 & -2.6; Firmicutes, 10.8 & 16.2;

Gemmatimonadetes, 2 & 3.3; Nitrospirae, -3.2 & -2; Planctomycetes, -3.7 & -2.5; Thaumarchaeota, -5.2 & -3.6; Verrucomicrobia, -2.5 & -2; Alphaproteobacteria, 1.4 & 1.7; Betaproteobacteria, 4 & 2; Deltaproteobacteria, -2.2 & -1.4; Gammaproteobacteria, 1.5 & 2.6. Normalized transcriptional activity (reads of 16S rRNA/reads of 16S rDNA) identified the Firmicutes and members within classes of the Proteobacteria as the most transcriptionally active. While abundant phyla tended to have high levels of normalized transcription, less abundant organisms like the Thaumarchaeota, were observed to have high normalized transcriptional activity especially under background conditions (Supplementary Fig. S5.7). In contrast, groups traditionally considered slow growers (e.g. Nitrospirae and Gemmatimonadetes) had low normalized transcription. It was also noted that while normalized transcription levels remained stable without urea, N deposition induced changes. These changes in normalized activity did not always match trends observed at individual DNA or RNA level (e.g. Firmicutes).

5.3.4. Shifts in N and moisture status trigger OTU response linked to divergent life strategies

Since Figure 5.3 only represents a taxonomic summary of all OTUs (irrespective of their response to treatments), it does not provide a clear indication of who is changing and why. To account for this, urea responsive OTUs were identified independently in RNA and DNA profiles (under each treatment) through a SIMPER analysis. OTUs accounting for 50% of the variance were analyzed (Figure 5.4). Response patterns for detected OTUs were conserved between RNA and DNA profiles. However, while some OTUs responded similarly to urea under varying moisture conditions, marked differences were observed with no detectable pattern based on taxonomy.

OTUs within the Proteobacteria identified in the SIMPER analysis did not display a conserved response to urea, however when lower taxonomic levels were examined patterns emerged. A consistent positive response was seen for OTUs within the class Betaproteobacteria and the family Hyphomicrobiaceae, amongst others. Positive responses to urea were also observed at the phylum level for the Firmicutes, Bacteroidetes, Actinobacteria, Gemmatimonadetes and Planctomycetes, although the level of response varied across lower taxonomic levels. In contrast, with only some exceptions, OTUs within the phyla Acidobacteria, Verrucomicrobia,

Nitrospirae, Candidate Division WS3 (also referred to as candidate phylum Latescibacteria) and the Thaumarchaeota all were negatively impacted by urea deposition.

To account for response patterns over time, we focused on OTUs that accounted for 30% of the variance in the SIMPER analysis (36 total), with individual OTU contributions ranging from 5 to 0.1 percent at the DNA level and 5 to 0.06 percent at the RNA level. Temporal patterns were conserved between DNA and RNA profiles (Supplementary Fig. S5.9, S5.10), despite differences in absolute abundance. Once again, moisture acted as a modulator of response with the extent of impact dependent on the OTU (Figure 5.5 and 5.6). While most functional groups responded immediately (at both DNA and RNA level), positively affected OTU responses were observed along all time points creating a succession of positively selected organisms. In contrast, negatively affected OTUs all responded within the first 2 time points indicating an immediate negative selective pressure (Figure 5.6). Large variances in absolute changes were observed, even within similar organisms (e.g. Pedobacter), with fold changes ranging from -10.5 to 410 across both positively and negatively affected OTUs. Despite this, OTU response was noted to correspond to taxonomy, with both the effect (positive or negative) and the extent of response (fold change or total abundance) in line with predicted ecological growth strategies (r vs. k) predicted for different taxa. To test this, we predicted rRNA operon copy numbers (*rrn*) for all 36 OTUs and compared them to the observed maximum abundance, max fold change in population or observed growth rate per day. We consistently observed a non-linear response with an asymptote reached at higher copy numbers (Figure 5.7). These trends were consistent independent of which moisture conditions were present at the time of response. To account for preferential response due to moisture, we selected the highest response for each organism and saw no clear difference in patterns. To account for potential biases due to uneven representation, OTUs were grouped into low (1-2 copies of *rrn*) or high (>2) copy number organisms (Supplementary Table S5.3). While significant changes ($p < 0.05$, Supplementary Fig. S5.11) were observed in most instances, exceptions were noted (e.g. growth rate under HM).

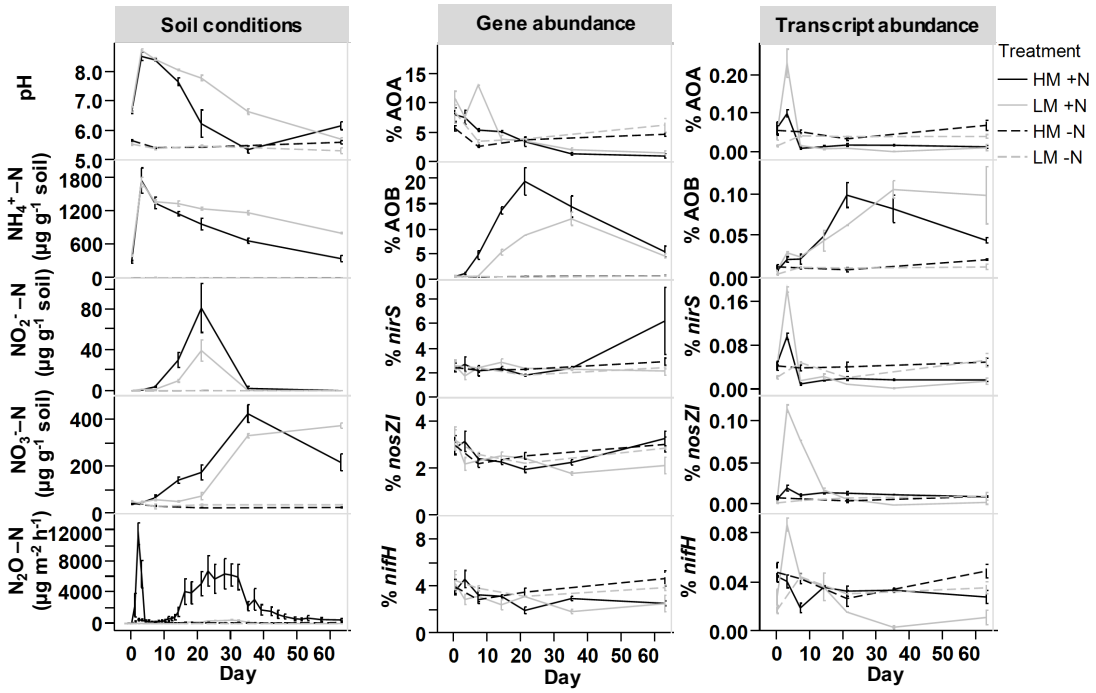

Figure 5.1. Chemical transformations and biological (functional group) response in soils treated with urea (+/- 1000 µg N/g dry soil) under two moisture conditions (LM = low moisture [-10kPa]; HM = high moisture [-1.0kPa]). Error bars are the standard error of the mean (n ≥ 3, except gene abundance data of day 7 [n=1; LM soil] and day 21 [n=1; LM soil]) for replicate mesocosms. Gene and transcript abundance were measured by qPCR targeting: nitrifiers (AOA, ammonia oxidizing archaea; AOB, ammonia oxidizing bacteria), denitrifiers (nirS, cytochrome cd $_1$-containing nitrite reductase; nosZI, nitrous oxide reductase) and nitrogen fixers (nifH, nitrogenase reductase). All qPCR results are normalized to 16S rRNA copy numbers and presented as percent of the nucleic acid pool.

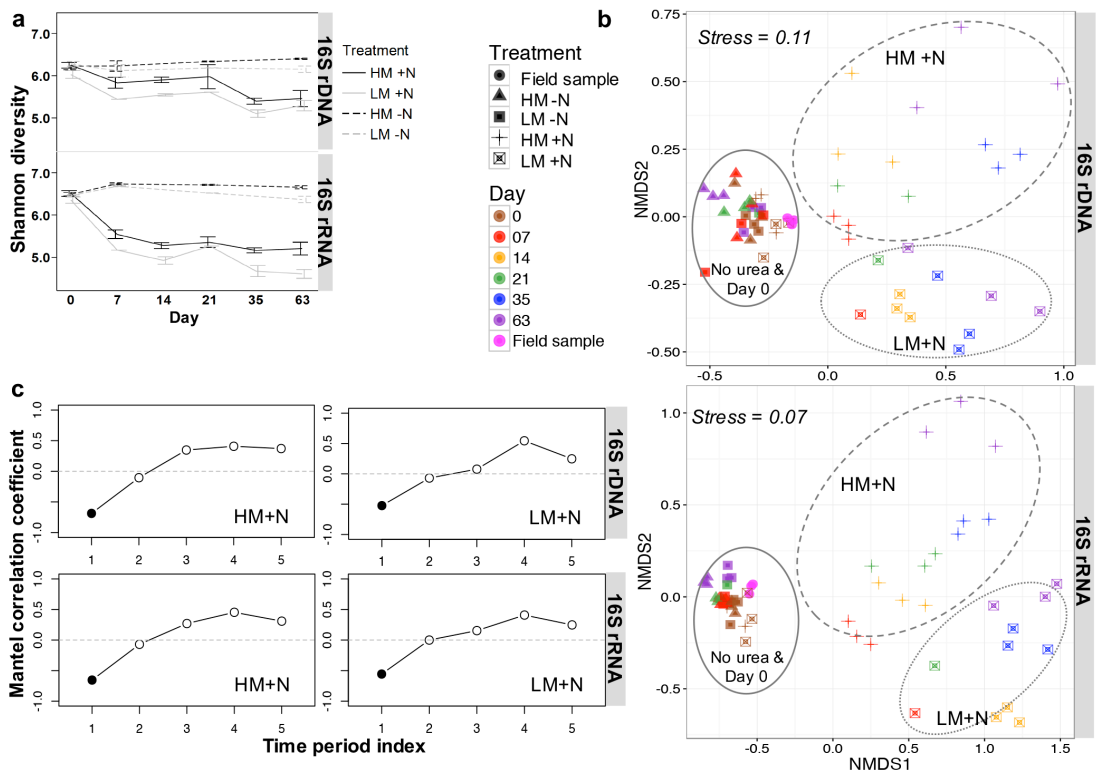

Figure 5.2. Total microbial community response (based on 16S rRNA gene amplicon profiling and clustering of sequences at OTU level (97% sequence similarity)) to urea (+/-1000 µg N/g dry soil) under two moisture conditions (LM = low moisture [-10kPa]; HM = high moisture [-1.0kPa]) at both DNA and RNA level. Error bars are the standard error of the mean (n = 3, except day 7 [n=1; LM soil] and day 21 [n=1; LM soil]) for replicate mesocosms. (a) Changes in microbial diversity (Shannon) index over time in response to treatment. (b) Non-metric multidimensional scaling (NMDS) ordination plots based on Bray-Curtis distances showing relationships among samples based on OTU level changes in community composition. (c) Mantel correlogram showing autocorrelation on community composition by performing sequential Mantel tests between the Bray-Curtis dissimilarities and the grouping of samples using a time period index (index 1 represents 0-7 days; 2 represents 7-14; 3 represents 14-21; 4 represents 21-35; 5 represents 35-63). Filled circles represent significant correlation ($p < 0.05$) in community composition at specific time periods, with open circles indicating no significant correlation.

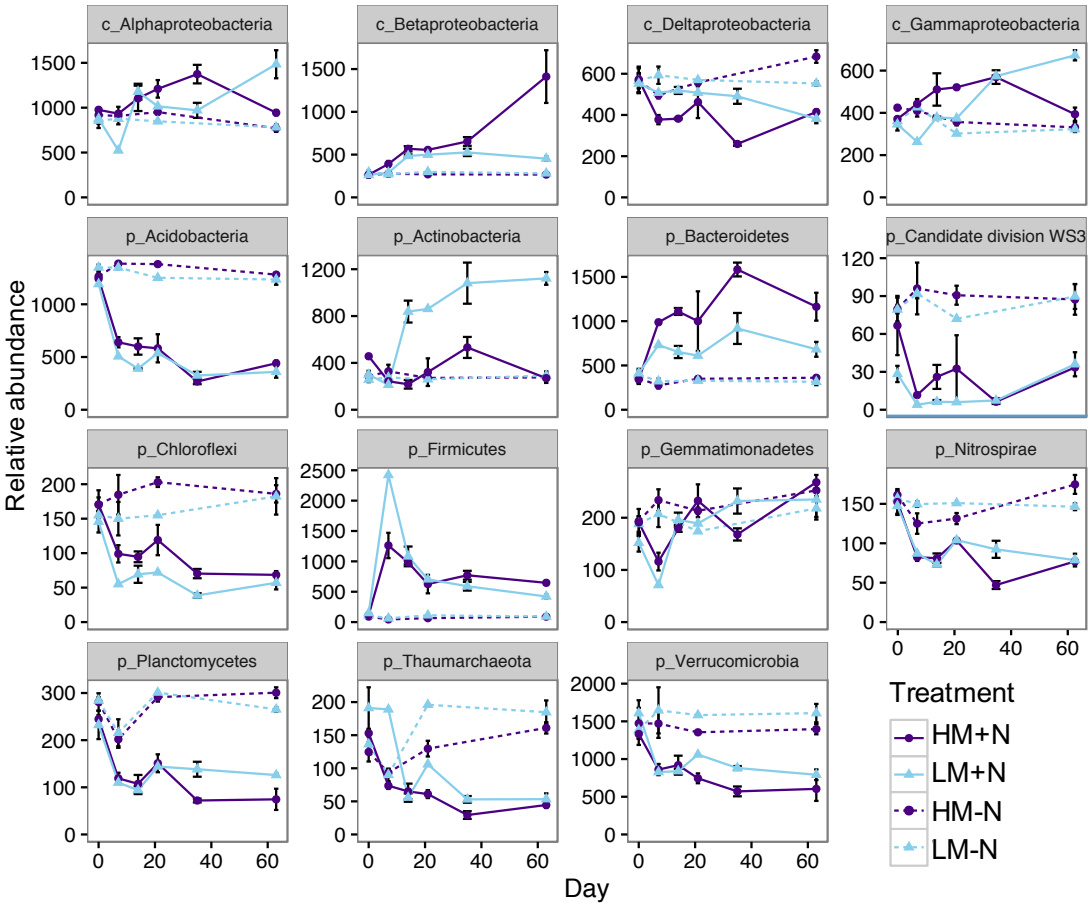

Figure 5.3. Phylum and class level (for Proteobacteria only) changes in abundance (DNA) representing relative contribution >1% of all detected phyla (based on OTUs clustered at 97% sequence similarity). A total of 7,400 sequences were examined per sample. Error bars are the standard error of the mean (n = 3, except day 7 [n=1; LM soil] and day 21 [n=1; LM soil]) for replicate mesocosms. Treatments = +/- N [+/-1000 µg N/g dry soil] under two moisture conditions (LM = low moisture [-10kPa]; HM = high moisture [-1.0kPa]). Abbreviations: c: Class; p: Phylum. See supplemental Fig. S8 for relative abundance

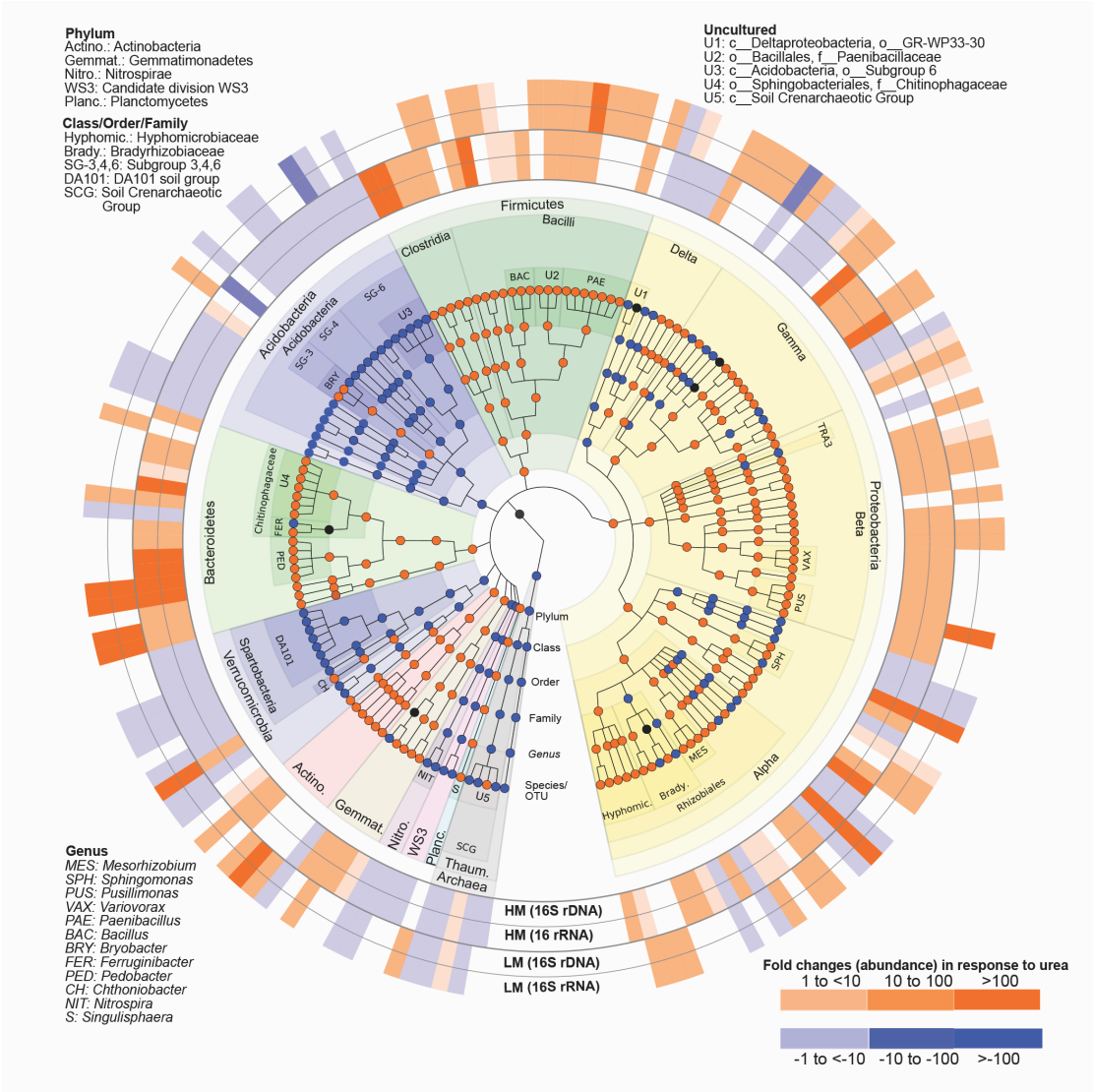

Figure 5.4. Taxonomic summary of OTUs responsive to urea treatment identified through similarity percentages (SIMPER) analysis (representing top 50% cumulative sum). The 4 outer rings represent fold changes in response to urea under high and low moisture content (MH & LM respectively) at either DNA or RNA level, with blank gaps indicating OTUs not identified in SIMPER analysis under the specified ring condition. Nodes on the tree (moving outwards from center) correspond to taxonomic level [Domain, Phylum, Class, Order, Family, Genus and Species/OTUs]. Nodes are colored based on dominant response (>50% conserved fold change response across OTUs within a node) with black notes indicating equal representation of positive and negatively responding OTUs. Shaded areas of branches delineate defined taxonomic groups.

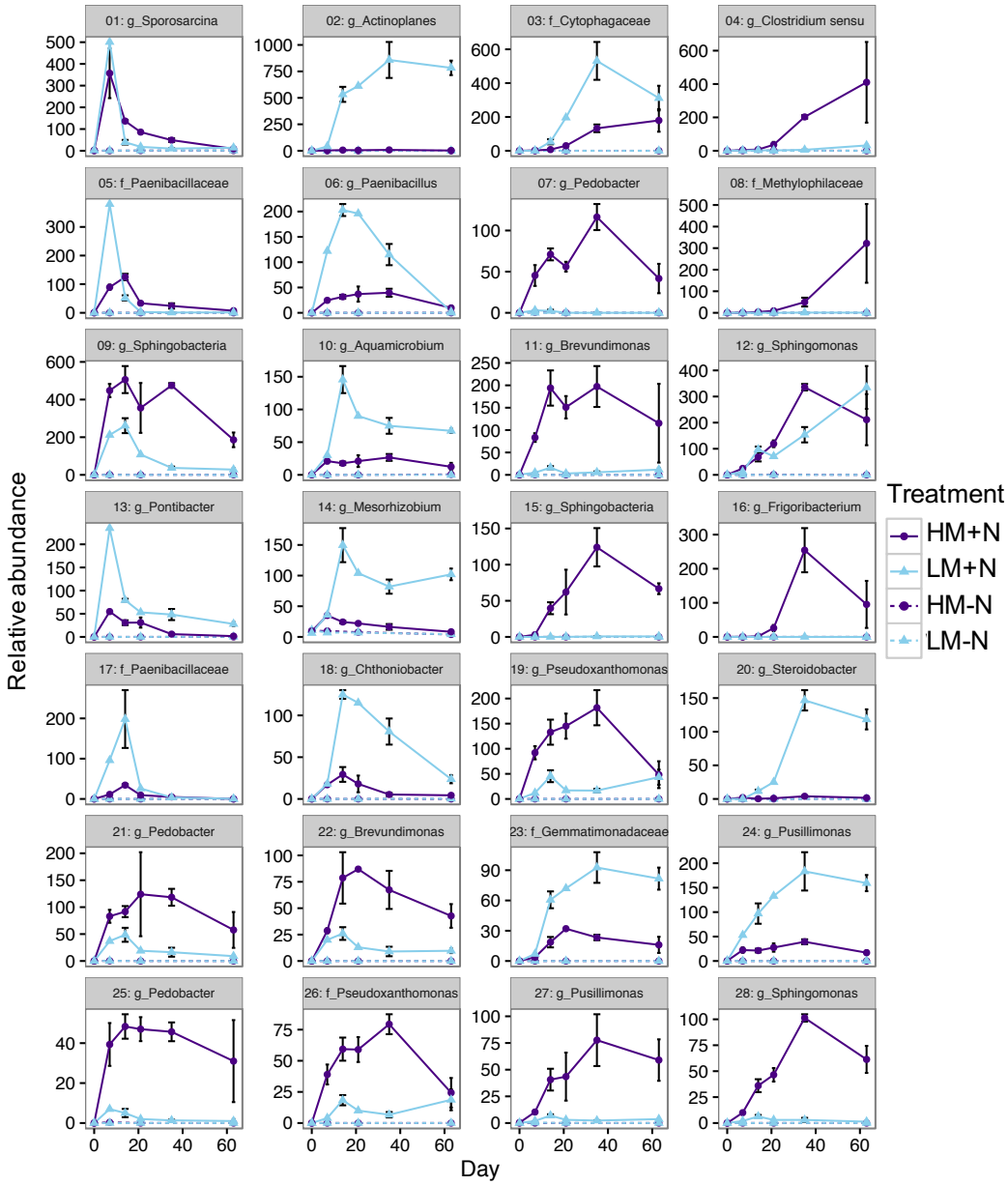

Figure 5.5. Population (16S rDNA) changes (abundance based on 7400 reads per samples) for OTUs identified as positively responsive to urea treatment based on similarity percentages (SIMPER) analysis (representing top 30% cumulative sum). Treatments = +/- N [+/-1000 µg N/g dry soil] under two moisture conditions (LM = low moisture [-10kPa]; HM = high moisture [-1.0kPa]).

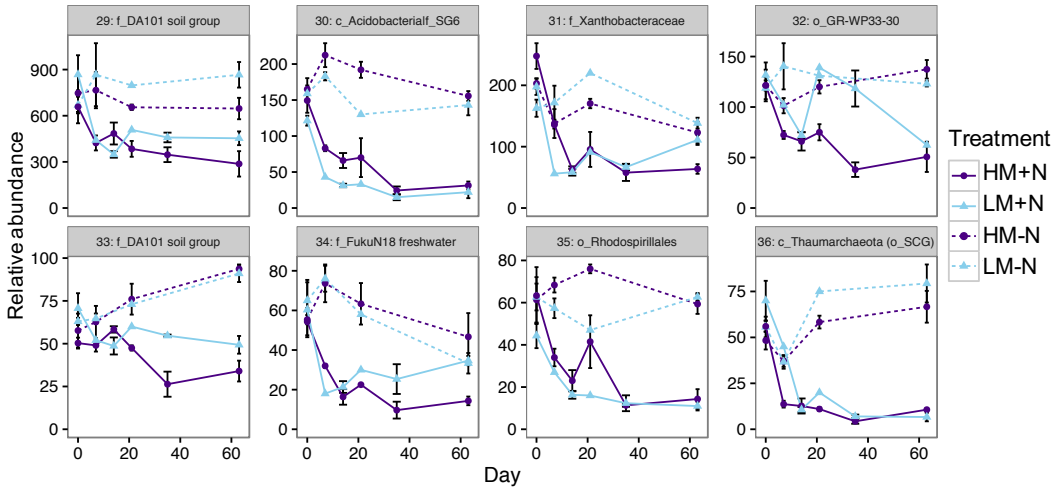

Figure 5.6. Population (16S rDNA) changes (abundance based on 7,400 reads per samples) for OTUs identified as negatively responsive to urea treatment based on similarity percentages (SIMPER) analysis (representing top 30% cumulative sum). Treatments = +/- N [+/-1000 µg N/g dry soil] under two moisture conditions (LM = low moisture [-10kPa]; HM = high moisture [-1.0kPa]).

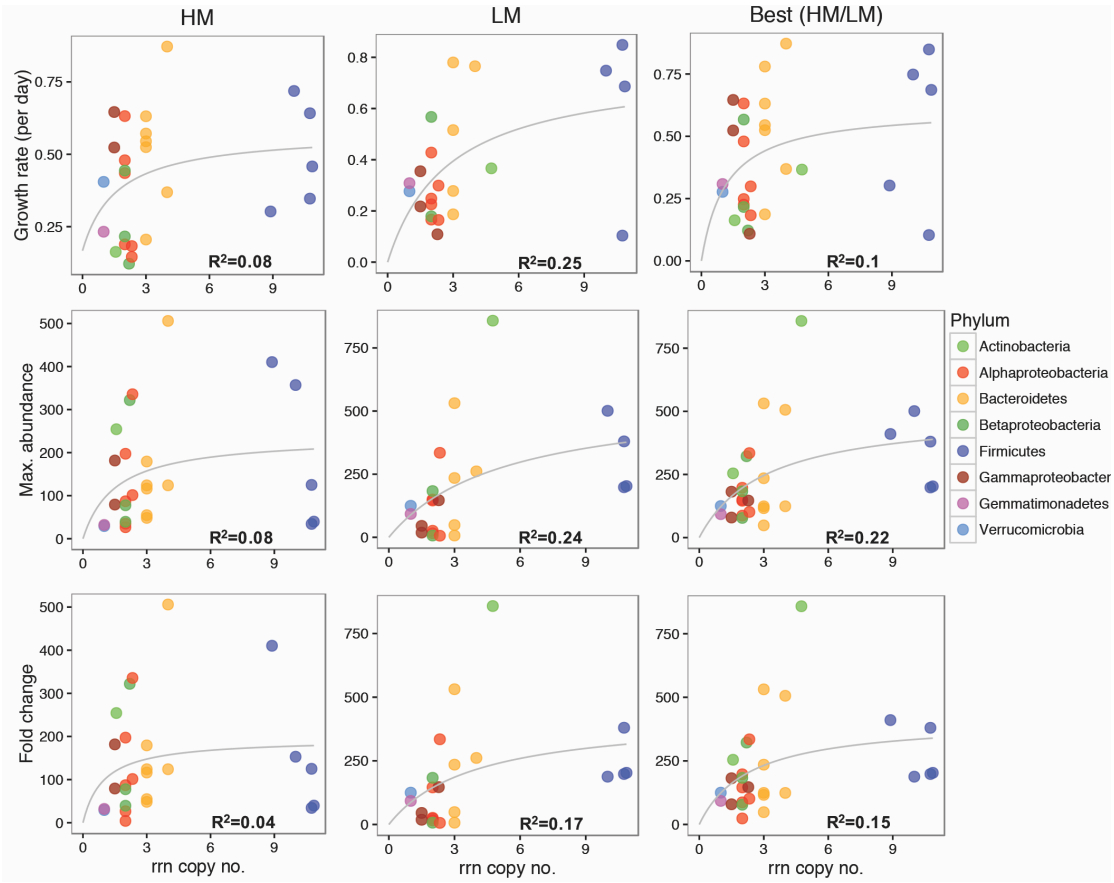

Figure 5.7. Relationship between predicted ribosomal RNA operon (*rrn*) copy numbers and growth rate (per day), maximum observed population change, or fold change in response to N treatment under both high moisture (HM) content, low moisture (LM) content and best growth either in HM or in LM (based on maximum observed growth). Copy number was estimated using *rrn* database (Stoddard *et al*., 2015). Copy number values were obtained by finding the closest match (lowest taxonomic level possible) to each OTU and retrieving the mean rRNA copy number for that group.

5.4. Discussion

Functional profiling (identification and quantification of specific functional genes/transcripts) is normally utilized to link chemical transformations to specific microbial populations capable of catalyzing reactions. However, functional groups are comprised of taxonomically diverse species of microbes with different lifestyle strategies that are unlikely to share a conserved response to an ecosystem disturbance (Ho *et al.*, 2012). While functional profiling allows us to measure the net response of a functional group, and could serve as a proxy for determining the importance of the group in a sample, it does not identify how specific organisms benefit from a catalyzed transformation. Here we used a controlled microcosm experiment to measure the response of soil communities to a disturbance in the form of changes in moisture and nitrogen (urea) deposition. Functional analysis (qPCR) demonstrated a biological response to urea, but differing responses to moisture depending on group (Figure 5.1). Responses are potentially linked to different life strategies amongst these groups. Ammonia oxidizers displayed contrasting population and expression profiles, suggesting niche differentiation driven by time and/or substrate concentration. AOA responded early, and declined as new N was made available while AOB responded later with population swings spanning from near detection limit to most dominant group. These observations match prior reports showing AOA prefer low N concentrations, while AOB respond vigorously to N deposition (Di *et al.*, 2010; Sterngren *et al.*, 2015). This has been interpreted as evidence for differing lifestyles for AOB and AOA, with AOA preferring nutrient poor conditions and AOB dominating in rich ones (Sterngren *et al.*, 2015). However, prior assertions that AOB are solely important for driving nitrification might be overstated given that transcriptional activity for both groups is comparable if compared at peak time (Di *et al.*, 2009). This contrasting use of energy between functionally redundant organisms might explain the low correlations between processes and the abundance of their respective functional populations (Rocca *et al.*, 2015). When we examine the response of other functional groups benefiting from influxes of N, like denitrifiers, we see no significant change in population sizes suggesting that either energy is being utilized for physiological maintenance or otherwise for redox balance/homeostasis (Hartsock and Shapleigh, 2011; Li *et al.*, 2012; Dietrich *et al.*, 2013). The distinction here being that we use the term physiological maintenance as it refers to the state of energetics in a cell where the energy consumed is used for functions other than the

production of new cell material (i.e. growth) (van Bodegom, 2007; Lipson, 2015). Alternatively, redox balance reactions are used to maintain viable metabolic processes by controlling the redox state of all the cellular components (Green and Paget, 2004). In contrast, organism adapted to low N concentrations, like N fixers, decline in response to exogenous N demonstrating real time selective pressure in a complex ecosystem. These responses also highlight the temporal nature of these relationships and how by following niche differentiation high number of functionally redundant organisms can be maintained (Stempfhuber *et al.*, 2015). However, the use of very high concentrations of urea (leading to rapid hydrolysis to ammonium followed by substantial nitrification) has major consequences for soil pH, physicochemical parameters, and potentially other factors (e.g. osmolarity). Without accounting for those it is unclear what the direct mechanism causing an increase or decrease in the relative abundance of a specific population is.

Despite this, our observations highlight how lifestyle preferences for organisms may be reflected in their dominance in the ecosystem. Prior work suggests that AOA dominate in soils with low N inputs, but AOB numbers are higher at times of high N loading or in ecosystems with consistent N deposition (Gong *et al.*, 2013; Sterngren *et al.*, 2015; Venterea *et al.*, 2015; Li *et al.*, 2016). This would suggest that a dynamic ecosystem with varying nutrient levels would select for a higher diversity of organisms that maintain ecosystem processes stable over time and space (Wang and Loreau, 2014). Indeed, our data supports this with alpha diversity (calculated based on 16S amplicon analysis at both DNA and RNA) decreasing in response to urea. This is inconsistent with plant responses to nutrient deposition in which multiple resources need to be added to elicit a response (Harpole *et al.*, 2016), although contrasting results have been observed (Suding *et al.*, 2005; Bai *et al.*, 2010; Song *et al.*, 2011; 2012). For microbes, high site to site variance is reported (De Schrijver *et al.*, 2011; Leff *et al.*, 2015), but similar negative responses are suggested and could be linked to increased competition in the absence of natural ecosystem variability. However, links between microbial and plant response suggest interplay between the response of macro and microbiota (Zeng *et al.*, 2016). While previous work suggests an important role for moisture in controlling community composition (Waldrop and Firestone, 2006), we only observed a modifier role in our experiment.

Although broad observations align with ecological theory, precise identification of responsive organisms is rarely carried out. Here we note that while at phylum level

clear responses (+/- fold change) are observed, variance is seen at the OTU level suggesting intra-taxonomic (i.e. same phylum but different species or OTUs) diversity. We hypothesized this reflects the life history strategies of the different organisms. Attempts to link specific transformations to organisms failed, potentially due to the succession of functionally redundant organisms that respond at different time with non-overlapping optima. That is, while functional gene abundance provides the population size of organisms capable of carrying out a process, the group may be composed of many OTUs with divergent life strategies or metabolic potentials that affect when they can respond. This makes functional gene measurement an average of all OTU subpopulations carrying that gene. However, community response allows us to identify OTUs responsive to N deposition, which when analyzed independently, provides insights into metabolic preferences (i.e. aerobic vs. anaerobic, nitrifier vs. denitrifier) based on time and response to treatments. Taxonomic groups regularly recognized as native to, or abundant in, oligotrophic conditions declined in the presence of urea. Most of these groups are still poorly understood, and included the Acidobacteria, Verrucomicrobia, Nitrospirae, Candidate Division WS3 (also referred to as candidate phylum Latescibacteria) and the Thaumarchaeota. These organisms are predicted to be slow growers with the Thaumarchaeal response confirming the AOA patterns observed at the functional level. In contrast, positively responding organisms are those generally associated with groups considered eutrophic or capable of fast response. This discrepancy based on life history strategies has been proposed and applied to microbes previously, and suggests that an organisms' ability to grow, utilize carbon, generate proteins and efficiently transform resources to biomass, amongst others, is related to its rRNA operon copy number (Klappenbach *et al.*, 2000; Stevenson and Schmidt, 2004; Dethlefsen and Schmidt, 2007; Roller *et al.*, 2016). When applied to communities, it is associated with microbial successions in which decreases in copy numbers are associated with later stages of succession including in soils (Nemergut *et al.*, 2015). For example, two OTUs matching the Verrucomicrobial OTU DA101 where found to be negatively affected by urea, and at least one was found to be highly abundant under background conditions. DA101 seems to be a common soil (and grassland) organism identified throughout the world (Felske and Akkermans, 1998; O'Farrell and Janssen, 1999; Brewer *et al.*, 2016). Based on growth (Sangwan *et al.*, 2005) and genome reconstructions (Brewer *et al.*, 2016), these organisms are predicted to be slow but efficient growers (k strategists). In contrast, most of the positively affected organisms seemed to posses higher *rrn*

copy numbers and included members of the Proteobacteria and Bacteroidetes in line with prior predictions (Fierer *et al.*, 2007). Statistical analysis supported this interpretation with low copy numbers (1-2) significantly associated to a negative response to N deposition, while high copy numbers (>2) were linked to increased capacity for growth, growth rate and maximum abundance. However, we found a non-linear relationship between increased *rrn* copy numbers and growth capacity, best fitted by models reaching an asymptote. These are first order models that suggest that while a benefit exists where increased copy numbers lead to increased growth rate, after a certain threshold other variables might limit any benefit. Alternatively, a decrease in growth rate might be observed with increasing copy numbers once a tradeoff threshold is passed (Lipson, 2015). However, when *rrn* copy numbers are log2 transformed, a significant linear fit was observed as seen in prior studies (Roller *et al.*, 2016). In our study these predictions are made complicated due to the observed intra-taxonomic variance that can arise from the lack of accurate knowledge of copy numbers for many organisms, or from metabolic plasticity at higher taxonomic levels. In addition, our analysis focused on N responsive organisms only, and with only 38 identified it indicates that most organisms were neither positively nor negatively affected. This could explain why certain organisms (e.g. Actinobacteria) expected to be k strategist, based on their ability to produce secondary metabolites (Abdelmohsen *et al.*, 2015) and compete with other organisms (Barka *et al.*, 2015), showed a positive response to N deposition. Alternatively, the low number of responsive organisms could indicate that our false discovery rate corrections were too restrictive.

These findings help us get closer to understanding not just the metabolic potential of organisms in soils, but the role specific pathways play for an organism. It also allows us to understand the repercussion of disturbances and management of soils on below ground biodiversity. The knowledge gained through these type of observations, and integration of life history strategies into microbial ecology, will get us one step closer to microbiome management as part of soil care.

CHAPTER 6

Conclusions and future perspectives

6.1. Summary

Pastoral farming in New Zealand contributes large amounts of nitrogen to soils, largely via livestock urine. Through a combination of soil nitrogen cycling processes, this nitrogen is often transformed to the gaseous product N_2O, a potent greenhouse gas and ozone depleter. Our understanding of the interconnecting pathways leading to the production and consumption of this N_2O are not well understood, especially under urine patch conditions. This PhD thesis contributes new insights into the N cycling process (i.e. denitrification and nitrification) in pasture soils to understand the emission potential of N_2O through the analysis of the edaphic factors, gas kinetics, the microbial community structure, and functional gene analysis.

6.1.1. Understanding of denitrification kinetics, C mineralization, pH, and their link to microbial diversity and richness in pasture soils

Soil pH is one of the most important edaphic factors regulating the emission ratio of N_2O or N_2O index **(chapter 2)** under anoxic conditions. We observed that low pH or acidic soils have more propensity to emit N_2O compared to slightly alkaline or neutral soil pH, and vice versa. Both soil pH and emission ratio of N_2O had a strong link to microbial community composition, diversity (Shannon) and richness. Our study suggests that pH imposes a general selective pressure on the entire microbial community and that resulted in changes in emission potential. Diversity (Shannon) and richness were higher in slightly alkaline or neutral soil pH where low emission ratio of N_2O was observed. The opposite pattern was observed in low soil pH where the emission ratio of N_2O was comparatively higher. Our results imply that higher microbial richness and diversity, and soil pH management (i.e. keeping the soil pH at neutral level) strategies in soils can overcome the higher emission ratio of N_2O through the rapid transformation of N_2O to N_2.

We observed a positive linear relationship between the rate of denitrification and the rate of C mineralization (under oxic and anoxic conditions). This may have implications in a soil management perspective as we can measure the rate of denitrification indirectly in nitrate-amended soils by estimating the rate of C mineralization.

6.1.2. Abundance and diversity of *nosZI* and *nosZII*, and how these link to emission ratio of N_2O

Nitrous oxide reductase (N_2OR) is purported to be the only sink of terrestrial N_2O. This enzyme is encoded by *nosZ*. Recent findings have shown that there are

two types of *nosZ* (clade I and clade II), with most *nosZI* belonging to the Proteobacteria (alpha) phylum, and most *nosZII* to the Bacteroidetes phylum. Recently, it has been shown that *nosZ (clade II)* are highly abundant in the natural environment (Sanford *et al.*, 2012; Orellana *et al.*, 2014; Jones *et al.*, 2013). Our results confirmed that irrespective of soil type, *nosZII* is highly abundant compared to *nosZI* in pasture soils (**chapter 3**). In addition, higher abundance of the *nosZII* gene was observed in slightly alkaline or neutral pH soils compared to acidic soils. Furthermore, a lower emission ratio of N_2O was observed from the highly abundant of the *nosZII* gene compared to lower abundance of *nosZII* in pasture soil. Our results suggest that both *nosZI* and *nosZII* are a phylogenetically diverse group of prokaryotes, with their abundance and activity in soils ultimately regulating the production and consumption of N_2O.

6.1.3. Does pH link to the emission ratio of N_2O under oxic urine patches?

Our denitrification study (NO_3^- amended pasture soils) showed a linear relationship between pH and emission ratio of N_2O under anoxic conditions (**chapter 2**). However, this trend was not observed under oxic urine patch conditions (**chapter 4**). The probable reason could be that urine patches disturb the soil pH as well as microbial community composition as seen in **chapter 5**.

6.1.4. Response of microbial community, diversity, and richness under urine patches

Urine patch contributed significant emission of N_2O (**Chapter 4 & 5**). However, it is still not known how microbial community composition changes under urine patch conditions, or which microbes are involved in N transformation process at DNA and transcription levels. We observed that soil urea treatment altered soil microbial community composition and reduced microbial diversity (Shannon) and richness. We suggested a model (**chapter 5**) that fast growing microbial populations utilized energy from the N-linked redox reactions for growth while others used it for physiological maintenance.

6.1.5. Abundance and activity of AOB and AOA under urine patches

Despite the higher abundance of AOA in pasture soils, asynchronous microbial activity was observed between AOA and AOB populations. AOA activity was observed during early N transformation process but then declined over time. On the other hand, the AOB population was initially very small (<1%) in pasture soils, but bloomed after just a few days (>10%). The immense growth of AOB was supported by energy utilization derived from the N transformation process. Hence,

understanding the growth and activity of AOA and AOB in pasture soils indicate the genetic potential for N transformation process which can be applied in soil management perspectives.

6.2. Future perspectives

Our studies linked N cycling processes and outcomes with edaphic factors and prokaryotic microbial communities in pasture soils but did not investigate the fungal communities and their role in N_2O emissions. Although, some progress has been made recently to target the fungal *nirK* gene (Long *et al.*, 2015; Wei *et al.*, 2015b), and show their symbiotic roles (Bender *et al.*, 2014), the overall contributions of fungal populations along with the prokaryotic communities, and their interactions in the N cycling process are still poorly understood.

We have identified pasture soil microbes which respond to urine treatments (i.e. N transformation process). However, their ecology and physiology are still not well known as they are mostly uncultured and their complete genomes are not yet sequenced. The isolation, culturing and genome sequencing of these nitrifiying and denitrifying microbes from the soil could open up new doors for a deeper understanding of the N cycling process.

Here, we quantified only a handful of N cycling genes through qPCR, giving a useful but narrow picture of the relationship between N cycling gene abundance and soil N transformations. In the future, metagenomic and metatranscriptomic quantification of all N cycling genes could give a more complete picture of N cycling gene abundances, expression and their relationship to N transformations in pasture urine

Our studies were conducted under laboratory conditions. This resulted in exclusion of some biological (e.g. grasses, plants, earthworms) and environmental factors (e.g. diurnal temperature variation, rainfall) from our experiments. Therefore, field level studies are important to corroborate our findings.

Supplementary Information

Supplementary materials for chapter 2

Supplementary Figures

Supplementary Fig. S2.1. Emission profile of N_2O production index (IN_2O) and $N_2O/(N_2O+N_2)$ product ratio over time. N_2O (µmol N/vial) and N_2 (µmol N/vial) emissions from the anoxic incubation of soils over time (1a-13a), and N_2O production index (IN_2O) and $N_2O/(N_2O+N_2)$ product ratio of denitrification over time (1b-13b). Soils were collected from Ireland (1: Moorepark, 2: Johnstown, 3: Solohead) and New Zealand (4: Warepa, 5: Otokia, 6: Wingatui, 7: Tokomairiro, 8: Mayfield, 9: Lismore, 10: Templeton, 11: Manawatu, 12: Horotiu and 13: Te Kowhai). Values represent the mean and standard error of triplicate flask results.

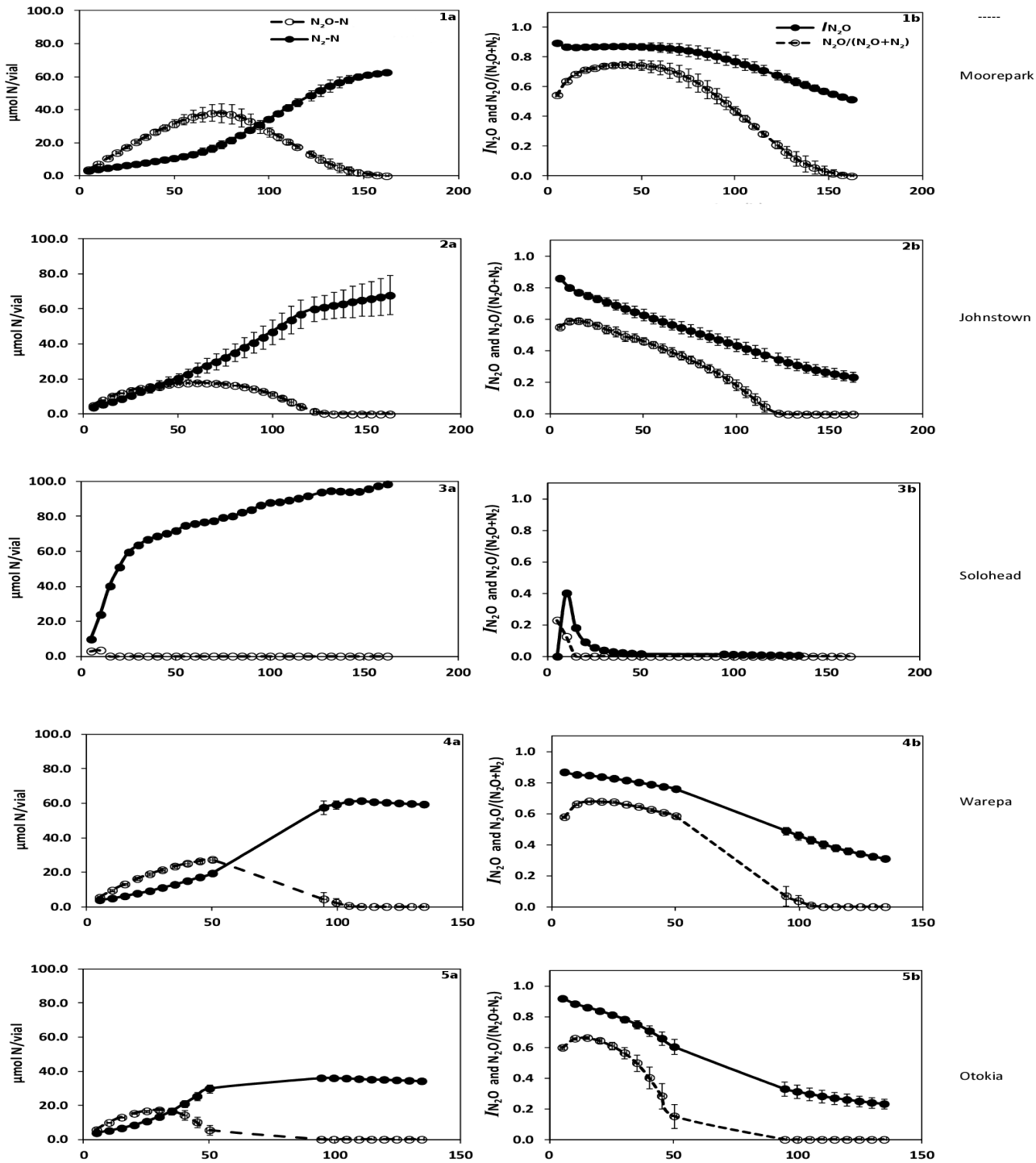

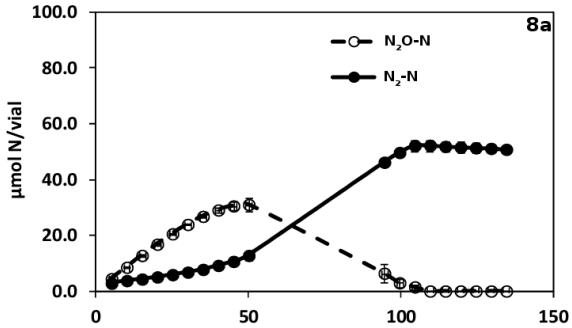

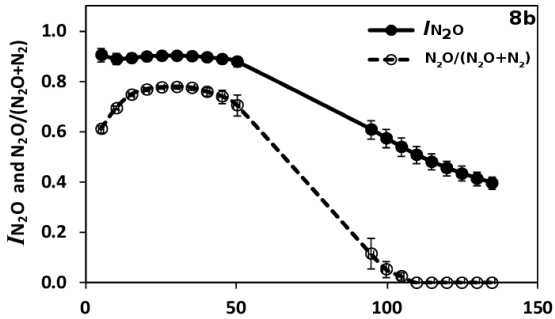

Mayfield

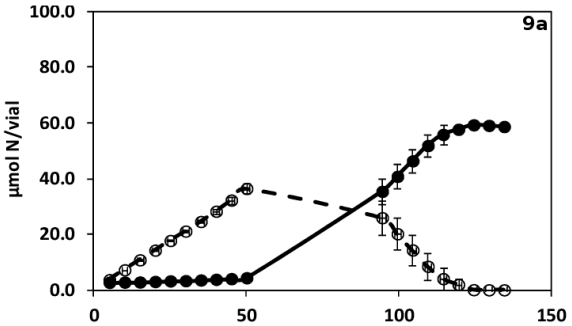

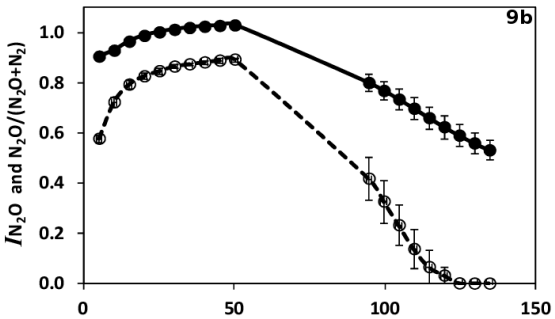

Lismore

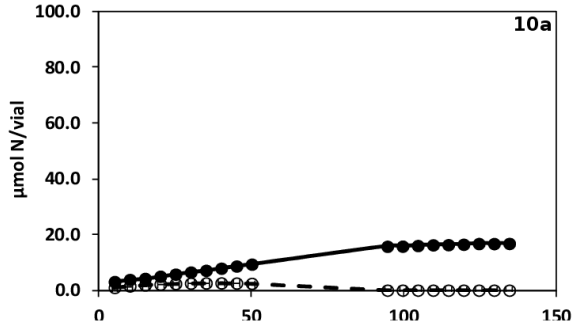

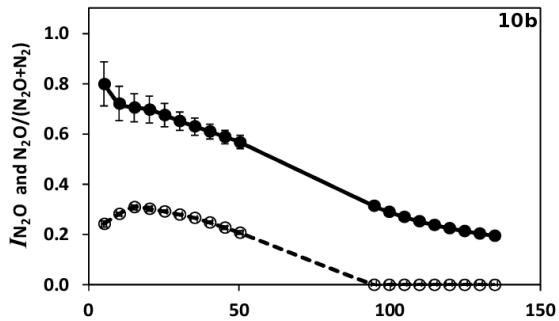

Templeton

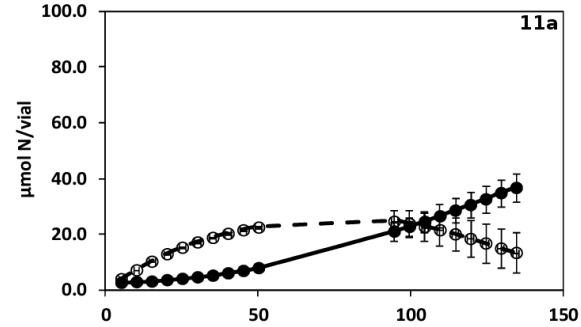

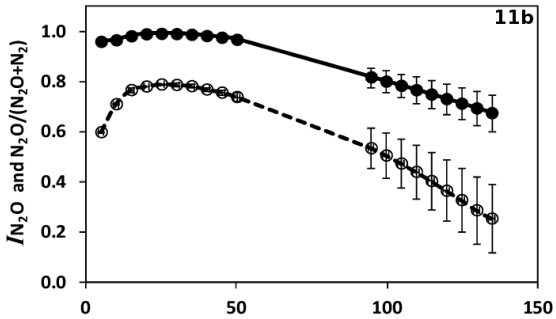

Manawatu

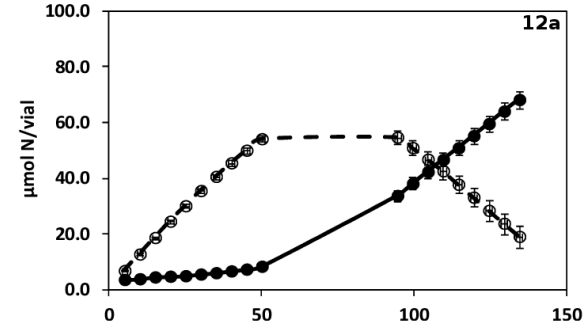

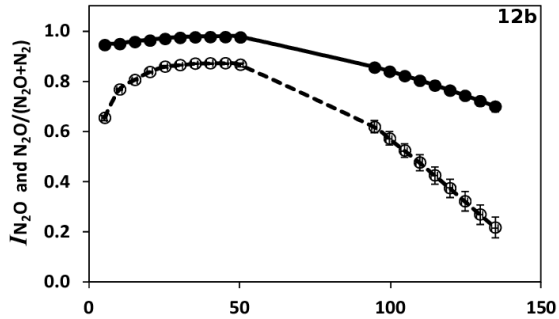

Horotiu

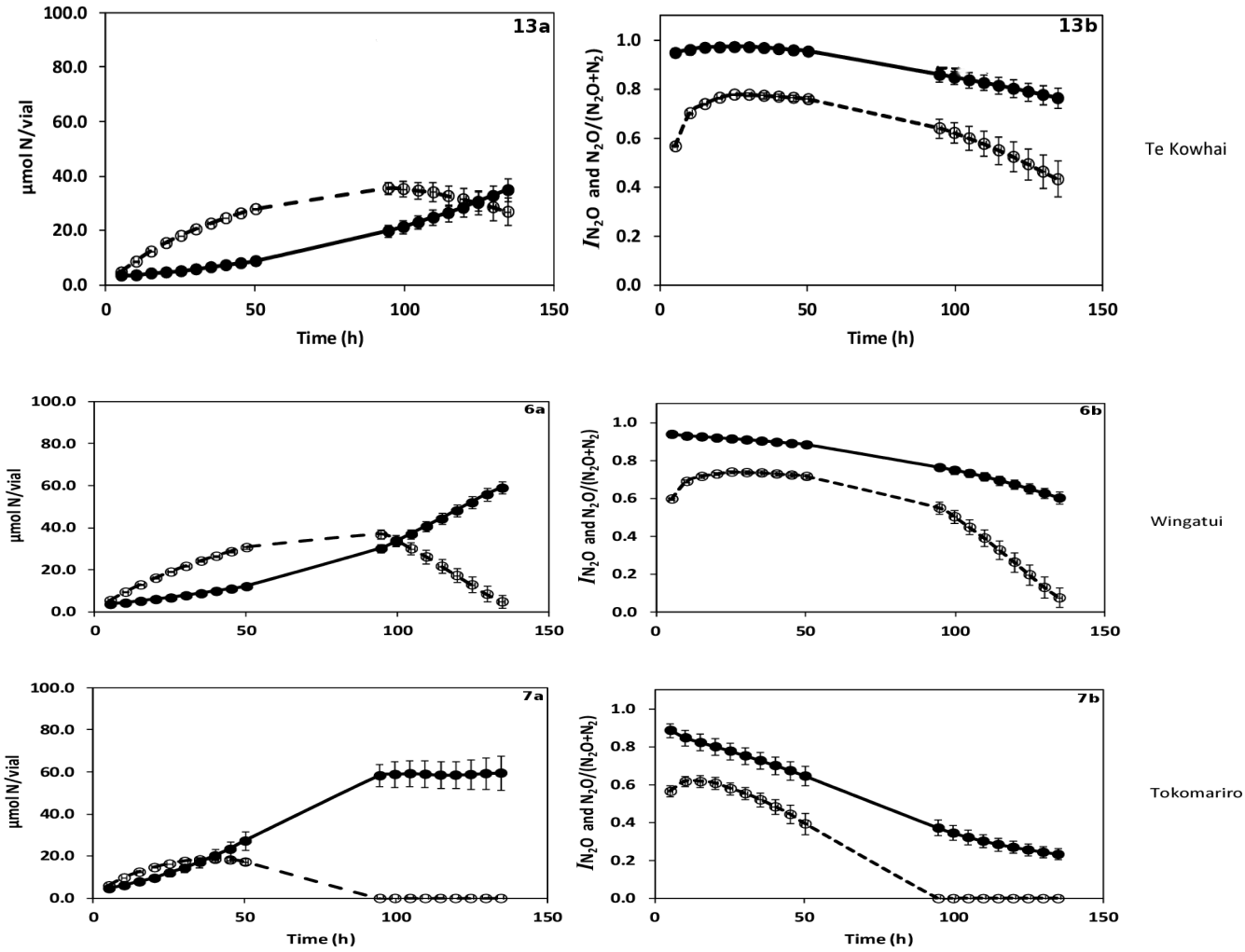
13a
13b
Te Kowhai
6a
6b
Wingatui
7a
7b
Tokomariro
µmol N/vial
I_{N_2O} and $N_2O/(N_2O+N_2)$
Time (h)

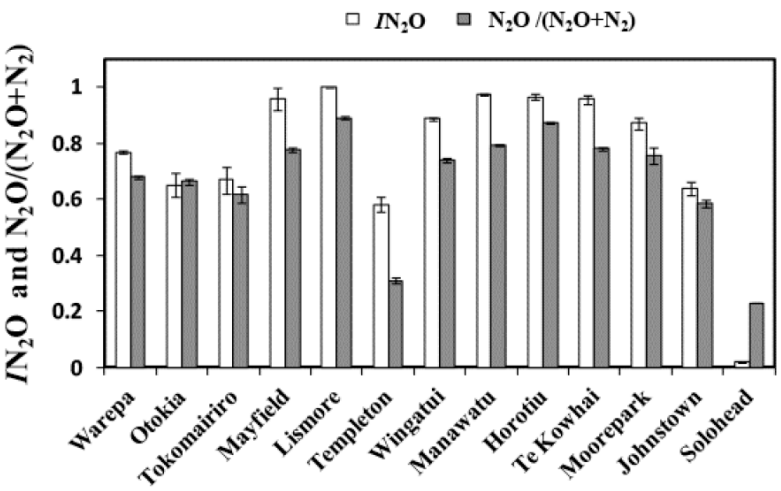

Supplementary Fig. S2.2. Maximum N_2O production index (IN_2O) and $N_2O/(N_2O+N_2)$ product ratio values observed in all soils. Values represent the mean and standard error of triplicate flask results.

Supplementary Tables

Supplementary Table S2.1. Physical and chemical characteristics of soil samples.

Soil	Country	Latitude/Longitude	Region	Soil type	Soil classification	Lowland/hill country	Drainage class	Management/farming practice
Horotiu	NZ	37°46'22"S , 175°21'13"E	Waikato	Silt loam	Typic Orthic Allophanic soil	Lowland	Freely	Intensively grazed flatland dairy pasture
Johnstown	IR	52°17'N, 6°30'W	Wexford	Gleysol	Luvic Gleysol	Lowland	Imperfectly	Moderately intensively grazed flatland dairy pasture
Lismore	NZ	43°47'S, 171°46'E	Canterbury	Stony soil	Pallic Orthic Brown	Lowland	Freely	Intensively grazed flatland pasture
Manawatu	NZ	43°7'S, 176°13'E	Manawatu	Fine sandy loam	Pallic Orthic Brown	Hill country	Freely	
Mayfield	NZ	43°48'S, 171°46'E	Canterbury	Silt loam	Typic Argillic Pallic Soils	Lowland	Imperfectly	Moderately intensively grazed flatland sheep pasture
Moorepark	IR	52°10'N, 8°15'W	Cork	Sandy loam brown earth	Haplic Cambisol	Lowland	Freely	Moderately intensively grazed flatland dairy pasture
Otokia	NZ	45°51'47"S,170°23'3"E	Otago	Silt loam	Fragic Perch-gley Pallic soil	Lowland	Poorly	Moderately intensively grazed flatland sheep pasture
Solohead	IR	52°51'N, 8° 21'W	Tipperary	Gley	Haplic Stagnosol	Lowland	Poorly	Moderately intensively grazed flatland dairy pasture
Te Kowhai	NZ	37°46'27"S, 175°21'5" E	Waikato	Silt loam	Typic Ochraqualf	Lowland	Poorly	Intensively grazed flatland dairy pasture
Templeton	NZ	43°37'S, 172°25'E	Canterbury	Silt loam	Immature Pallic Soil	Lowland	Imperfectly	Intensively grazed flatland pasture
Tokomairiro	NZ	46°18'S, 169°44'E	Otago	Deep silt loam	Fragic Perch-gley Pallic soil	Lowland	Imperfectly	Moderately intensively grazed flatland dairy pasture
Warepa	NZ	45°51'22"S, 170°23'44"E	Otago	Silt loam	Mottled Fragic Pallic soil	Hill country	Poorly	Moderately intensively grazed rolling sheep pasture
Wingatui	NZ	45°51'46" S, 170°23'6" E	Otago	Silt loam	Weathered Fluvial Recent soil	Lowland	Freely	Moderately intensively grazed flatland sheep pasture

Soil	Total C%	Total N%	C:N ratio	Soil Density (g/cm^3)	Soil Porosity (%)
Horotiu	10.90	1.15	9.5	0.83	68.3
Johnstown	2.46	0.21	12.0	1.18	52.0
Lismore	4.10	0.43	9.5	1.15	52.0
Manawatu	3.01	0.29	10.4	0.95	66.5
Mayfield	4.88	0.47	10.4		
Moorepark	2.66	0.27	9.8	1.19	54.0
Otokia	3.63	0.32	11.3	1.1	67.5
Solohead	6.08	0.62	9.8	1.09	57.2
Te Kowhai	7.71	0.76	10.1	1.04	64.2
Templeton	1.66	0.13	13.1	1.26	48.1
Tokomairiro	4.32	0.41	10.5	0.93	65.0
Warepa	2.63	0.17	15.7	0.91	
Wingatui	4.2	0.5	8.9	1.13	69.0

Table S2.3. Soil moisture content measurements (before and after adjustment of NH_4NO_3)

Sample name	Country	% Moisture (before flooding)	% Moisture (after flooding)
Warepa	NZ	47.3	49.4
Otokia	NZ	46.9	52.0
Wingatui	NZ	65.4	66.5
Tokomariro	NZ	43.6	49.5
Mayfield	NZ	38.2	43.3
Lismore	NZ	40.9	40.9
Templeton	NZ	24.5	21.6
Manawata	NZ	36.6	34.5
Horotiu	NZ	77.1	72.4
Te Kowhai	NZ	64.0	61.0
Moorpark	IRI	30.9	39.8
Johnstwon	IRI	29.7	41.3
Solohead	IRI	61.2	83.0

Table S2.2. Soil pH measurements. Soil pH values as determined using three different extraction methods (DI water, 0.01 M $CaCl_2$ and 2M KCl).

Soil	pH (H_2O)	pH ($CaCl_2$)	pH (KCl)
Warepa	6.06	5.67	4.75
Otokia	5.90	5.32	4.40
Tokomairiro	6.13	5.81	4.83
Mayfield	6.10	5.80	4.92
Lismore	5.75	5.50	4.50
Templeton	6.36	5.93	4.84
Wingatui	5.83	5.36	4.47
Manawatu	5.62	5.44	4.44
Horotiu	5.57	5.34	4.58
Te Kowhai	5.74	5.46	4.64
Moorepark	5.97	5.66	4.97
Johnstown	6.25	5.90	5.04
Solohead	7.03	6.92	6.39

Supplementary materials for chapter 3

Phylogenetic and functional potential links pH and N_2O emissions in pasture soils

Supplementary Methods

Analysis of microbial community composition

The rarified OTU table (biom file) was imported into R using the Phyloseq package (McMurdie and Holmes, 2013). To account for the multiple rarifications (10 total) abundances were normalized by dividing by 10 and rounding values to whole integers using the *transform_sample_counts()* command. Taxa (OTUs) with less than 1 count were removed using the *prune_taxa()* command. Alpha diversity (Shannon and richness) were calculated using the *estimate_richness()* command.

The NMDS plot was created using a Bray-Curtis distance matrix through Phyloseq. A Mantel test was performed to test the relationship between pH, as well as N_2O emission ratio, and microbial community composition using the Vegan package (Oksanen *et al.*, 2013). To determine grouping of samples a cluster analysis was performed in using the Pvclust package (method = Ward; distance matrix = Bray-Curtis; bootstrap value, n=1000) (Suzuki and Shimodaira, 2006). Clusters were marked boxes (red) at 95% confidence interval.

Identifying OTUs correlated to change in pH and $N_2O/(NO+N_2O+N_2)$

In R, the Phyloseq file was transformed into a matrix. The variables (pH and $N_2O/(NO+N_2O+N_2)$) were converted into new data frames (df). A Spearmans correlation test (*cor.test(variable$pH,x, method = "spearman")*) was performed and results were further processed by adjusting p-value using a false discovery rate adjustment based on the Benjamini & Hochberg method (*p.adjust(p.vals,method = "BH")*). Results were subsetted to include only data with an adjusted p-value of < 0.05 & Rho >= 0.5 | Rho <= -0.5. OTU names were then used to subset the full Phyloseq file based on the significantly correlated OTUs using the *subset_taxa()* command. The significant OTUs and their full taxonomic classification were exported from R as a text file before visualization using Graphlan (Asnicar *et al.*, 2015).

Normalization of metagenome sequences

Normalization was done based on equal number of sequence reads per sample (i.e. 2.63 million reads per sample).

Functional richness

Total functional richness (i.e. number of different functional genes) and functional richness at specific category (N-metabolism, level 3) were calculated from metagenome in MG-RAST (ID numbers 4644147.3 to 4644142.3) using KO annotation method with default MG-RAST settings (i.e. maximum e-value cutoff: 1e-5; minimum % identity cutoff: 60%; minimum alignment length cutoff: 15 aa). The functional richness data were exported from the MG-RAST and normalized based on equal number of sequence reads per sample (2.63 million reads per sample).

Supplementary Figures

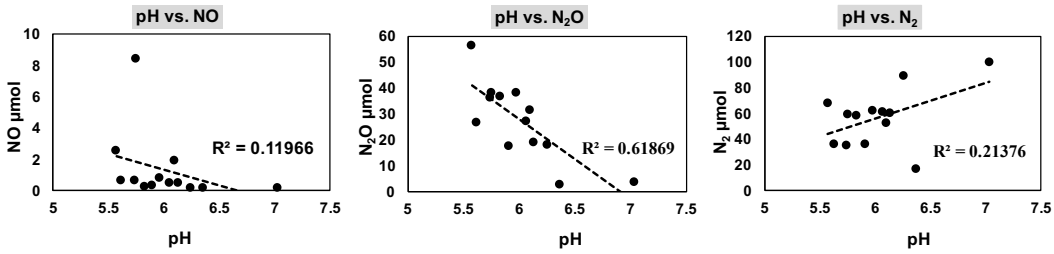

Supplementary Fig. S3.1. Relationship between soil pH and maximum emission of NO, N_2O and N_2 under anoxic incubation for all 13 soils.

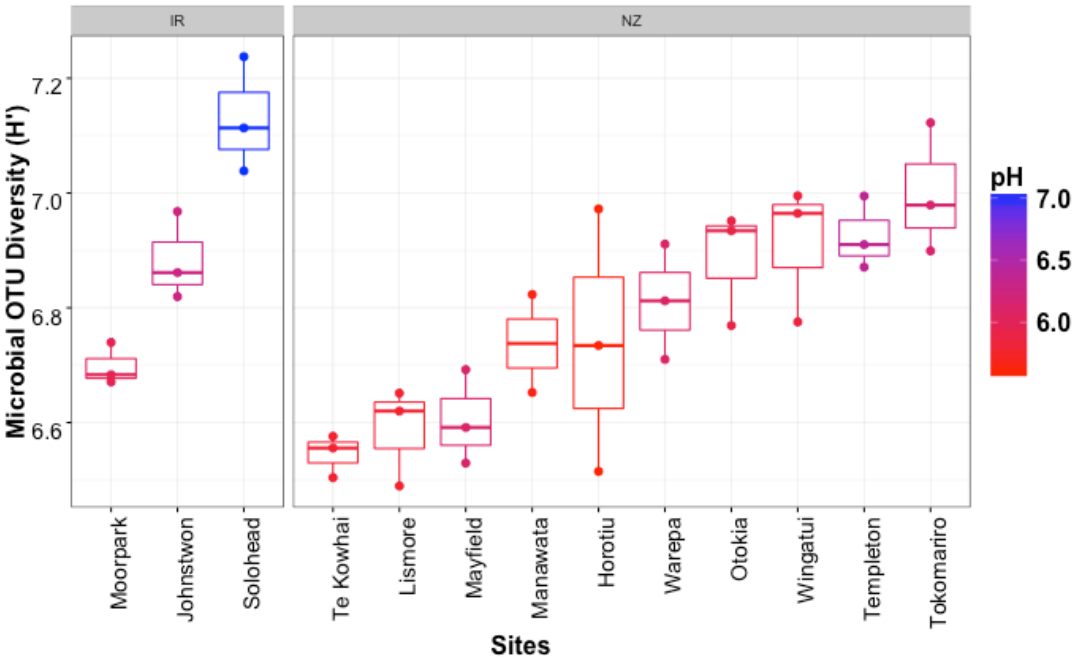

Supplementary Fig. S3.2. Shannon diversity based on microbial OTUs across all sites for both Irish (IR) and New Zealand (NZ) soils. Color gradient denotes influence of pH (R^2 = 0.49, $p<0.01$).

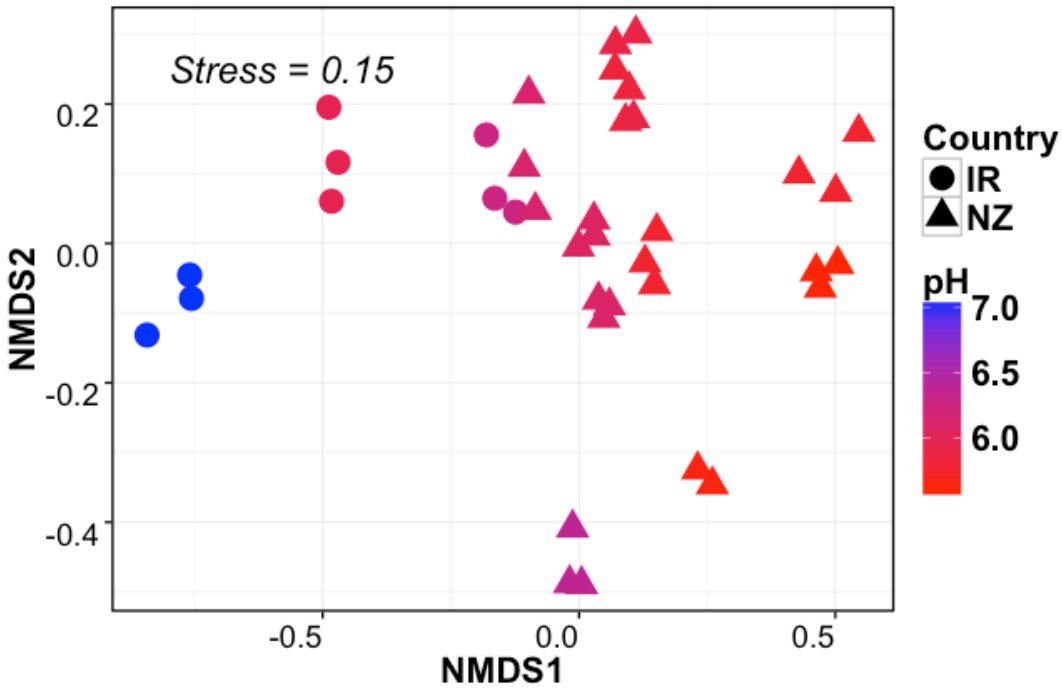

Supplementary Fig. S3.3. Microbial community dissimilarities of soils (Irish and New Zealand) with different pH as determined using NMDS (Bray-Curtis) ordination.

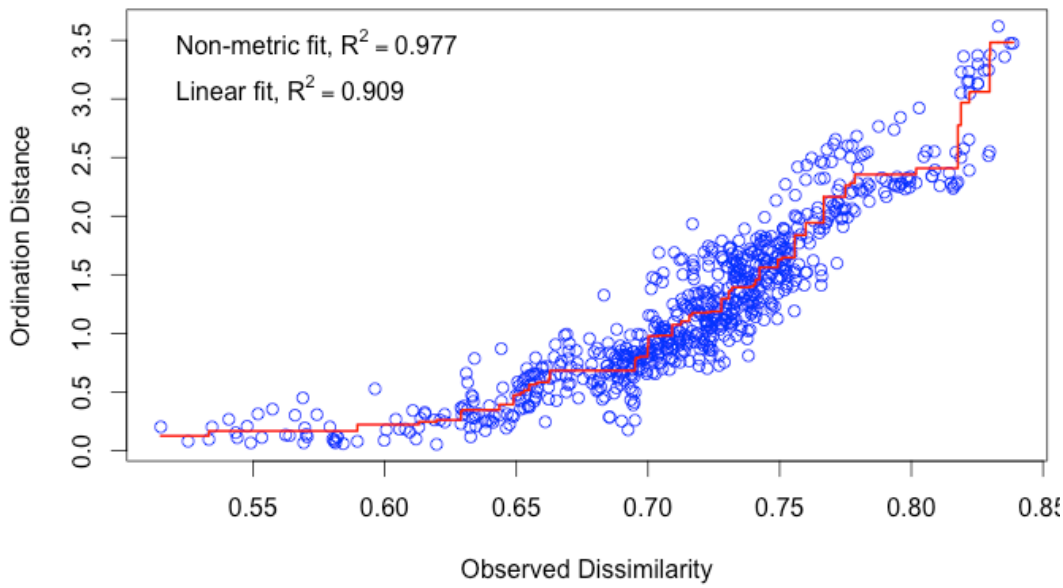

Supplementary Fig. S3.4. Stress plot for Figure 3.1E

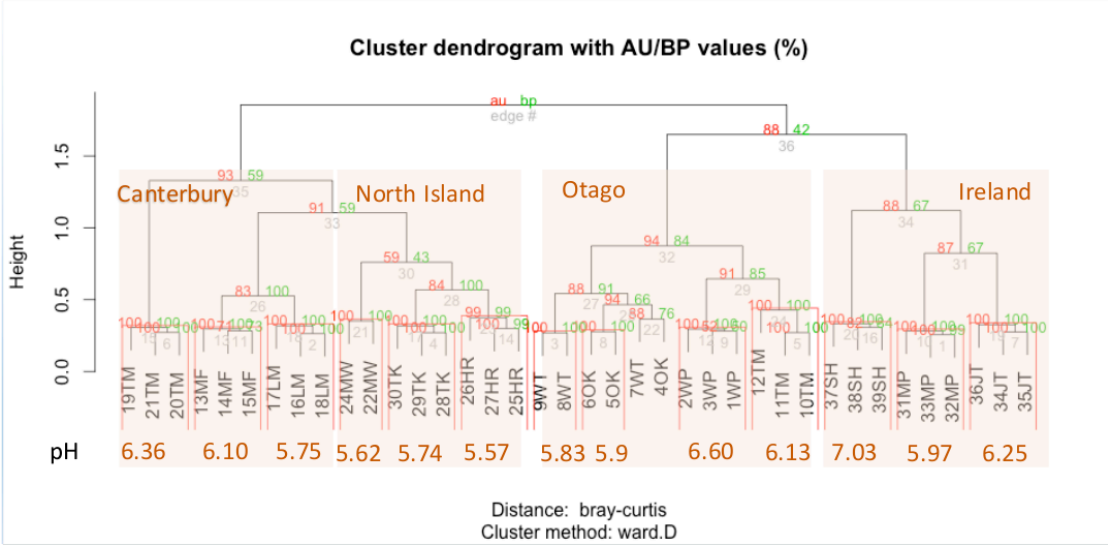

Supplementary Fig. S3.5 Pvclust tree using Bray-Curtis distance of 16S rRNA microbial community composition and including p values for each node [AU (approximately unbiased) BP (bootstrap probability)]. Red boxes mark clusters with 95% confidence. Clusters at lower confidence are labeled by region.

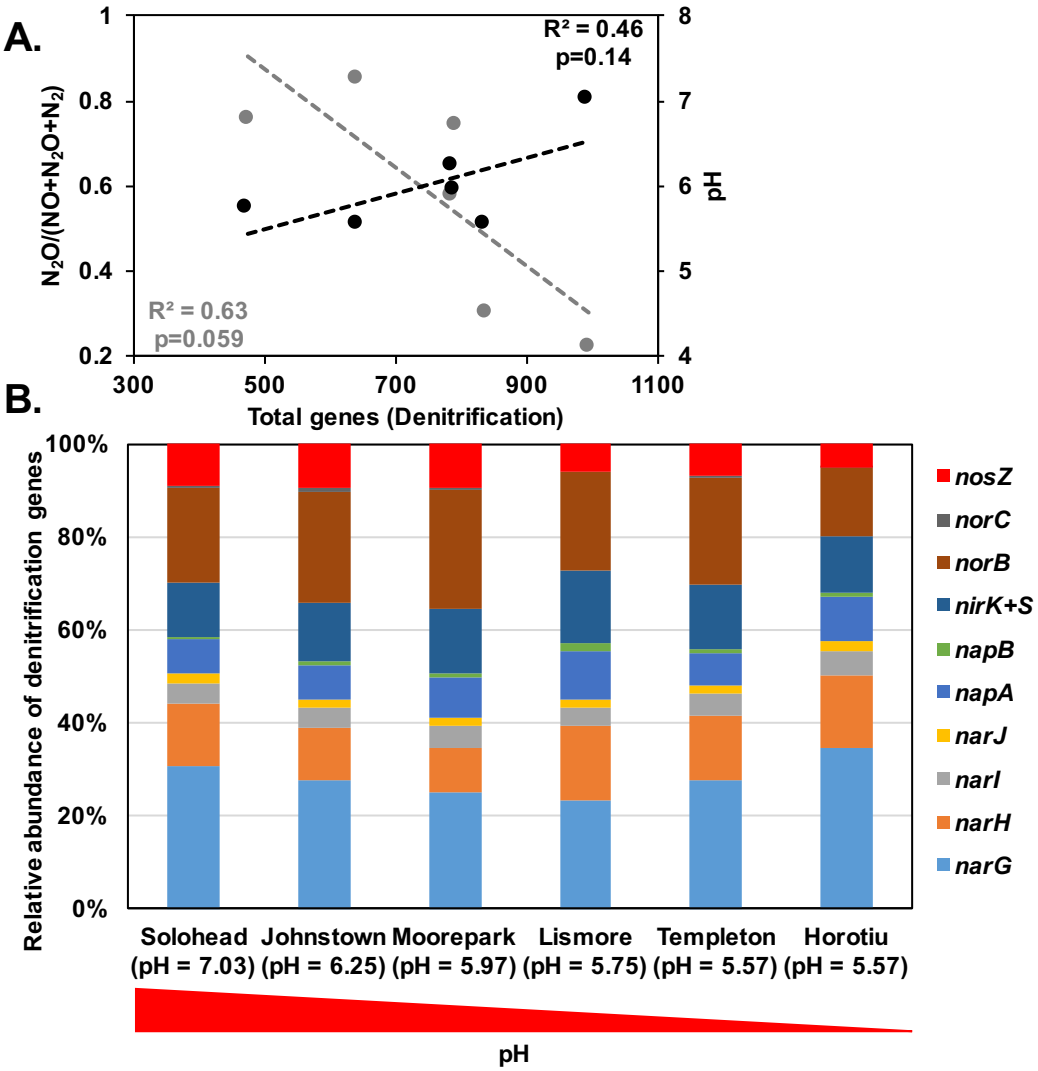

Supplementary Fig. S3.6. Relationships between total denitrification genes (genes per 2.63 million reads) & N_2O emission ratio ($N_2O/NO+N_2O+N_2$), and total denitrification genes (genes per 2.63 million reads) & pH (A). The black circles represent the relationship between denitrification genes & pH, and the gray circles represent the relationship between denitrification genes & N_2O emissions ratio. The bottom stack bar plot shows the relative abundance of denitrification genes according to pH gradient (high to low) (B). The abundance of denitrification genes was calculated from metagenome analysis (annotation source: KO) by detection of the following genes: *nosZ, norC, norB, nirK+S, napB, napA, narJ, narI, narG*.

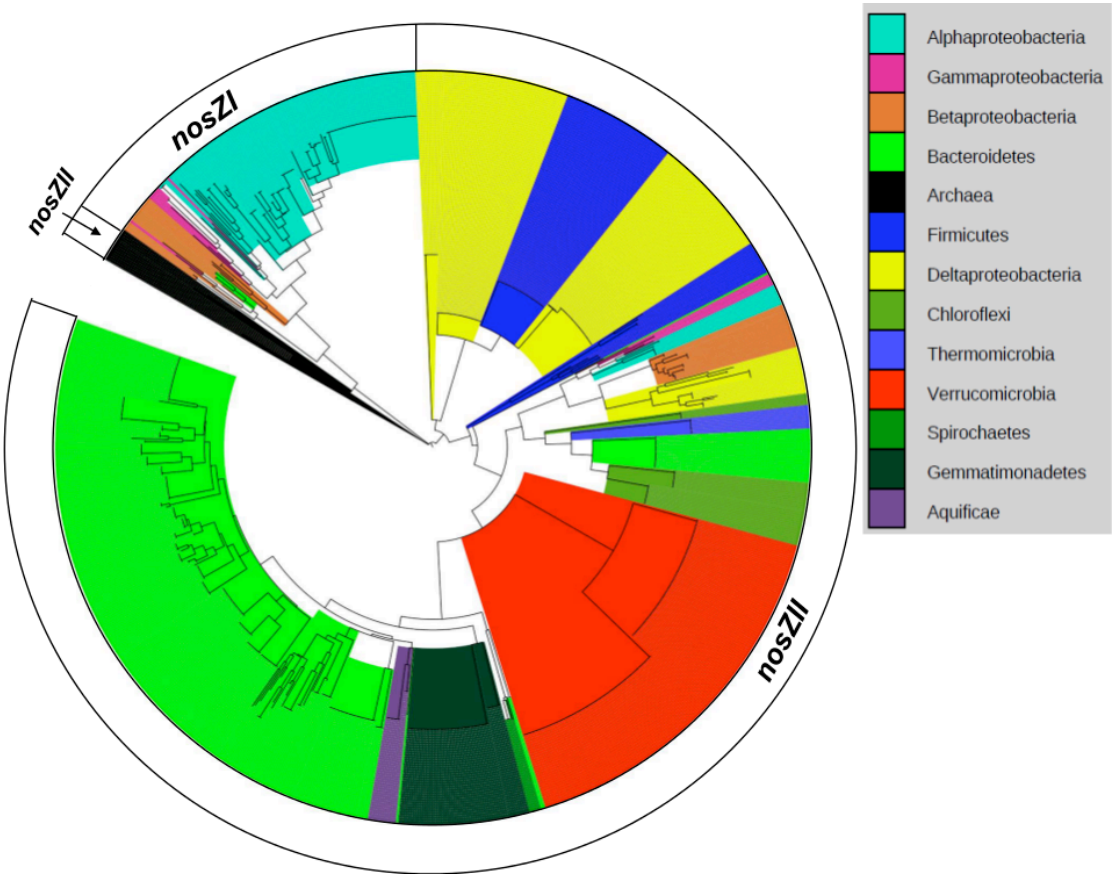

Supplementary Fig. S3.7. Maximum likelihood phylogeny of short-length *nosZ* amino-acid sequences (129 aa) obtained from metagenomes. A multiple sequence alignment was performed with CLUSTALW on MEGA 6. After alignment, sequences were trimmed outside of conserved (90-100 %) regions (at C terminal LGPLHT--- and at N terminal ---EPH) containing approx. 129 aa sequences. The phylogenetic tree was constructed preliminary with MEGA 6 using the maximum likelihood approach and JTT matrix-based model, and finally visualized with iTOL.

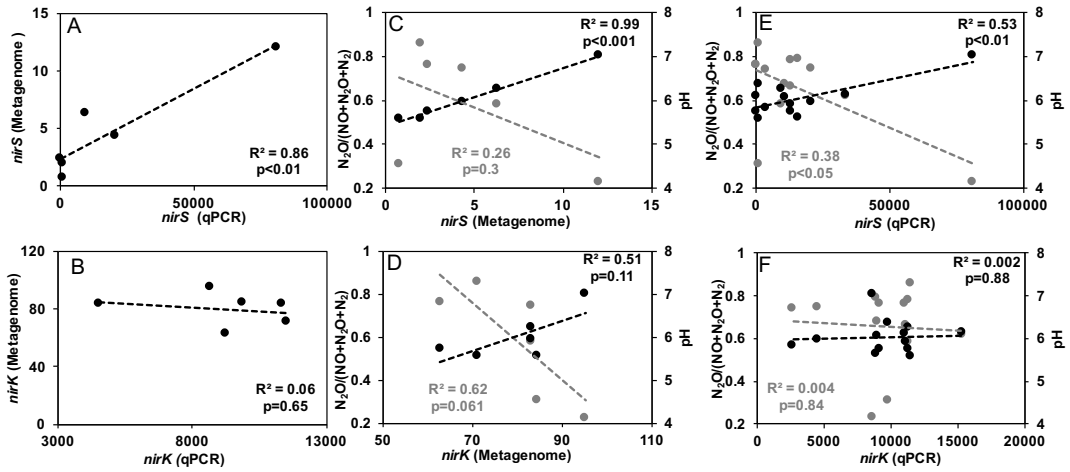

Supplementary Fig. S3.8. Relationship between abundance of *nir* genes (based on absolute quantification of metagenome & qPCR of *nirS* & *nirK*), $N_2O/(NO+N_2O+N_2)$ and pH. (A-B) Comparison of gene abundances based on either metagenomic (i.e. gene abundance per 2.63 million reads) or qPCR analysis (gene abundance per 5 ng soil DNA) for 6 soils. (C-D) Response of *nirS* and *nirK* abundances based on metagenomic analysis for 6 soils against $N_2O/(NO+N_2O+N_2)$ (gray) and pH (black). (E-F) Response of *nirS* and *nirK* abundances based on qPCR analysis for all 13 soils against $N_2O/(NO+N_2O+N_2)$ (gray) and pH (black).

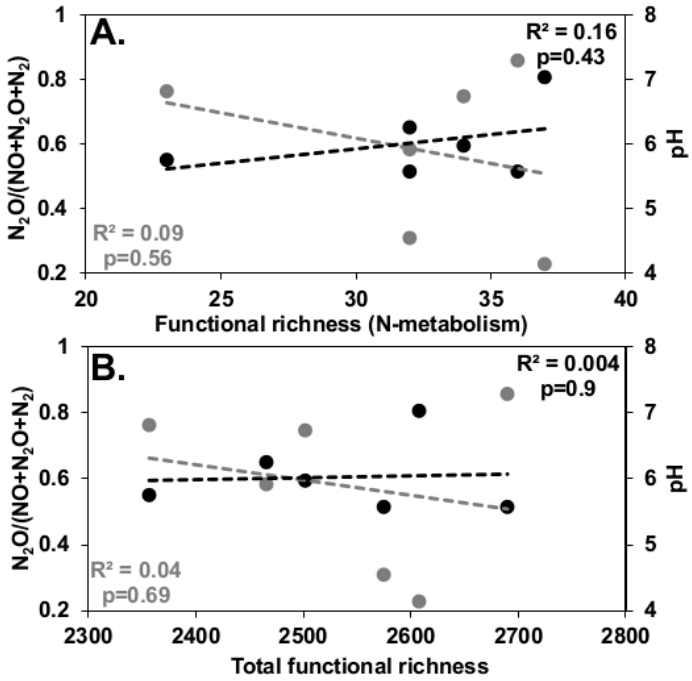

Supplementary Fig. S3.9. Relationship between functional richness (A: at N-metabolism level and B: total functional richness), N_2O emission ratio (gray) and pH (black). The x-axis denotes richness i.e. number of different genes per 2.63 million sequence reads. The functional richness was calculated from metagenome analysis (annotation source: KO).

Supplementary Table S3.1. The primers used in this study

Primer	Target group	Function	Amplicon (bp)	Sequences (5´-3´)	Polymerase	Cycling conditions & data acquisition	Efficiency (%) & R^2	References
UniF UniR	16S rRNA	Ribosomal RNA	180	ACTCCTACGGGAGGCAGCAGT ATTACCGCGGCTGCTGGC	Fast SYBR Green Master Mix	95°C for 10 minutes, followed by 40 cycles of 10 s at 95°C, 20 s at 65°C, then followed by 20 s at 72°C for fluorescent acquisition	106 & 0.99	(Hartman *et al.*, 2009)
cd3AF R3cd	*nirS*	NO_2^- reduction (cytochrome cd_1-containing)	425	GTSAACGTSAAGGARACSGG GASTTCGGRTGSGTCTTGA	Fast SYBR Green Master Mix	95°C for 10 minutes, followed by 40 cycles of 10 s at 95°C, 20 s at 58.5°C, 20 s at 72°C then followed by 20 s at 77°C for fluorescent acquisition	94.67 & 0.99	(Throbäck *et al.*, 2004; Yergeau *et al.*, 2007)
F1aCu R3Cu	*nirK*	NO_2^- reduction (Cu containing)	474	ATCATGGTSCTGCCGCG GCCTCGATCAGRTTGTGGTT	Luminaris HiGreen Low ROX qPCR Master Mix	95°C for 10 minutes, followed by 40 cycles of 10 s at 95°C, 30 s at 58.5, 40 s at 72°C then followed by 20 s at 80°C for fluorescent acquisition	96.89 & 0.99	(Throbäck *et al.*, 2004)
nosZ2F nosZ2R	*nosZ* I	N_2O reduction (Tat dependent)	267	CGCRACGGCAASAAGGTSMSSGT CAKRTGCAKSGCRTGGCAGAA	Fast SYBR Green Master Mix	95°C for 10 minutes, followed by 40 cycles of 10 s at 95°C, 20 s at 58.5°C, 20 s at 72°C then followed by 20 s at 75°C for fluorescent acquisition	99.3 & 0.99	(Henry *et al.*, 2006)
nosZ-II-F nosZ-II-R	*nosZ* II	N_2O reduction (Sec dependent)	690-720	CTIGGICCIYTKCAYAC GCIGARCARAAITCBGTRC	Luminaris HiGreen Low ROX qPCR Master Mix	95°C for 10 minutes, followed by 6 cycles of 15 s at 95°C, 30 s at 60-55°C (-1°C per cycle), 30 s 72°C, and then followed by 44 cycles of 15 s at 95°C, 30 s at 54°C, 30 s at 72°C and 30 s for fluorescent data acquisition (82°C).	66.12 & 0.99	(Jones *et al.*, 2013)

Supplementary materials for Chapter 4

Ruminant urine patch reveals significant sources of N_2O.

Supplementary Figures

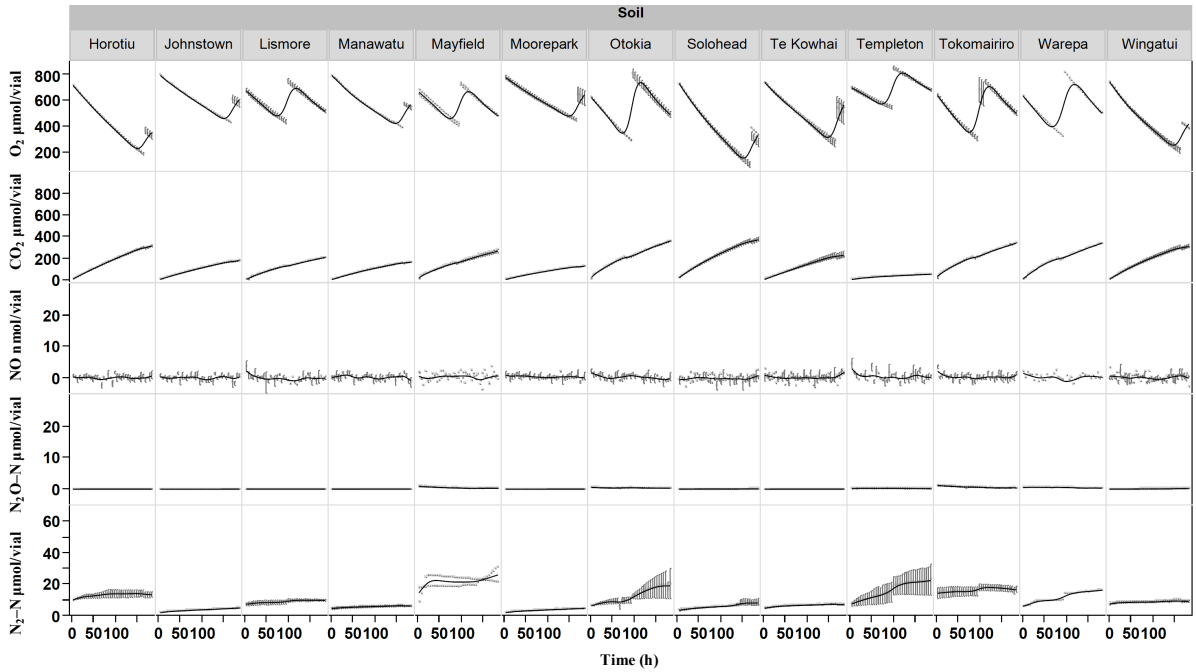

Supplementary Fig. S4.1 Gas kinetics (O_2, CO_2, NO, N_2O, N_2) of 13 different soil samples (10 New Zealand and 3 Ireland soils) under oxic incubation (without urine treatment).

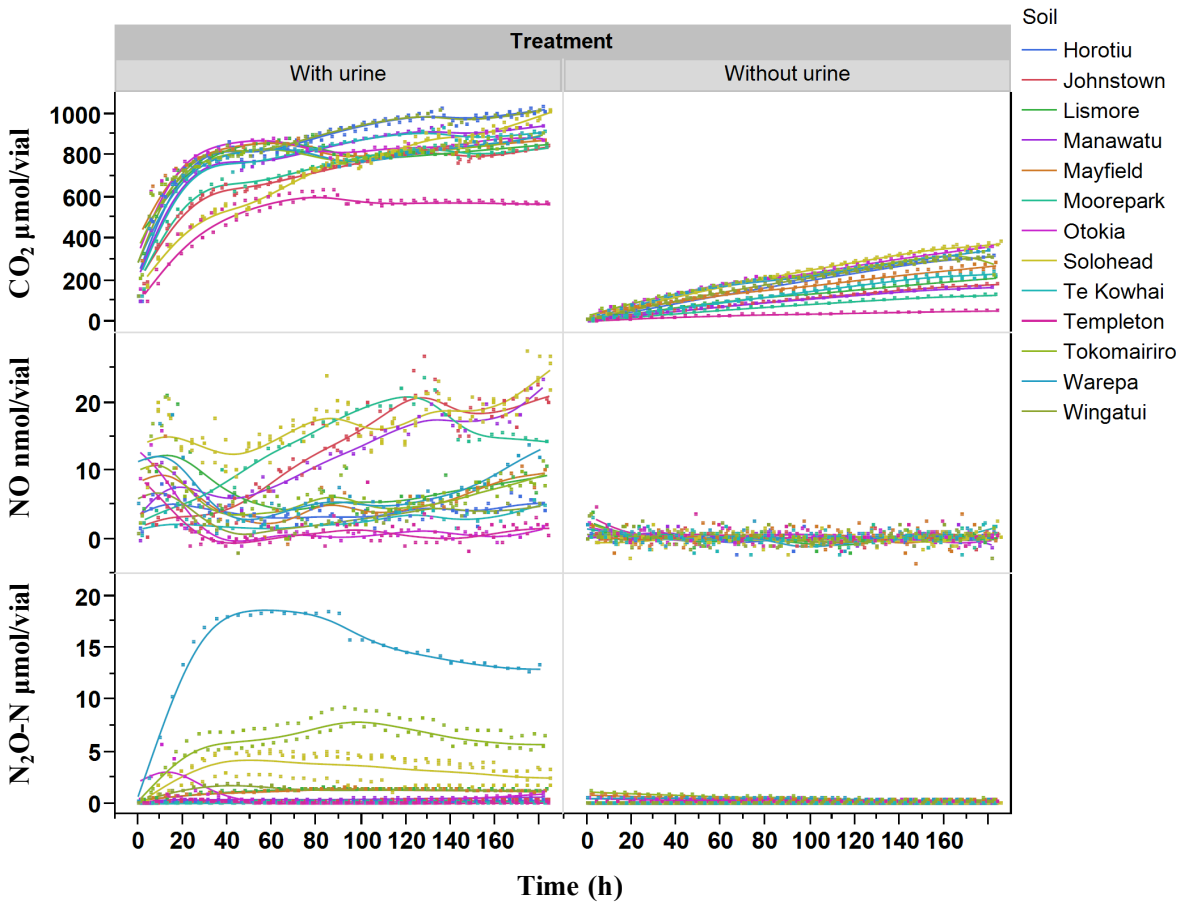

Supplementary Fig. S4.2. Emissions (CO_2, NO and N_2O) comparison between with urine and without urine.

Supplementary Table S4.1 Primer pairs used in this study

Primer	Target group	Function	Amplicon size (bp)	Sequence (5´-3´)	Polymerase used	Cycling & data acquisition	Efficiency (%) & R^2	References
UniF UniR	16S rRNA gene	Ribosomal RNA	180	ACTCCTACGGGAGGCAG CAGT ATTACCGCGGCTGCTGGC	Fast SYBR Green Master Mix	95°C for 10 minutes, followed by 40 cycles of 15 s at 95°C, 20 s at 65°C, then followed by 20 s at 72°C for fluorescent acquisition	99.3 & 0.99	(Hartman *et al.*, 2009)
Crenamo A23F Crenamo A616R	Archaeal *amoA* gene	Ammonia oxidation	628	ATGGTCTGGCTWAGACG GCCATCCATCTGTATGTC CA	Fast SYBR Green Master Mix	95°C for 10 minutes, followed by 6 cycles of 15 s at 95°C, 30 s at 60-55°C (-1°C per cycle), 30 s 72°C, and then followed by 36 cycles of 15 s at 95°C, 30 s at 54°C, 30 s at 72°C and 30 s for fluorescent data acquisition (75°C).	86.1 & 0.98	(Tourna *et al.*, 2008)
amoA1F amoAR1	Bacterial *amoA* gene	Ammonia oxidation	491	GGGGTTTCTACTGGTGGT CCCCTCGGGAAAGCCTTC TTC	Fast SYBR Green Master Mix	95°C for 10 minutes, followed by 45 cycles of 15 s at 95°C, 30 s at 57°C, 40 s at 72°C then followed by 20 s at 82°C for fluorescent acquisition	84.6 & 0.99	(Avrahami *et al.*, 2003)

Note: The efficiency and R^2 were calculated from the standard curve (10-fold dilution series) of each target (gene) from a single run in a 384-well plate.

Supplementary materials for chapter 5

Response to nitrogen addition reveals metabolic and ecological strategies of soil bacteria

Supplementary Methods

Analysis of microbial community composition

The rarified biom file was exported from Qiime and then processed in R using the phyloseq package (McMurdie and Holmes, 2013). To account for the multiple rarifications (10 total) abundances were first normalized by dividing by 10 followed by rounding values to whole integers using the *transform_sample_counts()* command. Taxa (OTUs) with less than 1 count were deleted using the *prune_taxa()* command. Alpha diversity (Shannon and richness) were calculated using the *estimate_richness()* command.

The NMDS plot was created using a Bray-Curtis distance matrix through "phyloseq" and "vegan" (Oksanen *et al.*, 2013) packages. Significant treatment effects by urea where determined using an Adonis test. To determine samples forming statistically significant groups, a cluster analysis was performed using the pvclust package (method = Ward; distance matrix = Bray-Curtis; bootstrap value, n = 1000) (Suzuki and Shimodaira, 2006). Significant groups (representing 95% confidence) were marked with boxes (red). To understand the temporal variation within microbial community in each treatment (4 treatments: HM+N [high moisture soil with urea]; LM+N [low moisture soil with urea]; HM-N [high moisture soil with no urea] and LM-N [high moisture soil with no urea]), a Mantel correlogram analysis was performed using "vegan" and "mpmcorrelogram" packages. Control samples with no N added were stable and only sampled 4 times (+N treatment was sampled 7 times).

Identifying OTUs affected by N treatment through SIMPER analysis

Both DNA and RNA data (16S sequencing reads) were subset into two groups based on moisture treatment (i.e. high moisture [HM] and low moisture [LM]). For each moisture treatment, OTUs identified within urea treated (+N) and untreated (-N) samples were compared after samples from day 0 (immediately after N application where removed). OTUs responsible for dissimilarities between N treatments for each moisture content were identified using similarity percentage analysis (SIMPER) (Clarke, 1993).

qPCR inhibition test

Low conc. of DNA and cDNA samples were used for qPCR templates to avoid PCR inhibition. This was tested on some DNA and cDNA samples by making a dilution series (low vs. high concentration of DNA or cDNA) along with qPCR standard curve.

Supplementary Table S5.1 Primer pairs used in this study

Primer	Target group	Function	Amplicon size (bp)	Sequence (5´-3´)	Polymerase used	Cycling & data acquisition	Efficiency (%) & R^2	References
UniF UniR	16S rRNA gene	Ribosomal RNA	180	ACTCCTACGGGAGGCAGCAGT ATTACCGCGGCTGCTGGC	Fast SYBR Green Master Mix	95°C for 10 minutes, followed by 40 cycles of 15 s at 95°C, 20 s at 65°C, then followed by 20 s at 72°C for fluorescent acquisition	99.3 & 0.99	(Hartman *et al.*, 2009)
CrenamoA 23F CrenamoA 616R	Archaeal *amoA* gene	Ammonia oxidation	628	ATGGTCTGGCTWAGACG GCCATCCATCTGTATGTCCA	Fast SYBR Green Master Mix	95°C for 10 minutes, followed by 6 cycles of 15 s at 95°C, 30 s at 60-55°C (-1°C per cycle), 30 s 72°C, and then followed by 36 cycles of 15 s at 95°C, 30 s at 54°C, 30 s at 72°C and 30 s for fluorescent data acquisition (75°C).	86.1 & 0.98	(Tourna *et al.*, 2008)
amoA1F amoAR1	Bacterial *amoA* gene	Ammonia oxidation	491	GGGGTTTCTACTGGTGGT CCCCTCGGGAAAGCCTTC TTC	Fast SYBR Green Master Mix	95°C for 10 minutes, followed by 45 cycles of 15 s at 95°C, 30 s at 57°C, 40 s at 72°C then followed by 20 s at 82°C for fluorescent acquisition	80.6 & 0.99	(Rotthauwe *et al.*, 1997; Avrahami *et al.*, 2003)
cd3AF R3cd	*nirS*	NO_2^- reduction (cytochrome cd_1-containing)	425	GTSAACGTSAAGGARACSGG GASTTCGGRTGSGTCTTGA	Fast SYBR Green Master Mix	95°C for 10 minutes, followed by 40 cycles of 10 s at 95°C, 20 s at 58.5°C, 20 s at 72°C then followed by 20 s at 77°C for fluorescent acquisition	94.2 & 0.99	(Throbäck *et al.*, 2004; Yergeau *et al.*, 2007)
nosZ2F nosZ2R	*nosZ I*	N_2O reduction (Tat dependent)	267	CGCRACGGCAASAAGGTSMSSG T CAKRTGCAKSGCRTGGCAGAA	Fast SYBR Green Master Mix	95°C for 10 minutes, followed by 40 cycles of 10 s at 95°C, 20 s at 58.5°C, 20 s at 72°C then followed by 20 s at 75°C for fluorescent acquisition	99.3 & 0.99	(Henry *et al.*, 2006)
nifHF nifHRb	*nifH*	Nitrogenase reductase	400	AAAGGYGGWATCGGYAARTCCA CCAC TGSGCYTTGTCYTCRCGGATBGG CAT	Fast SYBR Green Master Mix	95°C for 10 minutes, followed by 40 cycles of 10 s at 95°C, 20 s at 58.5°C, 20 s at 72°C then followed by 20 s at 77°C for fluorescent acquisition	94.6 & 0.99	(Rösch and Bothe, 2005)

Note: The efficiency and R^2 were calculated from the standard curve (10-fold dilution series) of each target (gene) from a single run in a 384-well plate.

Supplementary Table S5.2 Pairwise correlation between observed phylum (or class) abundance at DNA and RNA level for urea (+N) treated soils. Correlation analysis was done between DNA (16S rDNA) and RNA (16S rRNA) samples based on mean absolute abundance (per 7,400 sequence reads) at each time point (day 0, 7, 14, 21, 35, 63). Only Proteobacteria shown at class level.

Phylum or class	Lower 95%	Upper 95%	Correlation (r)	p-value
Acidobacteria	0.71	0.98	0.91	**<.0001**
Bacteroidetes	0.30	0.92	0.74	**0.0055**
CD WS3	0.58	0.96	0.86	**0.0003**
Chloroflexi	0.64	0.97	0.89	**0.0001**
Firmicutes	0.33	0.93	0.76	**0.004**
Gemmatimonadetes	-0.36	0.73	0.27	0.397
Nitrospirae	-0.30	0.76	0.33	0.2985
Planctomycetes	0.57	0.96	0.86	**0.0003**
Thaumarchaeota	0.33	0.93	0.76	**0.0041**
Verrucomicrobia	0.18	0.90	0.68	**0.0148**
Aplhaproteobacteria	-0.68	0.45	-0.17	0.6069
Betaproteobacteria	0.19	0.90	0.69	**0.0135**
Deltaproteobacteria	-0.08	0.84	0.51	0.087
Gammaproteobacteria	0.26	0.92	0.73	**0.0076**
Actinobacteria	-0.61	0.53	-0.06	0.8523

Note: Lower 95% and Upper 95% represent confidence limit. Statistically significant correlations ($p<0.05$) are in bold.

Supplementary Table S5.3: Two sample t-test for mean comparison between low copy number *rrn* (rRNA operon) samples (1-2) and high copy number of *rrn* samples (>2). The significant correlation ($p<0.05$) are showed as bold.

t-test (Welch)	Group1 mean (>2 *rrrn*)	Group2 mean (1-2 *rrrn*)	t value	df	p
HM (growth rate)	0.44	0.40	0.58	23.92	0.566
HM (Max. abundance)	176.62	7.88	3.20	30.66	**0.003**
HM (Fold change)	166.77	54.01	2.71	22.42	**0.013**
LM (growth rate)	0.45	0.36	0.97	20.38	0.342
LM (Max. abundance)	262.71	-9.55	3.55	21.62	**0.001**
LM (Fold change)	242.44	38.33	3.17	14.42	**0.006**
Best (HM/LM) (growth rate)	0.45	0.4	0.723	25.94	0.476
Best (HM/LM) (Max. abundance)	282.68	28.67	3.74	32.93	**0.0007**
Best (HM/LM) (Fold change)	267.87	78.51	3.52	22.45	**0.002**

Supplementary Figures

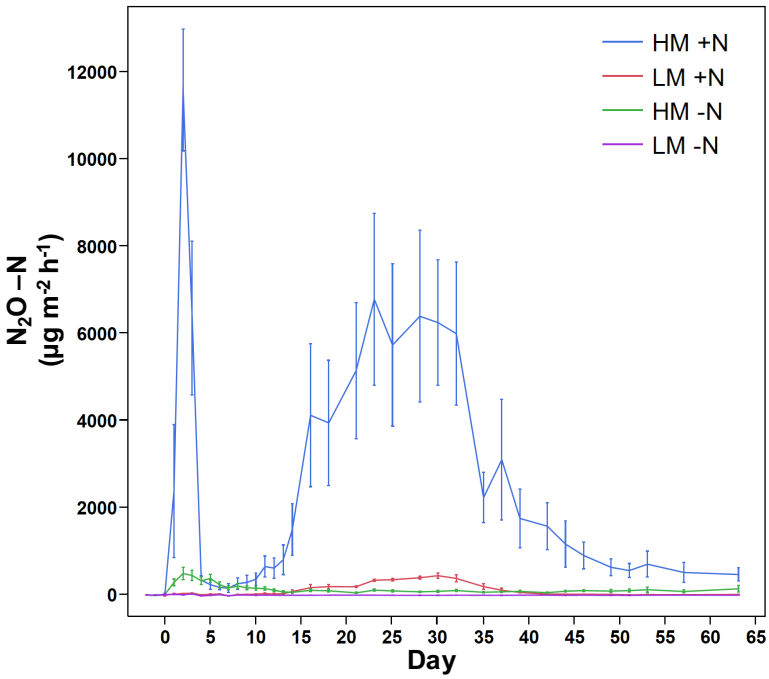

Supplementary Fig. S5.1. N_2O response in soils treated with urea (+/- 1000 µg N/g dry soil) under two moisture conditions (LM = low moisture [-10kPa]; HM = high moisture [-1.0kPa]). Error bars are the standard error of the mean (n ≥ 3) for replicate mesocosms.

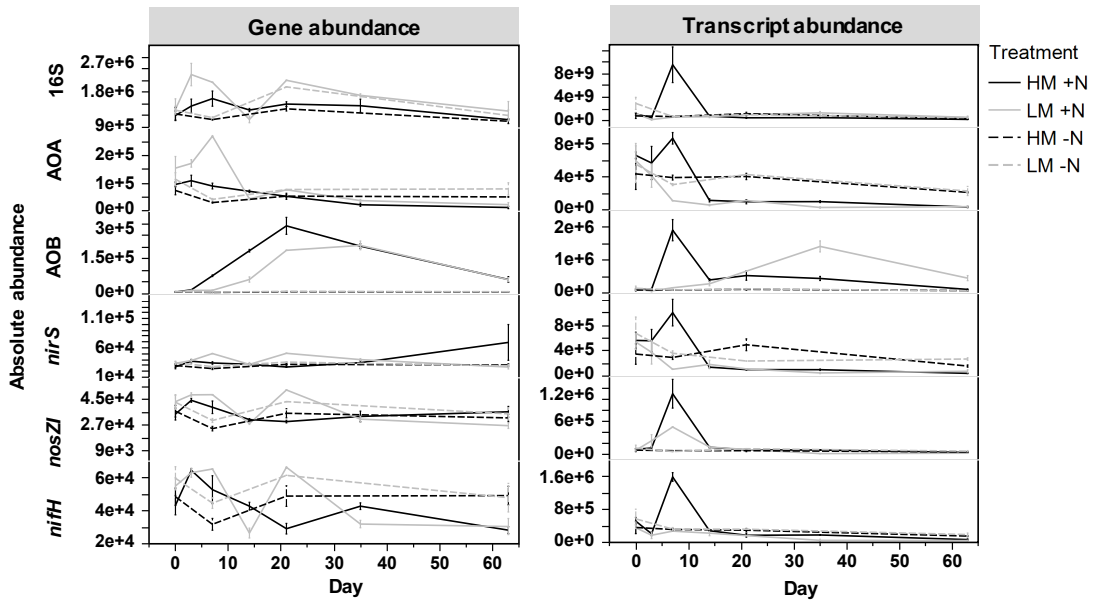

Supplementary Fig. S5.2. Functional group response (absolute quantification) in soils treated with urea (+/-1000 µg N/g dry soil) under two moisture conditions (LM = low moisture [-10kPa]; HM = high moisture [-1.0kPa]). Gene and transcript abundance were measured from DNA template (1 ng of DNA) and cDNA template (1 ng RNA). Error bars are the standard error of the mean (n = 3, except day 7 [n=1; LM soil] and day 21 [n=1; LM soil]) for replicate mesocosms. Absolute gene and transcript abundance were measured by qPCR targeting: 16S (total prokaryotic community), nitrifiers (AOA, ammonia oxidizing archaea; AOB, ammonia oxidizing bacteria), denitrifiers (*nirS,* cytochrome cd_1-containing nitrite reductase*; nosZI*, nitrous oxide reductase) and nitrogen fixers (*nifH*, nitrogenase reductase).

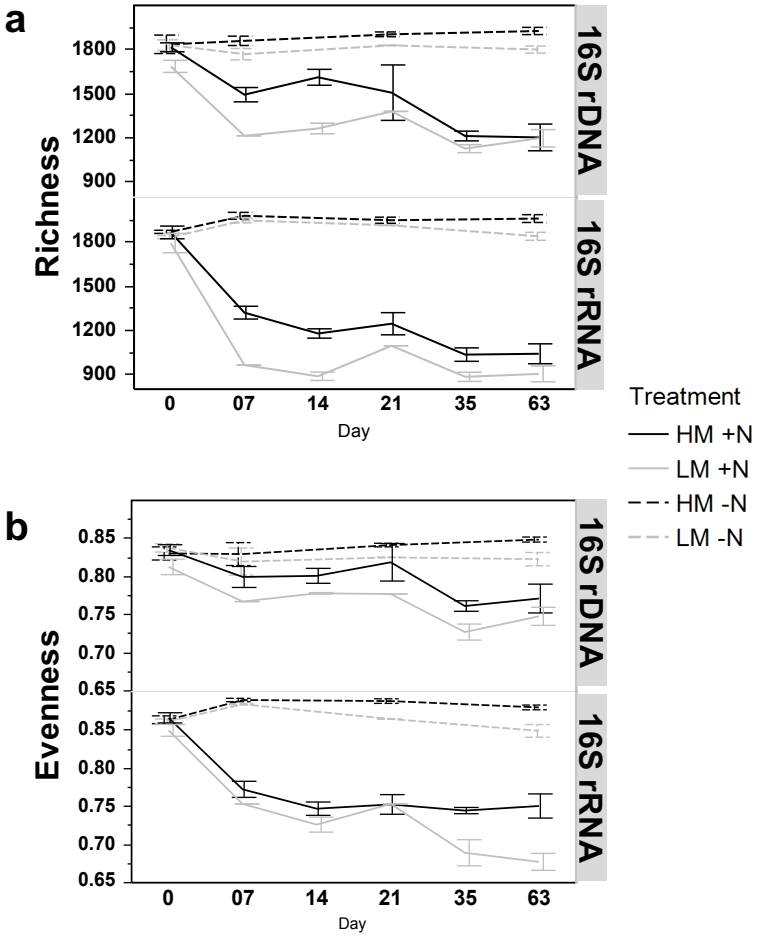

Supplementary Fig. S5.3. Changes in microbial a) Richness and b) Evenness (Pielou's) over time in response to treatment.

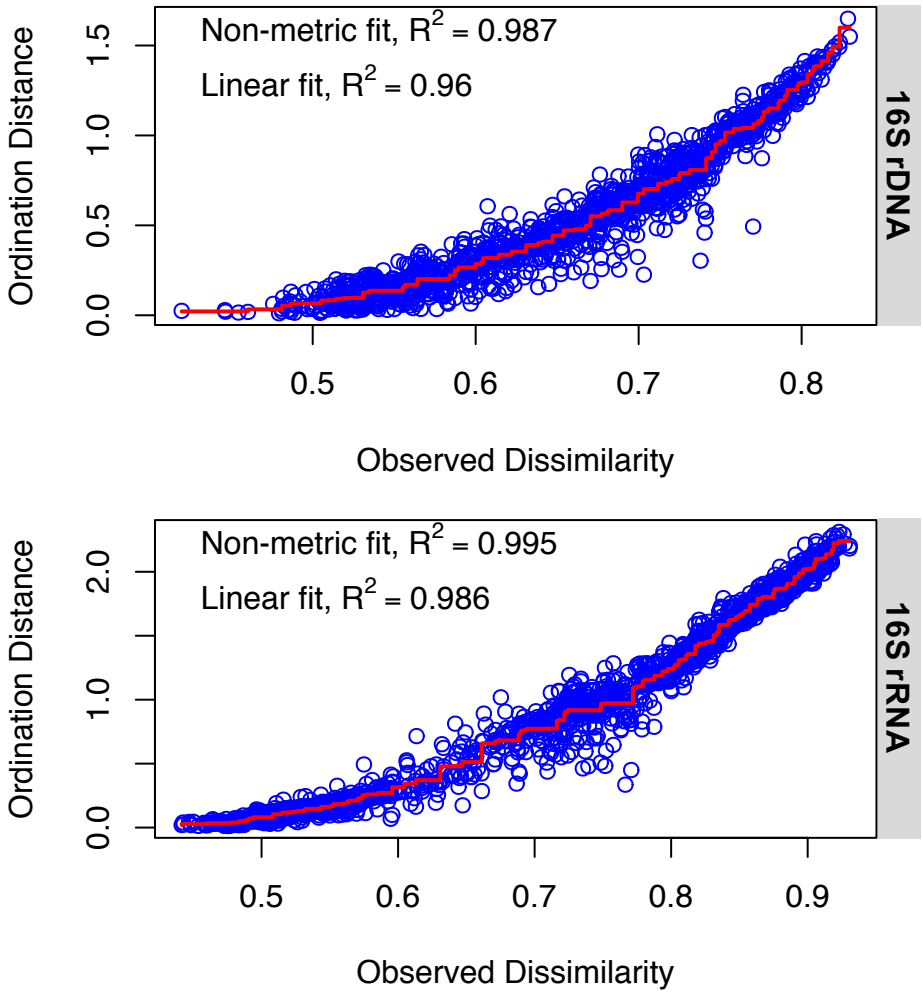

Supplementary Fig. S5.4. Stress plots for Fig. 5.2.b.

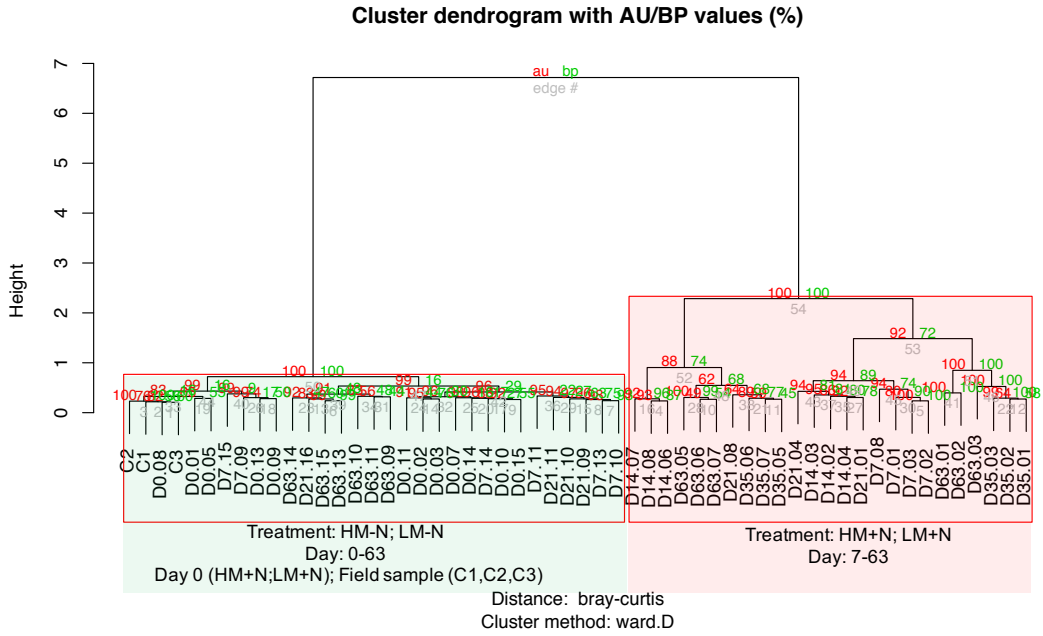

Supplementary Fig. S5.5. Pvclust tree displaying sample clustering based on Bray-Curtis distances calculated from 16S rRNA gene community composition and indicating significant clusters based on p values ([AU (approximately unbiased) BP (bootstrap probability)]) for each node. Red boxes mark clusters with 95% confidence. Bootstrap replication (n=1000). Two clusters: with urea (light red box) and no urea + day 0 N treated samples (light green box).

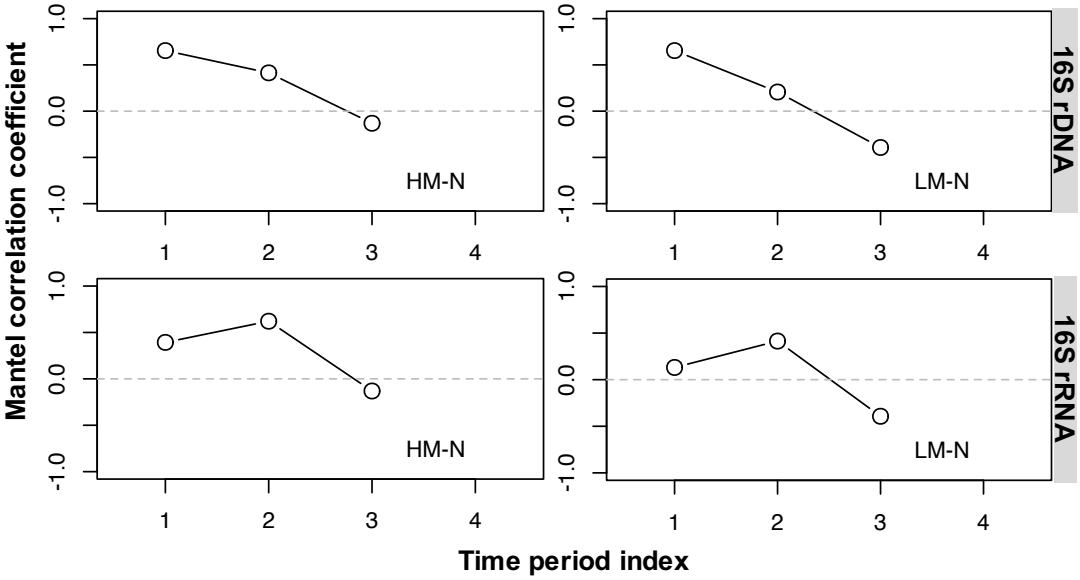

Supplementary Fig. S5.6. Mantel correlogram showing autocorrelation on community composition by performing sequential Mantel tests between the Bray-Curtis dissimilarities and the grouping of samples using a time period index (index 1 represents 0-7 days; 2 represents 7-21; 3 represents 21-63). Opened circles represent no significant correlations ($p > 0.05$) in community composition at specific time periods.

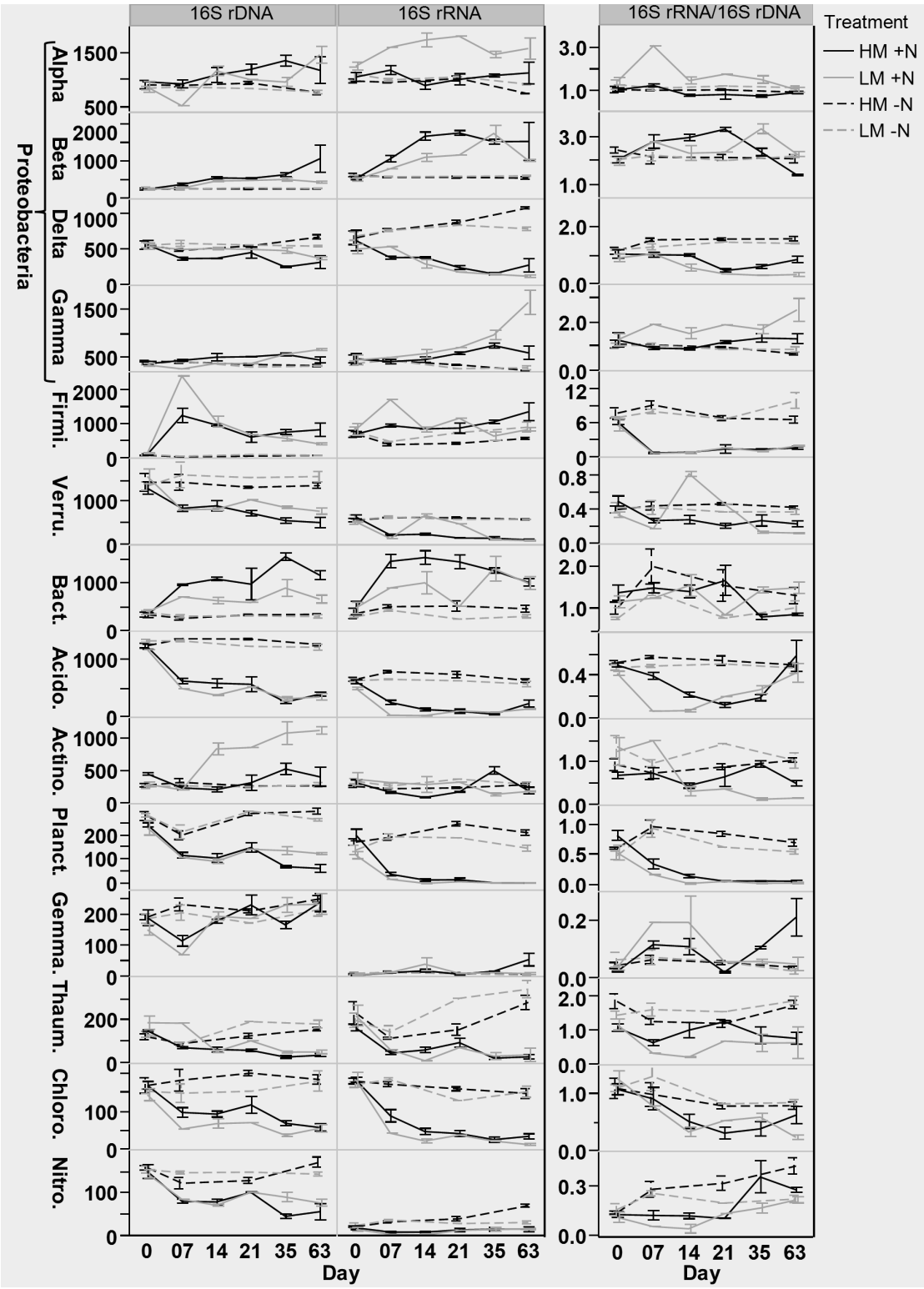

Supplementary Fig. S5.7 Changes in abundance (DNA), activity (RNA) and RNA/DNA ratio for phyla, or classes, representing top 11 phyla (based on OTUs clustered at 97% sequence similarity). A total of 7,400 sequences were examined per sample. Error bars are the standard error of the mean (n = 3, except day 7 [n=1; LM soil] and day 21 [n=1; LM soil]) for replicate mesocosms. Treatments =

+/- N [+/- 1000 µg N/g dry soil] under two moisture conditions (LM = low moisture [-10kPa]; HM = high moisture [-1.0kPa]). Abbreviations: Firmi., Firmicutes; Verru., Verrucomicrobia; Bact., Bacteroidetes; Acido., Acidobacteria; Actino., Actinobacteria; Planct., Planctomycetes; Gemma., Gemmatimonadetes; Thaum., Thaumarchaeota; Chloro., Chloroflexi, Nitro., Nitrospirae

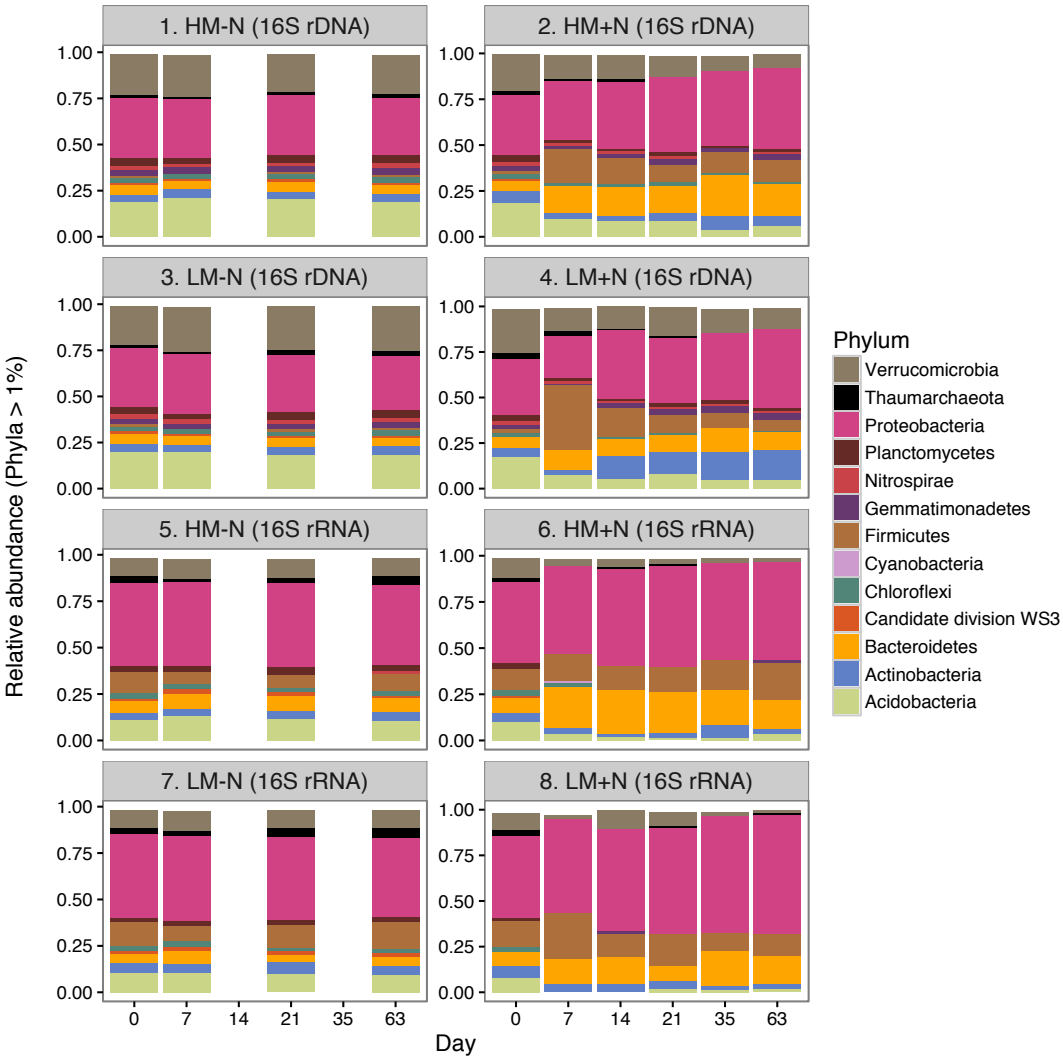

Supplementary Fig. S5.8 Phylum level changes (relative abundance) in genome (16S rDNA) and transcript (16S rRNA) levels representing relative contribution >1% of all detected phyla (based on OTUs clustered at 97% sequence similarity). A total of 7,400 sequences were examined per sample. Treatments = +/- N [+/- 1000 µg N /g dry soil] under two moisture conditions (LM = low moisture [-10kPa]; HM = high moisture [-1.0kPa]).

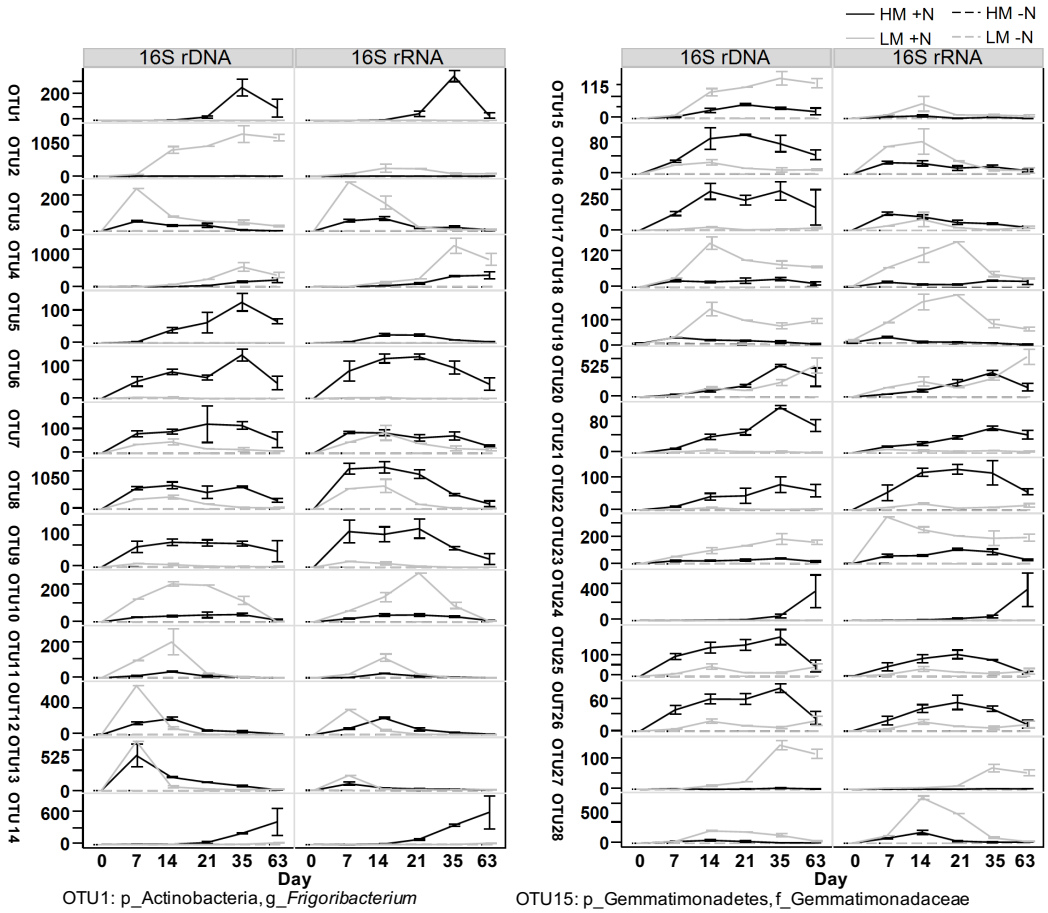

OTU1: p_Actinobacteria, g_*Frigoribacterium*
OTU2: p_Actinobacteria, g_*Actinoplanes*
OTU3: p_Bacteroidetes, g_*Pontibacter*
OTU4: p_Bacteroidetes, f_Cytophagaceae
OTU5: p_Bacteroidetes, f_Chitinophagaceae
OTU6: p_Bacteroidetes, g_ *Pedobacter*
OTU7: p_Bacteroidetes, g_*Pedobacter*
OTU8: p_Bacteroidetes, g_*Pedobacter*
OTU9: p_Bacteroidetes, g_*Pedobacter*
OTU10: p_Firmicutes, g_*Paenibacillus*
OTU11: p_Firmicutes, f_Paenibacillaceae
OTU12: p_Firmicutes,f_Paenibacillaceae
OTU13: p_Firmicutes, g_*Sporosarcina*
OTU14: p_Firmicutes, g_*Clostridium sensu stricto* (I)
OTU15: p_Gemmatimonadetes, f_Gemmatimonadaceae
OTU16: c_Alphaproteobacteria, g_*Brevundimonas*
OTU17: c_Alphaproteobacteria, g_*Brevundimonas*
OTU18: c_Alphaproteobacteria, g_*Aquamicrobium*
OTU19: c_Alphaproteobacteria, g_*Mesorhizobium*
OTU20: c_Alphaproteobacteria, g_*Sphingomonas*
OTU21: c_Alphaproteobacteria, g_*Sphingomonas*
OTU22: c_Betaproteobacteria, g_*Pusillimonas*
OTU23: c_Betaproteobacteria, g_*Pusillimonas*
OTU24: c_Betaproteobacteria, o_Methylophilaceae, f_OM43 clade
OTU25: c_Gammaproteobacteria, g_*Pseudoxanthomonas*
OTU26: c_Gammaproteobacteria, g_*Pseudoxanthomonas*
OTU27: c_ Gammaproteobacteria, g_*Steroidobacter*
OTU28: p_ Verrucomicrobia, g_*Chthoniobacter*

Supplementary Fig. S5.9 Transcriptional (16S rRNA) and population (16S rDNA) changes (abundance based on 7400 reads per samples) for OTUs identified as positively responsive to urea treatment based on similarity percentage (SIMPER) analysis (representing top 30% cumulative sum). Treatments = +/- N [+/- 1000 µg N/g dry soil] under two moisture conditions (LM = low moisture [-10kPa]; HM = high moisture [-1.0kPa]).

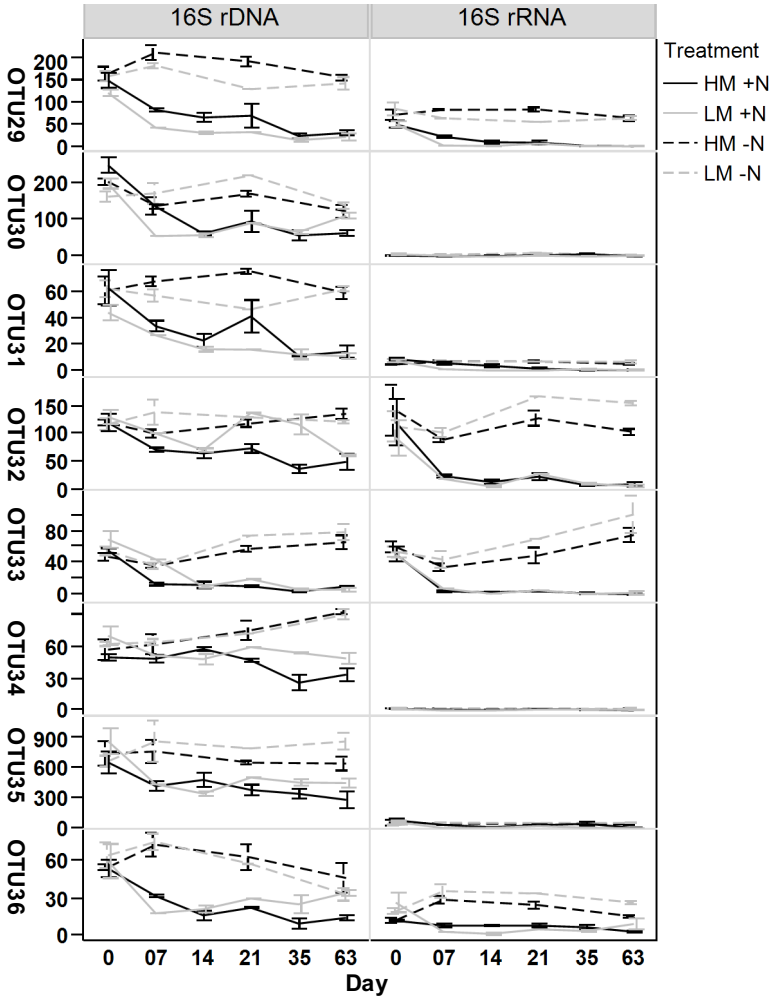

OTU29: c_Acidobacteria, o_Subgroup 6

OTU30: c_Alphaproteobacteria, f_Xanthobacteraceae

OTU31: c_Alphaproteobacteria, o_Rhodospirillales, f_I-10

OTU32: c_Deltaproteobacteria, o_GR-WP33-30

OTU33: p_Thaumarchaeota, c_Soil Crenarchaeotic Group(SCG)

OTU34: p_Verrucomicrobia, f_DA101 soil group

OTU35: p_Verrucomicrobia, f_DA101 soil group

OTU36: p_Verrucomicrobia, f_FukuN18 freshwater group

Supplementary Fig. S5.10 Transcriptional (16S rRNA) and population (16S rDNA) changes (abundance based on 7400 reads per samples) for OTUs identified as negatively responsive to urea treatment based on similarity percentage (SIMPER) analysis (representing top 30% cumulative sum). Treatments = +/- N [+/- 1000 µg N (urea)/g dry soil] under two moisture conditions (LM = low moisture [-10kPa]; HM = high moisture [-1.0kPa]).

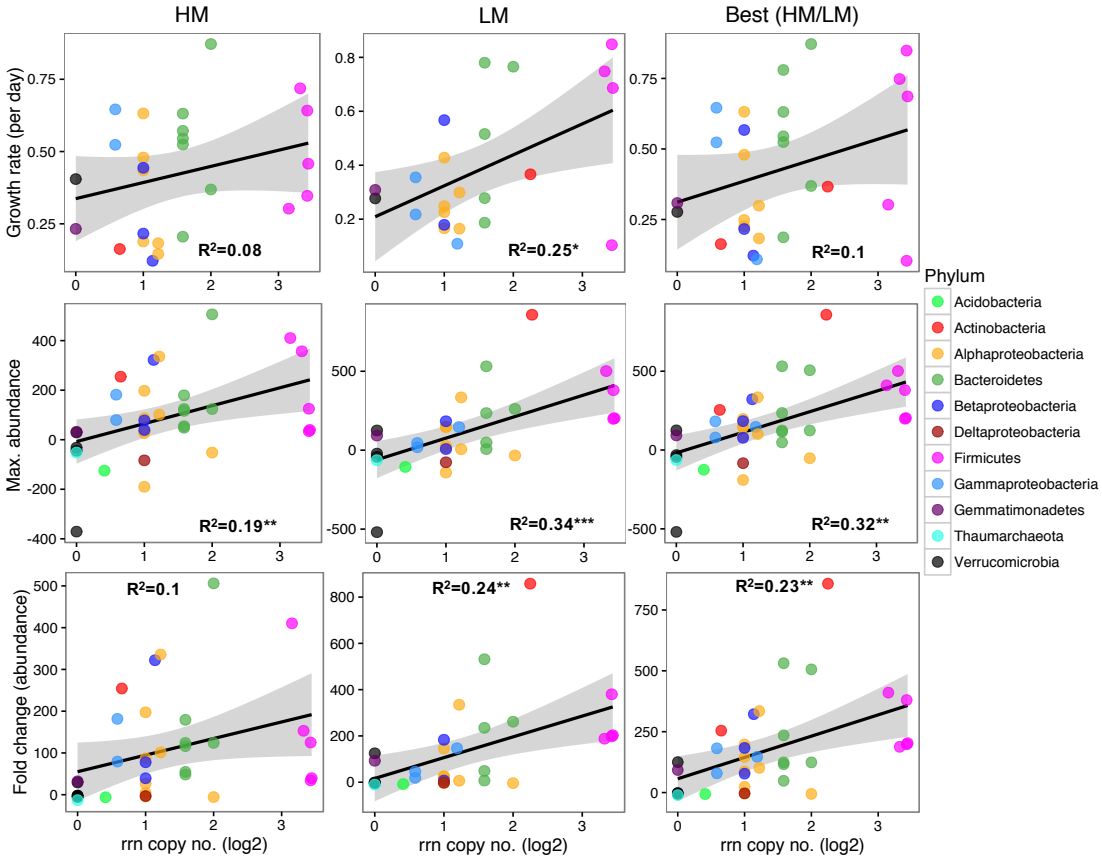

Supplementary Fig. S5.11 Relationship between predicted ribosomal RNA operon (*rrn*) copy numbers and observed growth rate (per day), maximum observed population change, or fold change in population abundance for OTUs responsive to N treatment under both high moisture (HM) content. Copy number was estimated using *rrn* database (Stoddard *et al.*, 2015). Predicted *rrn* copy numbers represent the mean rRNA copy number for the closest taxonomic match (at the lowest taxonomic level possible) for each OTU. The *rrn* copy numbers were log2 transformed before linear regression analysis. Significant "p" value is marked with an asterisk (*p<0.05; **p<0.01; ***p<0.001)

References

Abdelmohsen UR, Grkovic T, Balasubramanian S, Kamel MS, Quinn RJ, Hentschel U. (2015). Elicitation of secondary metabolism in actinomycetes. *Biotechnol Adv* **33**: 798–811.

Altschul SF, Gish W, Miller W, Myers EW, Lipman DJ. (1990). Basic local alignment search tool. *J Mol Biol* **215**: 403–410.

Arp D, Sayavedra-Soto L, Hommes N. (2002). Molecular biology and biochemistry of ammonia oxidation by *Nitrosomonas europaea*. *Arch Microbiol* **178**: 250–255.

Arp DJ, Chain PSG, Klotz MG. (2007). The impact of genome analyses on our understanding of ammonia-oxidizing bacteria. *Annu Rev Microbiol* **61**: 503–528.

Asnicar F, Weingart G, Tickle TL, Huttenhower C. (2015). Compact graphical representation of phylogenetic data and metadata with GraPhlAn. *PeerJ* **3**: e1029.

Avrahami S, Liesack W, Conrad R. (2003). Effects of temperature and fertilizer on activity and community structure of soil ammonia oxidizers. *Environ Microbiol* **5**: 691–705.

Azziz G, Monza J, Etchebehere C, Irisarri P. (2017). *nirS*- and *nirK*-type denitrifier communities are differentially affected by soil type, rice cultivar and water management. *Eur J Soil Biol* **78**: 20–28.

Bagos PG, Nikolaou EP, Liakopoulos TD, Tsirigos KD. (2010). Combined prediction of Tat and Sec signal peptides with hidden Markov models. *Bioinformatics* **26**: 2811–2817.

Bai Y, Wu J, Clark CM, Naeem S, Pan Q. (2010). Tradeoffs and thresholds in the effects of nitrogen addition on biodiversity and ecosystem functioning: evidence from inner Mongolia Grasslands. *Glob Change Biol* **16**: 358–372.

Bakken LR, Bergaust L, Liu B, Frostegard Å. (2012). Regulation of denitrification at the cellular level: a clue to the understanding of N_2O emissions from soils. *Phil Trans R Soc B* **367**: 1226–1234.

Baral KR, Thomsen AG, Olesen JE, Petersen SO. (2014). Controls of nitrous oxide emission after simulated cattle urine deposition. *Agr Ecosyst Environ* **188**: 103–110.

Barka EA, Vatsa P, Sanchez L, Gaveau-Vaillant N, Jacquard C, Klenk HP, *et al.* (2015). Taxonomy, physiology, and natural products of Actinobacteria. *Microbiol Mol Biol R* **80**: 1–43.

Bayer B, Vojvoda J, Offre P, Alves RJE, Elisabeth NH, Garcia JA, *et al.* (2015). Physiological and genomic characterization of two novel marine thaumarchaeal strains indicates niche differentiation. *ISME J* **10**: 1051–1063.

Bender SF, Plantenga F, Neftel A, Jocher M, Oberholzer H-R, hl LKO, *et al.* (2014). Symbiotic relationships between soil fungi and plants reduce N_2O emissions from soil. *ISME J* **8**: 1336–1345.

Bergaust L, Bakken LR, Frostegård Å. (2011). Denitrification regulatory phenotype, a new term for the characterization of denitrifying bacteria. *Biochm Soc Trans* **39**: 207–212.

Bergaust L, Mao Y, Bakken LR, Frostegard Å. (2010). Denitrification response patterns during the transition to anoxic respiration and posttranscriptional effects of suboptimal pH on nitrogen oxide reductase in *Paracoccus denitrificans*. *Appl Environ Microb* **76**: 6387–6396.

Berks BC, Richardson DJ, Reilly A, Willis AC, Ferguson SJ. (1995). The *napEDABC* gene cluster encoding the periplasmic nitrate reductase system of *Thiosphaera pantotropha*. *Biochem J* **309**: 983–992.

Bernhard M, Friedrich B, Siddiqui RA. (2000). *Ralstonia eutropha* TF93 is blocked in Tat-mediated protein export. *J Bacteriol* **182**: 581–588.

Braker G, Conrad R. (2011). Diversity, structure, and size of N_2O-producing microbial communities in soils—what matters for their functioning? *Adv Appl Microbiol* **75**: 33–70.

Brenzinger K, Dörsch P, Braker G. (2015). pH-driven shifts in overall and transcriptionally active denitrifiers control gaseous product stoichiometry in growth experiments with extracted bacteria from soil. *Front Microbiol* **6**: 961.

Brewer T, Handley K, Carini P, Gibert J, Fierer N. (2016). Genome reduction in an abundant and ubiquitous soil bacterial '*Candidatus Udaeobacter copiosus*'. *Nat Microbiol* **2**: 16198.

Burford JR, Bremner JM. (1975). Relationships between the denitrification capacities of soils and total, water-soluble and readily decomposable soil organic matter. *Soil Biol Biochem* **7**: 389–394.

Butterbach-Bahl K, Baggs EM, Dannenmann M, Kiese R, Zechmeister-Boltenstern S. (2013). Nitrous oxide emissions from soils: how well do we understand the processes and their controls? *Phil Trans R Soc B* **368**: 20130122.

Cabrera ML, Kissel DE, Bock BR. (1991). Urea hydrolysis in soil: Effects of urea concentration and soil pH. *Soil Biol Biochem* **23**: 1121–1124.

Caporaso JG, Kuczynski J, Stombaugh J, Bittinger K, Bushman FD, Costello EK, *et al.* (2010). QIIME allows analysis of high-throughput community sequencing data. *Nat Meth* **7**: 335–336.

Caporaso JG, Lauber CL, Walters WA, Berg-Lyons D, Huntley J, Fierer N, *et al.* (2012). Ultra-high-throughput microbial community analysis on the Illumina HiSeq and MiSeq platforms. *ISME J* **6**: 1621–1624.

Caranto JD, Vilbert AC, Lancaster KM. (2016). *Nitrosomonas europaea*

cytochrome P460 is a direct link between nitrification and nitrous oxide emission. *Proc Nat Acad Sci* **113**: 14704–14709.

Clarke KR. (1993). Non-parametric multivariate analyses of changes in community structure. *Aust J Ecol* **18**: 117–143.

Clough TJ, Lanigan GJ, de Klein C, Samad MS, Morales SE, Rex D, *et al.* (2017). Influence of soil moisture on codenitrification fluxes from a urea-affected pasture soil. *Sci Rep* **7**: 2185.

Cole CV, Duxbury J, Freney J, Heinemeyer O, Minami K, Mosier A, *et al.* (1997). Global estimates of potential mitigation of greenhouse gas emissions by agriculture. *Nutr Cycl Agroecosyst* **49**: 221–228.

Coyne MS, Arunakumari A, Averill BA, Tiedje JM. (1989). Immunological identification and distribution of dissimilatory heme cd_1 and nonheme copper nitrite reductases in denitrifying bacteria. *Appl Environ Microb* **55**: 2924–2931.

Čuhel J, Šimek M, Laughlin RJ, Bru D, Cheneby D, Watson CJ, *et al.* (2010). Insights into the effect of soil pH on N_2O and N_2 emissions and denitrifier community size and activity. *Appl Environ Microb* **76**: 1870–1878.

Daims H, Lücker S, Wagner M. (2016). A new perspective on microbes formerly known as nitrite-oxidizing bacteria. *Trends Microbiol* **24**: 699–712.

De Boer W, Kowalchuk GA. (2001). Nitrification in acid soils: micro-organisms and mechanisms. *Soil Biol Biochem* **33**: 853–866.

de Klein CA, Shepherd MA, van der Weerden TJ. (2014a). Nitrous oxide emissions from grazed grasslands: interactions between the N cycle and climate change — a New Zealand case study. *Curr Opin Environ Sustain* **9-10**: 131–139.

de Klein CAM, Barton L, Sherlock RR, Li Z, Littlejohn RP. (2003). Estimating a nitrous oxide emission factor for animal urine from some New Zealand pastoral soils. *Aust J Soil Res* **41**: 381–399.

de Klein CAM, Luo J, Woodward KB, Styles T, Wise B, Lindsey S, *et al.* (2014b). The effect of nitrogen concentration in synthetic cattle urine on nitrous oxide emissions. *Agr Ecosyst Environ* **188**: 85–92.

De Schrijver A, De Frenne P, Ampoorter E, Van Nevel L, Demey A, Wuyts K, *et al.* (2011). Cumulative nitrogen input drives species loss in terrestrial ecosystems. *Global Ecol Biogeogr* **20**: 803–816.

Delmont TO, Eren AM, Maccario L, Prestat E, Esen ÖC, Pelletier E, *et al.* (2015). Reconstructing rare soil microbial genomes using in situ enrichments and metagenomics. *Front Microbiol* **6**: 358.

Dethlefsen L, Schmidt TM. (2007). Performance of the translational apparatus varies with the ecological strategies of bacteria. *J Bacteriol* **189**: 3237–3245.

Di HJ, Cameron KC. (2016). Inhibition of nitrification to mitigate nitrate leaching

and nitrous oxide emissions in grazed grassland: a review. *J Soils Sediments* **16**: 1401–1420.

Di HJ, Cameron KC. (2002). Nitrate leaching in temperate agroecosystems: sources, factors and mitigating strategies. *Nutr Cycl Agroecosyst* **64**: 237–256.

Di HJ, Cameron KC, Shen J-P, Winefield CS, O'Callaghan M, Bowatte S, *et al.* (2010). Ammonia-oxidizing bacteria and archaea grow under contrasting soil nitrogen conditions. *Fems Microbiol Ecol* **72**: 386–394.

Di HJ, Cameron KC, Shen JP, Winefield CS, O'Callaghan M, Bowatte S, *et al.* (2009). Nitrification driven by bacteria and not archaea in nitrogen-rich grassland soils. *Nat Geosci* **2**: 621–624.

Dietrich LEP, Okegbe C, Price-Whelan A, Sakhtah H, Hunter RC, Newman DK. (2013). Bacterial community morphogenesis is intimately linked to the intracellular redox state. *J Bacteriol* **195**: 1371–1380.

Domeignoz-Horta LA, Spor A, Bru D, Breuil M-C, Bizouard F, Léonard J, *et al.* (2015). The diversity of the N_2O reducers matters for the N_2O:N_2 denitrification end-product ratio across an annual and a perennial cropping system. *Front Microbiol* **6**: 971.

Dreusch A, Bürgisser DM, Heizmann CW, Heizmann CW. (1997). Lack of copper insertion into unprocessed cytoplasmic nitrous oxide reductase generated by an R20D substitution in the arginine consensus motif of the signal peptide. *Biochim Biophys Acta* **1319**: 311–318.

Edgar RC. (2010). Search and clustering orders of magnitude faster than BLAST. *Bioinformatics* **26**: 2460–2461.

Felske, Akkermans. (1998). Prominent occurrence of ribosomes from an uncultured bacterium of the Verrucomicrobiales cluster in grassland soils. *Lett Appl Microbiol* **26**: 219–223.

Field SJ, Thorndycroft FH, Matorin AD, Richardson DJ, Richardson DJ, Watmough NJ. (2008). The respiratory nitric oxide reductase (NorBC) from *Paracoccus denitrificans*. *Methods Enzymol* **437**: 77–99.

Fierer N, Bradford MA, Jackson RB. (2007). Toward an ecological classification of soil bacteria. *Ecology* **88**: 1354–1364.

Firestone MK, Firestone RB, Tiedje JM. (1980). Nitrous oxide from soil denitrification: factors controlling its biological production. *Science* **208**: 749–751.

Fish JA, Chai B, Wang Q, Sun Y, Brown CT, Tiedje JM, *et al.* (2013). FunGene: the functional gene pipeline and repository. *Front Microbiol* **4**: 291.

Frame CH, Casciotti KL. (2010). Biogeochemical controls and isotopic signatures of nitrous oxide production by a marine ammonia-oxidizing bacterium. *Biogeosciences* **7**: 2695–2709.

Gardiner MJ, Radford T. (1980). Soil associations of Ireland and their land use potential: explanatory bulletin to soil map of Ireland. Soil Survey Bulletin No. 36. *An Forás Taluntais*, Dublin.

Gawlik BM, Lamberty A, Pauwels J, Blum WEH, Mentler A, Bussian B, *et al.* (2003). Certification of the European Reference Soil Set (IRMM-443—EUROSOILS). Part II. Soil-pH in suspensions of water and $CaCl_2$. *Sci Total Environ* **312**: 33–42.

Ge S, Wang S, Yang X, Qiu S, Li B, Peng Y. (2015). Detection of nitrifiers and evaluation of partial nitrification for wastewater treatment: A review. *Chemosphere* **140**: 85–98.

Godden JW, Turley S, Teller DC, Adman ET, Liu MY. (1991). The 2.3 angstrom X-ray structure of nitrite reductase from *Achromobacter cycloclastes*. *Science* **253**: 438–442.

Gong P, Zhang L, Wu Z, Shang Z, Li D. (2013). Does the nitrification inhibitor dicyandiamide affect the abundance of ammonia-oxidizing bacteria and archaea in a Hap-Udic Luvisol? *J Soil Sci Plant Nutr* **13**: 35–42.

Graham EB, Wieder WR, Leff JW, Weintraub SR, Townsend AR, Cleveland CC, *et al.* (2014). Do we need to understand microbial communities to predict ecosystem function? A comparison of statistical models of nitrogen cycling processes. *Soil Biol Biochem* **68**: 279–282.

Green J, Paget MS. (2004). Bacterial redox sensors. *Nat Rev Microbiol* **2**: 954–966.

Griffiths BS, Ritz K, Bardgett RD, Cook R, Christensen S, Ekelund F, *et al.* (2000). Ecosystem response of pasture soil communities to fumigation- induced microbial diversity reductions: an examination of the biodiversity–ecosystem function relationship. *Oikos* **90**: 279–294.

Griffiths B, Ritz K, Wheatley R. (2001). An examination of the biodiversity-ecosystem function relationship in arable soil microbial communities. *Soil Biol Biochem* **33**: 1713–1722.

Gubry-Rangin C, Kratsch C, Williams TA, McHardy AC, Embley TM, Prosser JI, *et al.* (2015). Coupling of diversification and pH adaptation during the evolution of terrestrial Thaumarchaeota. *Proc Nat Acad Sci* **112**: 9370–9375.

Haltia T, Brown K, Tegoni M, Cambillau C, Saraste M, Mattila K, *et al.* (2003). Crystal structure of nitrous oxide reductase from *Paracoccus denitrificans* at 1.6 Å resolution. *Biochem J* **369**: 77–88.

Hamonts K, Balaine N, Moltchanova E, Beare M, Thomas S, Wakelin SA, *et al.* (2013). Influence of soil bulk density and matric potential on microbial dynamics, inorganic N transformations, N_2O and N_2 fluxes following urea deposition. *Soil Biol Biochem* **65**: 1–11.

Harpole WS, Sullivan LL, Lind EM, Firn J, Adler PB, Borer ET, *et al.* (2016). Addition of multiple limiting resources reduces grassland diversity. *Nature* **537**: 93–96.

Hartman AL, Lough DM, Barupal DK, Fiehn O, Fishbein T, Zasloff M, *et al.* (2009). Human gut microbiome adopts an alternative state following small bowel transplantation. *Proc Nat Acad Sci* **106**: 17187–17192.

Hartsock A, Shapleigh JP. (2011). Physiological roles for two periplasmic nitrate reductases in *Rhodobacter sphaeroides* 2.4.3 (ATCC 17025). *J Bacteriol* **193**: 6483–6489.

Hassan J, Qu Z, Bergaust LL, Bakken LR. (2016). Transient accumulation of NO_2^- and N_2O during denitrification explained by assuming cell diversification by stochastic transcription of denitrification genes. *PLoS Comput Biol* **12**: e1004621.

Hatzenpichler R. (2012). Diversity, physiology, and niche differentiation of ammonia-oxidizing archaea. *Appl Environ Microb* **78**: 7501–7510.

Heikkilä MP, Honisch U, Wunsch P, Zumft WG. (2001). Role of the Tat transport system in nitrous oxide reductase translocation and cytochrome cd_1 biosynthesis in *Pseudomonas stutzeri*. *J Bacteriol* **183**: 1663–1671.

Heil J, Vereecken H, Brüggemann N. (2015). A review of chemical reactions of nitrification intermediates and their role in nitrogen cycling and nitrogen trace gas formation in soil. *Eur J Soil Sci* **67**: 23–39.

Henry S, Bru D, Stres B, Hallet S, Philippot L. (2006). Quantitative detection of the nosZ gene, encoding nitrous oxide reductase, and comparison of the abundances of 16S rRNA, *narG*, *nirK*, and *nosZ* genes in soils. *Appl Environ Microb* **72**: 5181–5189.

Herrero M, Henderson B, Havlík P, Thornton PK, Conant RT, Smith P, *et al.* (2016). Greenhouse gas mitigation potentials in the livestock sector. *Nat Clim Change* **6**: 452–461.

Ho A, Kerckhof F-M, Luke C, Reim A, Krause S, Boon N, *et al.* (2012). Conceptualizing functional traits and ecological characteristics of methane-oxidizing bacteria as life strategies. *Env Microbiol Rep* **5**: 335–345.

Hooper AB, Vannelli T, Bergmann DJ, Arciero DM. (1997). Enzymology of the oxidation of ammonia to nitrite by bacteria. *Antonie Van Leeuwenhoek* **71**: 59–67.

Howes BD, Abraham Z, Lowe DJ, Bruser T. (1994). EPR and electron nuclear double resonance (ENDOR) studies show nitrite binding to the type 2 copper centers of the dissimilatory nitrite reductase of *Alcaligenes xylosoxidans* (NCIMB 11015) *Biochemistry* **33**: 3171–3277.

Hu H-W, Chen D, He J-Z. (2015). Microbial regulation of terrestrial nitrous oxide formation: understanding the biological pathways for prediction of emission rates. *FEMS Microbiol Rev* **39**: 729–749.

Inatomi K-I, Hochstein LI. (1996). The purification and properties of a copper nitrite reductase from *Haloferax denitrificans*. *Curr Microbiol* **32**: 72–76.

IPCC. (2007). Climate Change 2007: Synthesis Report. Contribution of Working Groups I, II and III to the Fourth Assessment report of the intergovernmental panel on climate change. Geneva, Switzerland.

ISO. (2005). Soil quality—determination of pH (ISO 10390: 2005).

Jahangir MMR, Khalil MI, Johnston P, Cardenas LM, Hatch DJ, Butler M, *et al.* (2012). Denitrification potential in subsoils: A mechanism to reduce nitrate leaching to groundwater. *Agr Ecosyst Environ* **147**: 13–23.

Jia Z, Conrad R. (2009). Bacteriarather than Archaea dominate microbial ammonia oxidation in an agricultural soil. *Environ Microbiol* **11**: 1658–1671.

Jones CM, Graf D, Bru D, Philippot L, Hallin S. (2013). The unaccounted yet abundant nitrous oxide-reducing microbial community: a potential nitrous oxide sink. *ISME J* **7**: 417–426.

Jones CM, Spor A, Brennan FP, Breuil MC. (2014). Recently identified microbial guild mediates soil N_2O sink capacity. *Nat Clim Change* **4**: 801–805.

Jung M-Y, Well R, Min D, Giesemann A, Park S-J, Kim J-G, *et al.* (2014). Isotopic signatures of N_2O produced by ammonia-oxidizing archaea from soils. *ISME J* **8**: 1115–1125.

Kern M, Simon J. (2015). Three transcription regulators of the Nss family mediate the adaptive response induced by nitrate, nitric oxide or nitrous oxide in *Wolinella succinogenes*. *Environ Microbiol* **18**: 2899–2912.

Klappenbach JA, Dunbar JM, Schmidt TM. (2000). rRNA operon copy number reflects ecological strategies of bacteria. *Appl Environ Microb* **66**: 1328–1333.

Klotz MG, Stein LY. (2007). Nitrifier genomics and evolution of the nitrogen cycle. *FEMS Microbiol Lett.* **278**:146–156.

Knowles R. (1982). Denitrification. *Microbiol Rev* **46**: 43–70.

Koch H, Lücker S, Albertsen M, Kitzinger K, Herbold C, Spieck E, *et al.* (2015). Expanded metabolic versatility of ubiquitous nitrite-oxidizing bacteria from the genus *Nitrospira*. *Proc Nat Acad Sci* **112**: 11371–11376.

Kool DM, Hoffland E, Abrahamse SPA, van Groenigen JW. (2006). What artificial urine composition is adequate for simulating soil N_2O fluxes and mineral N dynamics? *Soil Biol Biochem* **38**: 1757–1763.

Kuenen JG, Robertson LA. (1994). Combined nitrification-denitrification processes. *FEMS Microbiol Rev* **15**: 109–117.

Lampe C, Dittert K, Sattelmacher B, Wachendorf M, Loges R, Taube F. (2006). Sources and rates of nitrous oxide emissions from grazed grassland after

application of ^{15}N-labelled mineral fertilizer and slurry. *Soil Biol Biochem* **38**: 2602–2613.

Lauber CL, Hamady M, Knight R, Fierer N. (2009). Pyrosequencing-based assessment of soil pH as a predictor of soil bacterial community structure at the continental scale. *Appl Environ Microb* **75**: 5111–5120.

Leff JW, Jones SE, Prober SM, Barberán A, Borer ET, Firn JL, *et al.* (2015). Consistent responses of soil microbial communities to elevated nutrient inputs in grasslands across the globe. *Proc Nat Acad Sci* **112**: 10967–10972.

Leininger S, Urich T, Schloter M, Schwark L, Qi J, Nicol GW, *et al.* (2006). Archaea predominate among ammonia-oxidizing prokaryotes in soils. *Nature* **442**: 806–809.

Lesschen JP, Velthof GL, De Vries W, Kros J. (2011). Differentiation of nitrous oxide emission factors for agricultural soils. *Environ Pollut* **159**: 3215–3222.

Levine UY, Teal TK, Robertson GP, Schmidt TM. (2011). Agriculture's impact on microbial diversity and associated fluxes of carbon dioxide and methane. *ISME J* **5**: 1683–1691.

Li C, Di HJ, Cameron KC, Podolyan A, Zhu B. (2016). Effect of different land use and land use change on ammonia oxidiser abundance and N_2O emissions. *Soil Biol Biochem* **96**: 169–175.

Li Y, Katzmann E, Borg S, Schuler D. (2012). The periplasmic nitrate reductase Nap is required for anaerobic growth and involved in redox control of magnetite biomineralization in *Magnetospirillum gryphiswaldense*. *J Bacteriol* **194**: 4847–4856.

Lipson DA. (2015). The complex relationship between microbial growth rate and yield and its implications for ecosystem processes. *Front Microbiol* **6**: 615.

Liu B, Frostegard Å, Bakken LR. (2014). Impaired reduction of N_2O to N_2 in acid soils is due to a posttranscriptional interference with the expression of *nosZ*. *mBio* **5**: e01383–14.

Liu B, Mørkved PT, Frostegård Å, Bakken LR. (2010). Denitrification gene pools, transcription and kinetics of NO, N_2O and N_2 production as affected by soil pH. *Fems Microbiol Ecol* **72**: 407–417.

Locey KJ, Lennon JT. (2016). Scaling laws predict global microbial diversity. *Proc Nat Acad Sci* **113**: 5970–5975.

Long A, Song B, Fridey K, Silva A. (2015). Detection and diversity of copper containing nitrite reductase genes (*nirK*) in prokaryotic and fungal communities of agricultural soils. *Fems Microbiol Ecol* **91**: 1–9.

Loreau M, Naeem S, Inchausti P, Bengtsson J, Grime JP, Hector A, *et al.* (2001). Biodiversity and ecosystem functioning: current knowledge and future challenges. *Science* **294**: 804–808.

Lücker S, Nowka B, Rattei T, Spieck E. (2013). The genome of *Nitrospina gracilis* illuminates the metabolism and evolution of the major marine nitrite oxidizer. *Front Microbiol* **4**: 1–19.

Lücker S, Wagner M, Maixner F, Pelletier E, Koch H, Vacherie B, *et al.* (2010). A Nitrospira metagenome illuminates the physiology and evolution of globally important nitrite-oxidizing bacteria. *Proc Nat Acad Sci* **107**: 13479–13484.

Maharjan B, Venterea RT. (2013). Nitrite intensity explains N management effects on N_2O emissions in maize. *Soil Biol Biochem* **66**: 229–238.

Marchler-Bauer A, Bryant SH. (2004). CD-Search: protein domain annotations on the fly. *Nucleic Acids Res* **32**: W327–W331.

McCarty GW, Bremner JM. (1992). Availability of organic carbon for denitrification of nitrate in subsoils. *Biol Fertil Soils* **14**: 219–222.

McMillan AMS, Pal P, Phillips RL, Palmada T, Berben PH, Jha N, *et al.* (2016). Can pH amendments in grazed pastures help reduce N_2O emissions from denitrification? - The effects of liming and urine addition on the completion of denitrification in fluvial and volcanic soils. *Soil Biol Biochem* **93**: 90–104.

McMurdie PJ, Holmes S. (2013). phyloseq: an R package for reproducible interactive analysis and graphics of microbiome census data. *PLoS ONE*. **8:** e61217.

Meincke M, Bock E, Kastrau D, Kroneck PMH. (1992). Nitrite oxidoreductase from Nitrobacter hamburgensis: redox centers and their catalytic role. *Arch Microbiol* **158**: 127–131.

Meyer F, Paarmann D, D'Souza M, Olson R, Glass EM, Kubal M, *et al.* (2008). The metagenomics RAST server – a public resource for the automatic phylogenetic and functional analysis of metagenomes. *BMC Bioinformatics* **9**: 386.

Moir J, Crossman LC, Spiro S, Richardson DJ. (1996). The purification of ammonia monooxygenase from *Paracoccus denitrficans*. *FEBS Lett* **387**: 71–74.

Moir JWB, Baratta D, Richardson DJ, Ferguson SJ. (1993). The purification of a *cd1*- type nitrite reductase from, and the absence of a copper- type nitrite reductase from, the aerobic denitrifier *Thiosphaera pantotropha*; the role of pseudoazurin as an electron donor. *Eur J Biochem* **212**: 377–385.

Molstad L, Dörsch P, Bakken LR. (2007). Robotized incubation system for monitoring gases (O_2, NO, N_2O N_2) in denitrifying cultures. *J Microbiol Meth* **71**: 202–211.

Morales SE, Cosart T, Holben WE. (2010). Bacterial gene abundances as indicators of greenhouse gas emission in soils. *ISME J* **4**: 799–808.

Morales SE, Holben WE. (2013). Functional response of a near-surface soil microbial community to a simulated underground CO_2 storage leak. *PLoS ONE* **8**:

e81742.

Morales SE, Jha N, Saggar S. (2015). Biogeography and biophysicochemical traits link N_2O emissions, N_2O emission potential and microbial communities across New Zealand pasture soils. *Soil Biol Biochem* **82**: 87–98.

Mosier A, Kroeze C, Nevison C, Oenema O, Seitzinger S, Van Cleemput O. (1998). Closing the global N_2O budget: nitrous oxide emissions through the agricultural nitrogen cycle. *Nutr Cycl Agroecosyst* **52**: 225–248.

Mosier AR. (1998). Soil processes and global change. *Biol Fertil Soils* **27**: 221–229.

Moura JJG, Brondino CD, Trinc o J, Rom o MJO. (2004). Mo and W bis-MGD enzymes: nitrate reductases and formate dehydrogenases. *J Biol Inorg Chem* **9**: 791–799.

Myhre G, Shindell D, Bréon FM, Collins W, Fuglestvedt J, Huang J, *et al.* (2013). Anthropogenic and Natural Radiative Forcing. *In*: *Climate Change 2013*: *The Physical Science Basis*. Contribution of Working Group I to the Fifth Assessment Report of the Intergovernmental Panel on Climate Change. Cambridge University Press, Cambridge.

Mørkved PT, Dörsch P, Bakken LR. (2007). The N_2O product ratio of nitrification and its dependence on long-term changes in soil pH. *Soil Biol Biochem* **39**: 2048–2057.

Natale P, Brüser T, Driessen AJM. (2008). Sec- and Tat-mediated protein secretion across the bacterial cytoplasmic membrane—distinct translocases and mechanisms. *Biochim Biophys Acta* **1778**: 1735–1756.

Nemergut DR, Knelman JE, Ferrenberg S, Bilinski T, Melbourne B, Jiang L, *et al.* (2015). Decreases in average bacterial community rRNA operon copy number during succession. *ISME J* **10**: 1147–1156.

Ngugi DK, Blom J, Stepanauskas R, Stingl U. (2016). Diversification and niche adaptations of *Nitrospina*- like bacteria in the polyextreme interfaces of Red Sea brines. *ISME J* **10**: 1383–1399.

Nicholls DG, Ferguson SJ (2013). 5 - Respiratory Chains. In: Bioenergetics (Fourth Edition). *Bioenergetics (Fourth Edition)*. Academic Press: Boston, pp 91–157.

Nicol GW, Leininger S, Schleper C, Prosser JI. (2008). The influence of soil pH on the diversity, abundance and transcriptional activity of ammonia oxidizing archaea and bacteria. *Environ Microbiol* **10**: 2966–2978.

Nishizawa T, Quan A, Kai A, Tago K, Ishii S, Shen W, *et al.* (2014). Inoculation with N_2-generating denitrifier strains mitigates N_2O emission from agricultural soil fertilized with poultry manure. *Biol Fertil Soils* **50**: 1001–1007.

Obia A, Cornelissen G, Mulder J, Dörsch P. (2015). Effect of soil pH increase by biochar on NO, N_2O and N_2 production during denitrification in acid soils. *PLoS ONE* **10**: e0138781.

Oenema O, Wrage N, Velthof GL, van Groenigen JW, Dolfing J, Kuikman PJ. (2005). Trends in global nitrous oxide emissions from animal production systems. *Nutr Cycl Agroecosyst* **72**: 51–65.

Ohshima T, Sugiyama M, Uozumi N, Iijima S. (1993). Cloning and sequencing of a gene encoding nitrite reductase from *Paracoccus denitrificans* and expression of the gene in *Escherichia coli*. *J Ferment Bioeng* **76**: 82–88.

Oksanen J, Blanchet FG, Kindt R, Legendre P. (2013). Vegan: Community ecology package (2013) R package version 2.0-7. https://cran.r-project.org/package=vegan.

Orellana LH, Rodriguez-R LM, Higgins S, Chee-Sanford JC, Sanford RA, Ritalahti KM, *et al.* (2014). Detecting nitrous oxide reductase (*nosZ*) genes in soil metagenomes: method development and implications for the nitrogen cycle. *mBio* **5**: e01193.

Ostrom NE, Sutka R, Ostrom PH, Grandy AS, Huizinga KM, Gandhi H, *et al.* (2010). Isotopologue data reveal bacterial denitrification as the primary source of N_2O during a high flux event following cultivation of a native temperate grassland. *Soil Biol Biochem* **42**: 499–506.

O'Farrell KA, Janssen PH. (1999). Detection of Verrucomicrobia in a Pasture Soil by PCR-Mediated Amplification of 16S rRNA Genes. *Appl Environ Microb* **65**: 4280–4284.

Pachauri RK, Allen MR, Barros VR, Broome J, Cramer W, Christ R, *et al.* (2014). Climate Change 2014: Synthesis Report. Contribution of Working Groups I, II and III to the Fifth Assessment Report of the Intergovernmental Panel on Climate Change. *EPIC3Geneva, Switzerland, IPCC, 151 p, pp 151, ISBN: 978-92-9169-143-2*. http://epic.awi.de/37530/.

Paustian L, Babcock B, Hatfield JL, Lal R, McCarl BA, McLaughlin S, *et al.* (2004). Agricultural mitigation of greenhouse gases: Science and policy options. 18.

Philippot L. (2002). Denitrifying genes in bacterial and Archaeal genomes. *Biochim Biophys Acta* ***1577****:* 355–376.

Philippot L, Andert J, Jones CM, Bru D. (2011). Importance of denitrifiers lacking the genes encoding the nitrous oxide reductase for N_2O emissions from soil. *Glob Change Biol* **17**: 1497–1504.

Philippot L, Spor AE, nault CHE, Bru D, Bizouard F, Jones CM, *et al.* (2013). Loss in microbial diversity affects nitrogen cycling in soil. *ISME J* **7**: 1609–1619.

Pratscher J, Dumont MG, Conrad R. (2011). Ammonia oxidation coupled to CO_2 fixation by archaea and bacteria in an agricultural soil. *Proc Nat Acad Sci* **108**:

4170–4175.

Prosser JI, Nicol GW. (2012). Archaeal and bacterial ammonia-oxidisers in soil: the quest for niche specialisation and differentiation. *Trends Microbiol* **20**: 523–531.

Ptacnik R, Solimini AG, Andersen T, Tamminen T, Brettum P, Lepistö L, *et al.* (2008). Diversity predicts stability and resource use efficiency in natural phytoplankton communities. *Proc Nat Acad Sci* **105**: 5134–5138.

Qu Z, Bakken LR, Molstad L, Frostegård Å, Bergaust LL. (2016). Transcriptional and metabolic regulation of denitrification in *Paracoccus denitrificans* allows low but significant activity of nitrous oxide reductase under oxic conditions. *Environ Microbiol* **18**: 2951–2963.

Qu Z, Wang J, Almøy T, Bakken LR. (2014). Excessive use of nitrogen in Chinese agriculture results in high $N_2O/(N_2O+N_2)$ product ratio of denitrification, primarily due to acidification of the soils. *Glob Change Biol* **20**: 1685–1698.

Quast C, Pruesse E, Yilmaz P, Gerken J, Schweer T, Yarza P, *et al.* (2012). The SILVA ribosomal RNA gene database project: improved data processing and web-based tools. *Nucleic Acids Res* **41**: D590–D596.

R Development Core Team. (2008). R: A language and environment for statistical computing. *R Foundation for Statistical Computing, Vienna, Austria*. http://www.R-project.org.

Rasmussen T, Berks BC, Butt JN, Thomson AJ. (2002). Multiple forms of the catalytic centre, Cu_Z, in the enzyme nitrous oxide reductase from *Paracoccus pantotrophus*. *Biochem J* **364**: 807–815.

Raut N, Dörsch P, Sitaula BK, Bakken LR. (2012). Soil acidification by intensified crop production in South Asia results in higher $N_2O/(N_2 + N_2O)$ product ratios of denitrification. *Soil Biol Biochem* **55**: 104–112.

Ravishankara AR, Daniel JS, Portmann RW. (2009). Nitrous oxide (N_2O): the dominant ozone-depleting substance emitted in the 21st Century. *Science* **326**: 123–125.

Reddy KR, Rao PSC, Jessup RE. (1982). The Effect of Carbon Mineralization on Denitrification Kinetics in Mineral and Organic Soils. *Soil Sci Soc Am J* **46**: 62–68.

Regaert D, Aubinet M, Moureaux C. (2015). Mitigating N_2O emissions from agriculture : A review of the current knowledge on soil system modelling, environmental factors and management practices influencing emissions. *J Soil Sci Environ Manage* **6**: 178–186.

Richardson D, Felgate H, Watmough N, Thomson A, Baggs E. (2009). Mitigating release of the potent greenhouse gas N2O from the nitrogen cycle – could enzymic regulation hold the key? *Trends Biotechnol* **27**: 388–397.

Rinke C, Schwientek P, Sczyrba A, Ivanova NN, Anderson IJ, Cheng JF, *et al.* (2013). Insights into the phylogeny and coding potential of microbial dark matter. *Nature* **499**: 431–437.

Robertson GP. (2000). Greenhouse gases in intensive agriculture: contributions of individual gases to the radiative forcing of the atmosphere. *Science* **289**: 1922–1925.

Rocca JD, Hall EK, Lennon JT, Evans SE, Waldrop MP, Cotner JB, *et al.* (2015). Relationships between protein-encoding gene abundance and corresponding process are commonly assumed yet rarely observed. *ISME J* **9**: 1693–1699.

Roller BRK, Stoddard SF, Schmidt TM. (2016). Exploiting rRNA operon copy number to investigate bacterial reproductive strategies. *Nat Microbiol* **1**: 16160.

Rotthauwe JH, Witzel KP, Liesack W. (1997). The ammonia monooxygenase structural gene *amoA* as a functional marker: molecular fine-scale analysis of natural ammonia-oxidizing populations. *Appl Environ Microb* **63**: 4704–4712.

Rousk J, Bååth E, Brookes PC, Lauber CL, Lozupone C, Caporaso JG, *et al.* (2010). Soil bacterial and fungal communities across a pH gradient in an arable soil. *ISME J* **4**: 1340–1351.

Rösch C, Bothe H. (2005). Improved assessment of denitrifying, N_2-fixing, and total-community bacteria by terminal restriction fragment length polymorphism analysis using multiple restriction enzymes. *Appl Environ Microb* **71**: 2026–2035.

Russenes AL, Korsaeth A, Bakken LR, Dörsch P. (2016). Spatial variation in soil pH controls off-season N_2O emission in an agricultural soil. *Soil Biol Biochem* **99**: 36–46.

Saggar S, Jha N, Deslippe J, Bolan NS, Luo J, Giltrap DL, *et al.* (2013). Denitrification and N_2O:N_2 production in temperate grasslands: processes, measurements, modelling and mitigating negative impacts. *Sci Total Environ* **465**: 173–195.

Sahrawat KL. (2008). Factors affecting nitrification in soils. *Commun Soil Sci Plan* **39**: 1436–1446.

Samad MS, Bakken LR, Nadeem S, Clough TJ, de Klein CAM, Richards KG, *et al.* (2016a). High-resolution denitrification kinetics in pasture soils link N_2O emissions to pH, and denitrification to C mineralization. *PLoS ONE* **11**: e0151713.

Samad MS, Biswas A, Bakken LR, Clough TJ, de Klein CAM, Richards KG, *et al.* (2016b). Phylogenetic and functional potential links pH and N_2O emissions in pasture soils. *Sci Rep* **6**: 35990.

Samad MS, Johns C, Richards KG, Lanigan GJ, de Klein CAM, Clough TJ, *et al.* (2017). Response to nitrogen addition reveals metabolic and ecological strategies of soil bacteria. *Mol Ecol*, 1–15.

Sanford RA, Sanford RA, Wagner DD, Wagner DD, Wu Q, Wu Q, *et al.* (2012). Unexpected nondenitrifier nitrous oxide reductase gene diversity and abundance in soils. *Proc Nat Acad Sci* **109**: 19709–19714.

Sangwan P, Kovac S, Davis KER, Sait M, Janssen PH. (2005). Detection and cultivation of soil verrucomicrobia. *Appl Environ Microb* **71**: 8402–8410.

Santoro AE, Buchwald C, McIlvin MR. (2011). Isotopic signature of N_2O produced by marine ammonia-oxidizing archaea. *Science* **333**: 1282–1285.

Schnitzer SA, Klironomos JN, HilleRisLambers J, Kinkel LL, Reich PB, Xiao K, *et al.* (2011). Soil microbes drive the classic plant diversity–productivity pattern. *Ecology* **92**: 296–303.

Senbayram M, Chen R, Budai A, Bakken L, Dittert K. (2012). N_2O emission and the $N_2O/(N_2O+N_2)$ product ratio of denitrification as controlled by available carbon substrates and nitrate concentrations. *Agr Ecosyst Environ* **147**: 4–12.

Sherlock RR, Goh KM. (1985). Dynamics of ammonia volatilization from simulated urine patches and aqueous urea applied to pasture. II. Theoretical derivation of a simplified model. *Fert Res* **6**: 3–22.

Shiina Y, Itakura M, Choi H, Saeki Y, Hayatsu M, Minamisawa K. (2014). Relationship between soil type and N_2O reductase genotype (*nosZ*) of indigenous soybean Bradyrhizobia: *nosZ*-minus populations are dominant in Andosols. *Microb Environ* **29**: 420–426.

Shoun H, Kim D-H, Uchiyama H, Sugiyama J. (1992). Denitrification by fungi. *FEMS Microbiol Lett* **94**: 277–281.

Simon J, Einsle O, Kroneck PMH, Zumft WG. (2004). The unprecedented nosgene cluster of *Wolinella succinogenesencodes* a novel respiratory electron transfer pathway to cytochrome cnitrous oxide reductase. *FEBS Lett* **569**: 7–12.

Song L, Bao X, Liu X, Zhang F. (2012). Impact of nitrogen addition on plant community in a semi-arid temperate steppe in China. *J Arid Land* **4**: 3–10.

Song L, Bao X, Liu X, Zhang Y, Christie P, Fangmeier A, *et al.* (2011). Nitrogen enrichment enhances the dominance of grasses over forbs in a temperate steppe ecosystem. *Biogeosciences* **8**: 2341–2350.

Sorokin DY, cker SLU, Vejmelkova D, Kostrikina NA, Kleerebezem R, Rijpstra WIC, *et al.* (2012). Nitrification expanded: discovery, physiology and genomics of a nitrite-oxidizing bacterium from the phylum *Chloroflexi*. *ISME J* **6**: 2245–2256.

Spieck E, Aamand J, Bartosch S. (1996). Immunocytochemical detection and location of the membrane-bound nitrite oxidoreductase in cells of *Nitrobacter* and *Nitrospira*. *FEMS Microbiol Lett* **139**: 71–76.

Spiro S. (2012). Nitrous oxide production and consumption: regulation of gene expression by gas-sensitive transcription factors. *Phil Trans R Soc B* **367**: 1213–

1225.

Stahl DA, de la Torre JR. (2012). Physiology and diversity of ammonia-oxidizing archaea. *Annu Rev Microbiol* **66**: 83–101.

Starkenburg SR, Chain PSG, Sayavedra-Soto LA, Hauser L, Land ML, Larimer FW, *et al.* (2006). Genome sequence of the chemolithoautotrophic nitrite-oxidizing bacterium *Nitrobacter winogradskyi* Nb-255. *Appl Environ Microb* **72**: 2050–2063.

Stein LY, Yung YL. (2003). Production, isotopic composition, and atmospheric fate of biologically produced nitrous oxide. *Annu Rev Earth Planet Sci* **31**: 329–356.

Stempfhuber B, Richter-Heitmann T, Regan KM, Kölbl A, Wüst PK, Marhan S, *et al.* (2015). Spatial interaction of archaeal ammonia-oxidizers and nitrite-oxidizing bacteria in an unfertilized grassland soil. *Front Microbiol* **6**: 1567.

Sterngren AE, Hallin S, Bengtson P. (2015). Archaeal ammonia oxidizers dominate in numbers, but bacteria drive gross nitrification in N-amended grassland soil. *Front Microbiol* **6**: 1350.

Stevenson BS, Schmidt TM. (2004). Life History Implications of rRNA Gene Copy Number in *Escherichia coli*. *Appl Environ Microb* **70**: 6670–6677.

Stoddard SF, Smith BJ, Hein R, Roller BRK, Schmidt TM. (2015). *rrn*DB: improved tools for interpreting rRNA gene abundance in bacteria and archaea and a new foundation for future development. *Nucleic Acids Res* **43**: D593–D598.

Suding KN, Collins SL, Gough L, Clark C, Cleland EE, Gross KL, *et al.* (2005). Functional- and abundance-based mechanisms explain diversity loss due to N fertilization. *Proc Nat Acad Sci* **102**: 4387–4392.

Suzuki R, Shimodaira H. (2006). Pvclust: an R package for assessing the uncertainty in hierarchical clustering. *Bioinformatics* **22**: 1540–1542.

Syakila A, Kroeze C. (2011). The global nitrous oxide budget revisited. *Greenhouse Gas Meas Manage* **1**: 17–26.

Szukics U, Abell GCJ, Hödl V, Mitter B, Sessitsch A, Hackl E, *et al.* (2010). Nitrifiers and denitrifiers respond rapidly to changed moisture and increasing temperature in a pristine forest soil. *Fems Microbiol Ecol* **72**: 395–406.

Šimek M, Cooper JE. (2002). The influence of soil pH on denitrification: progress towards the understanding of this interaction over the last 50 years. *Eur J Soil Sci* **53**: 345–354.

Taylor AE, Zeglin LH, Wanzek TA, Myrold DD, Bottomley PJ. (2012). Dynamics of ammonia-oxidizing archaea and bacteria populations and contributions to soil nitrification potentials. *ISME J* **6**: 2024–2032.

Throbäck IN, Enwall K, Jarvis Å, Hallin S. (2004). Reassessing PCR primers targeting *nirS*, *nirK* and *nosZ* genes for community surveys of denitrifying bacteria with DGGE. *Fems Microbiol Ecol* **49**: 401–417.

Tian H, Lu C, Ciais P, Michalak AM, Canadell JG, Saikawa E, *et al.* (2016). The terrestrial biosphere as a net source of greenhouse gases to the atmosphere. *Nature* **531**: 225–228.

Tiedje JM, Firestone MK, Firestone MK, Firestone RB, Firestone RB, Tiedje JM. (1980). Nitrous oxide from soil denitrification: factors controlling its biological production. *Science* **208**: 749–751.

Tilman D. (1999). The ecological consequences of changes in biodiversity: A search for general principles. *Ecology* **80**: 1455–1474.

Tilman D, Fargione J, Wolff B, D'Antonio C, Dobson A, Howarth R, *et al.* (2001). Forecasting agriculturally driven global environmental change. *Science* **292**: 281–284.

Tilman D, Isbell F, Cowles JM. (2014). Biodiversity and ecosystem functioning. *Annu Rev Ecol Evol Syst* **45**: 471–493.

Tilman D, Tilman D, Cassman KG, Cassman KG, Matson PA, Matson PA, *et al.* (2002). Agricultural sustainability and intensive production practices. *Nature* **418**: 671–677.

Tourna M, Freitag TE, Nicol GW, Prosser JI. (2008). Growth, activity and temperature responses of ammonia-oxidizing archaea and bacteria in soil microcosms. *Environ Microbiol* **10**: 1357–1364.

Valentine DL. (2007). Adaptations to energy stress dictate the ecology and evolution of the Archaea. *Nat Rev Microbiol* **5**: 316–323.

van Bodegom P. (2007). Microbial maintenance: a critical review on its quantification. *Microb Ecol* **53**: 513–523.

Van Cleemput O, Samater AH. (1996). Nitrite in soils: accumulation and role in the formation of gaseous N compounds. *Fert Res* **45**: 81–89.

Van Der Heijden MGA, Bardgett RD, van Straalen NM. (2008). The unseen majority: soil microbes as drivers of plant diversity and productivity in terrestrial ecosystems. *Ecol Letters* **11**: 296–310.

van der Oost J, De Boer APN, de Gier J-WL, Heizmann CW, Stouthamer AH, Van Spanning RJM. (1994). The heme-copper oxidase family consists of three distinct types of terminal oxidases and is related to nitric oxide reductase. *FEMS Microbiol Lett* **121**: 1–9.

van Groenigen JW, Schils RLM, Velthof GL, Kuikman PJ, Oudendag DA, Oenema O. (2008). Mitigation strategies for greenhouse gas emissions from animal production systems: synergy between measuring and modelling at different scales. *Aust J Exp Agric* **48**: 46–53.

van Kessel MAHJ, Speth DR, Albertsen M, Nielsen PH, Camp den HJMO, Kartal B, *et al.* (2015). Complete nitrification by a single microorganism. *Nature* **528**: 555–559.

Venterea RT, Clough TJ, Coulter JA, Breuillin-Sessoms F, Wang P, Sadowsky MJ, *et al.* (2015). Ammonium sorption and ammonia inhibition of nitrite-oxidizing bacteria explain contrasting soil N_2O production. *Sci Rep* **5**: 12153.

Vitousek PM, Mooney HA, Lubchenco J, Melillo JM. (1997). Human domination of Earth's ecosystems. *Science* **277**: 494–499.

Vogel C, Marcotte EM. (2012). Insights into the regulation of protein abundance from proteomic and transcriptomic analyses. *Nat Rev Genet* **13**: 228–232.

Wagg C, Bender SF, Widmer F, van der Heijden MGA. (2014). Soil biodiversity and soil community composition determine ecosystem multifunctionality. *Proc Nat Acad Sci* **111**: 5266–5270.

Waldrop MP, Firestone MK. (2006). Response of microbial community composition and function to soil climate change. *Microb Ecol* **52**: 716–724.

Wallenstein MD, Myrold DD, Firestone M, Voytek M. (2006). Environmental controls on denitrifying communities and denitrification rates: insights from molecular methods. *Ecol Appl* **16**: 2143–2152.

Wei W, Isobe K, Nishizawa T, Zhu L, Shiratori Y, Ohte N, *et al.* (2015a). Higher diversity and abundance of denitrifying microorganisms in environments than considered previously. *ISME J*. **9**: 1954–1965.

Wei W, Isobe K, Shiratori Y, Nishizawa T, Ohte N, Ise Y, *et al.* (2015b). Development of PCR primers targeting fungal *nirK* to study fungal denitrification in the environment. *Soil Biol Biochem* **81**: 282–286.

Wertz S, Degrange V, Prosser JI, Poly F, Commeaux C, Freitag T, *et al.* (2006). Maintenance of soil functioning following erosion of microbial diversity. *Environ Microbiol* **8**: 2162–2169.

Whittaker M, Bergmann D, Arciero D. (2000). Electron transfer during the oxidation of ammonia by the chemolithotrophic bacterium *Nitrosomonas europaea*. *Biochim Biophys Acta* **1459**: 346–355.

Wittebolle L, Marzorati M, Clement L, Balloi A, Daffonchio D, Heylen K, *et al.* (2009). Initial community evenness favours functionality under selective stress. *Nature* **458**: 623–626.

Wrage N, Velthof GL, Van Beusichem ML. (2001). Role of nitrifier denitrification in the production of nitrous oxide. *Soil Biol Biochem* **33**: 1723–1732.

Yergeau E, Kang S, He Z, Zhou J, Kowalchuk GA. (2007). Functional microarray analysis of nitrogen and carbon cycling genes across an Antarctic latitudinal transect. *ISME J* **1**: 163–179.

Zaman M, Nguyen ML, Matheson F, Blennerhassett JD, Quin BF. (2007). Can soil amendments (zeolite or lime) shift the balance between nitrous oxide and dinitrogen emissions from pasture and wetland soils receiving urine or urea-N? *Aust J Soil Res* **45**: 543–553.

Zeng J, Liu X, Song L, Lin X, Zhang H, Shen C, *et al.* (2016). Nitrogen fertilization directly affects soil bacterial diversity and indirectly affects bacterial community composition. *Soil Biol Biochem* **92**: 41–49.

Zhu X, Burger M, Doane TA, Horwath WR. (2013). Ammonia oxidation pathways and nitrifier denitrification are significant sources of N_2O and NO under low oxygen availability. *Proc Nat Acad Sci* **110**: 6328–6333.

Zimmerman AR, Benner R. (1994). Denitrification, nutrient regeneration and carbon mineralization in sediments of Galveston Bay, Texas, USA. *Mar Ecol Prog Ser*. **114**: 275-288.

Zumft WG. (1997). Cell biology and molecular basis of denitrification. *Microbiol Mol Biol R* **61**: 533–616.

Zumft WG, Heizmann CW, Kroneck PMH. (2006). Respiratory Transformation of Nitrous Oxide (N_2O) to Dinitrogen by Bacteria and Archaea. *Adv Microb Physiol* **52**: 107–227.